1960

The influence of blast and earth pressure loadings on the dynamic response of flexible underground two-hinged arches.

Walls, Worthen Allen

University of Illinois

THE INFLUENCE OF BLAST AND EARTH PRESSURE LOADINGS ON THE DYNAMIC RESPONSE OF FLEXIBLE UNDERGROUND TWO-HINGED ARCHES

WORTHEN ALLEN WALLS

THE INFLUENCE OF BLAST AND EARTH PRESSURE LOADINGS ON THE DYNAMIC RESPONSE OF FLEXIBLE UNDERGROUND TWO-HINGED ARCHES

BY

WORTHEN ALLEN WALLS

B.S., University of Arkansas, 1948
M.S., University of Illinois, 1954

THESIS

SUBMITTED IN PARTIAL FULFILLMENT OF THE REQUIREMENTS
FOR THE DEGREE OF DOCTOR OF PHILOSOPHY IN CIVIL ENGINEERING
IN THE GRADUATE COLLEGE OF THE
UNIVERSITY OF ILLINOIS, 1960

URBANA, ILLINOIS

ACKNOWLEDGMENTS

This thesis was undertaken under a postgraduate educational program sponsored by the United States Navy for Civil Engineer Corps Officers. The author expresses his appreciation to the United States Navy and to the Bureau of Yards and Docks, United States Navy, for the opportunity of participating in this program.

Appreciation for timely personal interest and encouragement is expressed to Dr. N. M. Newmark, Head, Department of Civil Engineering, University of Illinois, under whose immediate supervision this thesis was prepared.

The author is deeply indebted to Dr. J. D. Haltiwanger, Professor of Civil Engineering, for constructive criticism throughout the preparation of the thesis, and to Dr. J. L. Merritt, Assistant Professor of Civil Engineering, for frequent exchanges of ideas.

TABLE OF CONTENTS

TABLE OF CONTENTS (Continued)

CHAPTER I

INTRODUCTION

1.1 General Statement of the Problem

When a nuclear weapon explodes, a high pressure wave develops and moves away from the point of the explosion, traveling over the ground surface and through the ground. A shallow-buried arch subjected to this pressure responds in various ways, depending on the orientation of the structure relative to the direction of travel of the blast wave, the parameters of the blast loading, and the properties of the soil surrounding the arch. If the arch is oriented with its longitudinal axis perpendicular to the direction of travel of the blast wave, the windward side of the arch is subjected to the pressure a few milliseconds before the leeward side. This unsymmetrical sequence of loading produces flexural stresses and deflection in the arch. The deflection of the arch into the surrounding soil gives rise to an unsymmetrical passive earth pressure loading.

An understanding of how these loadings occur and their effects on the arch is necessary for the proper consideration of the design of the arch rib.

1.2 Purpose of this Thesis

When the arch rib is subjected to the above described loads it responds in a configuration which is a function of an infinite number of shapes or modes of vibration, since the arch rib has distributed mass and elasticity. An infinitely large number of coordinates would be required to specify the position of the deflected arch. The participation of each mode depends on the spatial distribution of the loads along the arch rib

as well as the time variation of the dynamic load in relation to the natural frequencies of vibration of each mode.

The distortion of the arch rib is a function of the stiffness of the rib, the passive earth pressure loading resulting from the stiffness of the soil surrounding the arch, the distribution of the soil and dynamic loads, the time variation of the dynamic load, and the support condition of the abutments. It is convenient to consider the earth pressure loading due to the stiffness of the soil as an integral part of the resistance of the arch. For flexible arches, the stiffness of the soil is greatly in excess of the stiffness of the arch rib, consequently the properties of the arch rib may be neglected. Henceforth, unless specifically designated otherwise, the resistance of the arch rib means the resistance given to the arch by the soil.

Design of structures for dynamic loading is usually based on the principle of conservation of energy. When the dynamic load acts on the structural element, the element deflects. Work is done on the structure by the load at any point as that point deflects. Due to the speed of the loading, kinetic energy of motion is given to the mass of the element, and, as the element deflects, strain energy is stored. The strain energy may involve both elastic and plastic action. A general statement of the principle of conservation of energy is:

work done = kinetic energy + strain energy

To evaluate this equation the displacement of any point on the structure under the load must be known. The strain energy is the sum of all the strain energy in the element, and may be caused by compressive, flexural, torsional and shear stresses in the element. The kinetic energy is the energy of translation or rotation of all the masses in the element.

The evaluation of these quantities would be exceedingly difficult if no more than the arch rib were involved. Evaluation of the energy stored in the soil is a hopeless task, impossible for practical purposes. Fortunately, the principal modes of response of the arch rib are a symmetrical mode corresponding to the compression stresses and an antisymmetrical mode corresponding to the flexural stresses. This allows a considerable simplification to be made in the treatment of the problem.

A single-degree-of-freedom system consists of a lumped mass restrained by a weightless spring. When this system is subjected to a load, only one coordinate is required to fully define the position of the mass. By assuming that the antisymmetrical mode of response of the arch rib is defined by the radial deflection of a point at the quarterpoint of the arch, which is the point of maximum deflection of the arch, the entire deflected shape of the arch may be defined with one coordinate, and the arch may be considered a single-degree-of-freedom system. In essence this neglects any tangential movements of the arch rib associated with the radial deflection.

After representing the action of the arch rib as that of a single-degree-of-freedom system, dynamic equivalence relations should be established between the actual and idealized masses, spring stiffnesses, and loads acting on the two systems. However, for the purposes of this study, this refinement is omitted. Instead, the following assumptions are made:

(1) The mass of the single-degree-of-freedom system is equal to the unit mass of the arch, which is obtained by uniformly distributing along the arch rib the weight of the soil which creates the passive earth pressure.

(2) The resistance function of the single-degree-of-freedom system is equal to the unit resistance given the arch by the earth pressure.

(3) The forcing function on the single-degree-of-freedom system is equal to the unit pressure of the forcing function acting on the arch rib.

Once the mass, resistance function, and forcing function acting on the single-degree-of-freedom system have been defined, the response of the system may be determined by the well-known differential equation of motion of such a system:

$$m\ddot{x} + kx = p(t)$$

where $\ddot{x}$ = the second derivative of the displacement with respect to time

kx = the resistance of the system as a function of the displacement

m = mass of the system

$p(t)$ = the externally applied force as a function of time

The main purpose of this thesis is to investigate the response of various arch ribs under a limited range of variables when acted upon by blast pressure. In order to do this, it is necessary to relate the parameters of the single-degree-of-freedom system to those of the actual structure under investigation.

1.3 Method of Approach

The blast pressure acting on the surface of the ground causes vertical and horizontal pressures in the soil. These pressures are a function of the maximum surface pressure, and are time-dependent upon a pressure wave which passes through the soil. Pressure-time relations of these pressures are formulated.

These pressures are assumed to be principal stresses, the resultant of which acts radially on the arch. The tangential component is omitted. The total radial load which results from these pressures is designated as

a load profile $p_r(\varphi,t)$, which is then represented as a distributed load by the series $\sum p_n(t) \sin \frac{n\pi\varphi}{\theta}$

where $$p_n(t) = \frac{2}{\theta R} \int_o^\theta p_r(\varphi,t) \sin \frac{n\pi\varphi}{\theta} \, Rd\varphi$$

θ = central angle of the arch

R = arch radius

An analogous, uniformly-distributed, antisymmetrical, time-dependent load, $p_a(t)$, is then determined. This load has the same general effect on the entire haunch of the arch as the load $\sum p_n(t) \sin \frac{n\pi\varphi}{\theta}$. The pressure-time diagram for $p_a(t)$ and the numerical relation between $p_a(t)$ and the dynamic load $\sum p_n(t) \sin \frac{n\pi\varphi}{\theta}$ are established by equating their effects at various times as though they both acted statically. The analogous antisymmetrical load $p_a(t)$ defines the forcing function acting on the arch and also on the single-degree-of-freedom system.

The unit, horizontal, passive earth pressure acting on the arch is determined by Rankine's theory for passive earth pressure. The unit vertical pressure acting on the arch is found by statics. These two pressures are assumed to be principal stresses, and their radial resultant is assumed to resist the movement of the arch. The tangential component is omitted. The total radial soil load is designated as a load profile $p_r(\varphi)$, and is represented as a distributed load by the series $\sum p_n \sin \frac{n\pi\varphi}{\theta}$

where $$p_n = \frac{2}{\theta R} \int_o^\theta p_r(\varphi) \sin \frac{n\pi\varphi}{\theta} \, Rd\varphi$$

An analogous, uniformly-distributed, antisymmetrical load which has the same general effect on the entire haunch of the arch as the load

$\sum p_n \sin \frac{n\pi\varphi}{\theta}$ is determined by statics. The passive earth pressure is assumed to reach its maximum value when a point located at $\theta/4$ on the arch rib deflects radially an amount equal to 0.001R. In addition, the resistance diagram of this pressure is assumed to be elasto-plastic. The analogous antisymmetrical load defines the unit resistance of the arch rib and also the resistance function for the single-degree-of-freedom system.

The weight of the soil that causes the passive earth pressure is determined by Rankine's theory and by statics. This weight is assumed to be uniformly distributed along the arch rib and defines the unit mass of the arch rib and also the mass of the single-degree-of-freedom system.

The response of the equivalent single-degree-of-freedom system is determined by a method developed by Dr. N. M. Newmark for blast resistant design, Reference (8).

CHAPTER II

GENERAL DISCUSSION OF THE VARIABLES

The variables of the problem may be divided into three general groups corresponding to the blast loading, the earth pressure loading, and the configuration of the arch rib.

2.1 Blast Pressure Loading

The blast forces acting on the arch rib are conceived to act as a pressure wave passing through the soil, Figure 2.1. The direction and velocity of the propagation of this wave in the soil is assumed to be related to the shock velocity of the surface pressure wave, U, and to the seismic velocity of the soil surrounding the arch, C_s. The magnitude of C_s is assumed to be less than U.

Within the stressed-soil zone, the vertical pressure $p_v(t)$ is assumed to be equal to the surface overpressure $P_s(t)$, but to have a different pressure-time curve to allow for the retardation effects on the shock transmitted through the soil. The horizontal pressure $p_h(t)$ is assumed to be proportional to the vertical pressure.

The time of arrival t_a of the pressure wave at any point in the soil, or on the arch, is determined by the propagation velocity of the wave. The time of rise t_r of the vertical pressure to its maximum value P_m is assumed to be a function of the vertical transit time t_t of the pressure wave. The rate of decay of the earth pressure wave is assumed to be the same as that for the surface pressure. These relations are shown qualitatively in Figure 2.2.

Study of Figure 2.1 indicates that as the shock velocity of the blast wave increases relative to the seismic velocity of the soil, the

unsymmetrical loading decreases, since the pressure wave approaches the arch more nearly vertically. For the usual range of these variables the earth pressure wave qualitatively approaches the arch as shown in Figure 2.1.

It should be noted that this pressure wave is considered to have been induced solely by the surface pressure. The direct ground shock wave associated with a nuclear weapon explosion is not considered in this thesis. Reference (1) states that for pressures of less than 300 psi and for depths of less than fifty feet the direct ground shock may be ignored.

The arch is assumed to be acted upon by the radial resultant of the vertical and horizontal pressures. If the ratio of the horizontal pressure to the vertical pressure is as great as 1:1, the radial pressure is equal to the vertical pressure. Moreover, the total radial force increases as the ratio of the horizontal to the vertical pressure increases.

The effect of the rise time may be seen in Figure 2.2. The pressure wave arrives at some point φ_1 on the arch, Figure 2.1, and the pressure increases to its maximum value in some time t_r. At some adjacent point φ_2 the pressure is at a different level, depending on the relative arrival and rise times. Reference (2) recommends that the rise time be taken equal to one-half the vertical transit time.

The following range of variables will be studied in this paper:

P_m = 100 and 200 psi with U = 3000 and 4000 fps

C_s = 1000 and 2000 fps

t_r = t_t and 1/2 t_t

p_h/p_v = 0.25, 0.50, 0.75 and 1.00

2.2. Passive Earth Pressure Loading

The unsymmetrical blast load on the arch causes the arch to deflect into the soil on the leeward side. This deflection brings into action the

passive earth pressure of the soil as well as the inertia of the mass of soil associated with this pressure, since the blast load acts dynamically. This pressure contributes materially to the resistance of the arch and must be considered.

While precise evaluation of the passive earth pressure under static conditions is complex, evaluation under dynamic conditions is equally, or even more, complex. The passive earth pressure can vary in the length of the arch due either to the properties of the soil or to the construction technique used in placing the backfill. Rankine's theory has been chosen as the simplest method for evaluating this passive earth pressure.

In the application of Rankine's formulas, Reference (3), the unit weight of the soil is assumed to be 120 pounds per cubic foot and the angle of internal friction is assumed to be thirty degrees.

2.3 Structures Considered

The blast loading on arches with central angles of 180 and 120 degrees and radii of 150 and 300 inches is investigated to determine the effect of the soil variables, arch geometry, and relative rise time on the arch loading, and to determine a conventionalized dynamic loading function. Subsequently investigated is the response of arches with central angles of 180 and 120 degrees and radii of 200 to 600 inches to this conventionalized dynamic loading function.

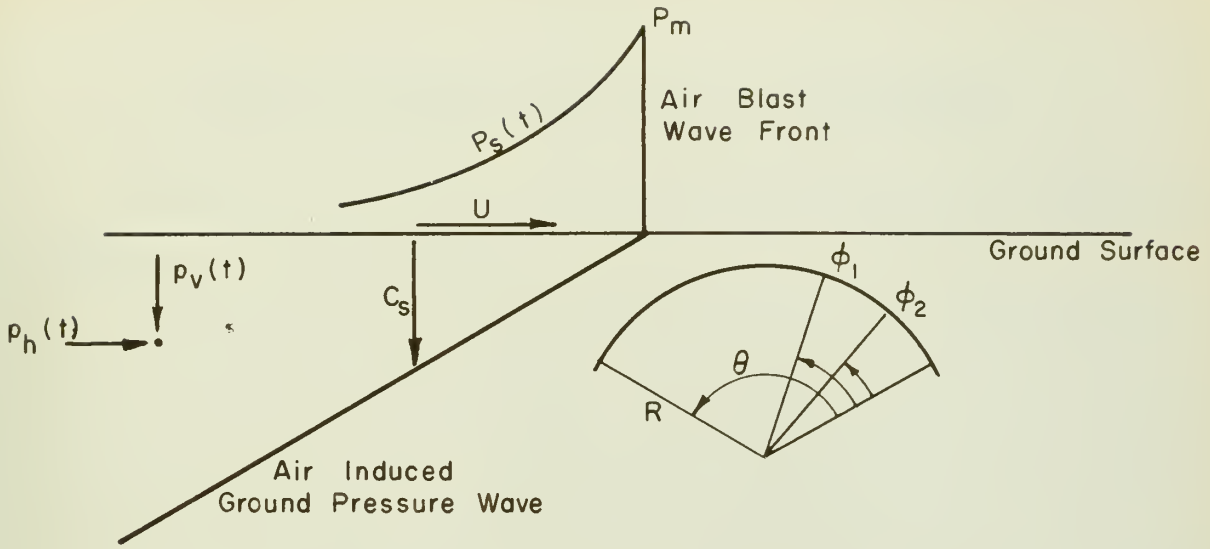

Figure 2.1 Underground Arch Subjected to Blast Pressure

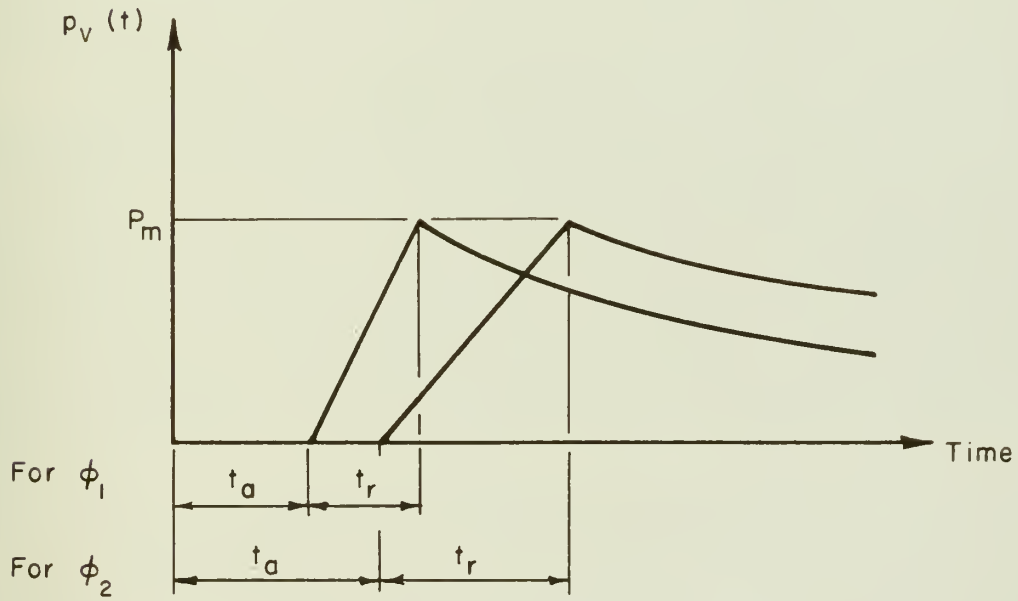

Figure 2.2 Vertical Pressure-Time Diagram for φ

CHAPTER III

GENERAL RELATIONS COMMON TO EACH LOADING FUNCTION

To predict the effect of the loads on the arch rib, the loads must be defined in a convenient manner.

Certain general relations may be derived for defining either the blast load or the earth pressure load. These general relations concern the transformation of stress with direction, the method used to determine the value of the coefficients $p_n(t)$ and p_n for the distributed radial load functions $\sum p_n(t) \sin \frac{n\pi \varphi}{\theta}$ and $\sum p_n \sin \frac{n\pi \varphi}{\theta}$ which represent the actual load on the arch, and the basis for assuming analogous loads to represent these distributed loads.

For purposes of dynamic analysis, the arch is idealized to a single-degree-of-freedom system. The time-dependent load $\sum p_n(t) \sin \frac{n\pi \varphi}{\theta}$ is replaced by a uniformly-distributed, antisymmetrical, time-dependent load $p_a(t)$, and the distributed earth pressure load $\sum p_n \sin \frac{n\pi \varphi}{\theta}$ is replaced by a uniformly-distributed antisymmetrical load p_a. These antisymmetrical loads act outwardly on one half of the arch, and they act inwardly on the other half.

The direction of the analogous earth load is opposite to that of the analogous blast load. These antisymmetrical loads define the effects of the actual loads on the arch haunch.

The values of these analogous loads are found by the application of the principles of statics. The value of the analogous load for the soil pressure may be found by equating the moment produced by the distributed load $\sum p_n \sin \frac{n\pi \varphi}{\theta}$ at a point $\theta/4$ to those of the analogous antisymmetrical load p_a at the same point. The replacement of the dynamic load $\sum p_n(t) \sin \frac{n\pi \varphi}{\theta}$ with an analogous load requires that a basic assumption be made. It is

assumed that if two generally similar static loads produce equal static effects on a structure at a specified point, then the same two loads applied dynamically with similar pressure-time diagrams of equal duration would cause equal dynamic effects at the same point. Of course the dynamic effects of the loads are not defined. The point considered is $\theta/4$.

To determine the analogous loads, the moments caused by the anti-symmetrical loads $p_a(t)$ and p_a are equated with the moments caused by the distributed loads $\sum p_n(t) \sin \frac{n\pi \varphi}{\theta}$ and $\sum p_n \sin \frac{n\pi \varphi}{\theta}$ respectively. In addition, the effect of a uniform compressive load on the central third of the arch coupled with a uniform outward load on the outer thirds of the arch is determined. This load provides an analogous load for study of the crown of the arch.

3.1 Stress Transformation with Direction

Let it be assumed that a horizontal unit stress p_h and a vertical unit stress p_v are acting on a segment $Rd\Phi$ of a semicircular arch rib located at the angle Φ measured from the right abutment. Assuming that p_v and p_h are principal stresses, the radial pressure $p_r(\Phi)$ at Φ may be found by the well-known method for determining the relations between stresses at a point on different planes passing through the point, Reference (4).

$Rd\Phi$ may be assumed to be a plane surface for an infinitesimal segment. The vertical projection of the plane $Rd\Phi$ is $Rd\Phi \cos \Phi$; the horizontal projection is $Rd\Phi \sin \Phi$. Equating the sum of the radial forces to zero yields the following:

$$p_r(\Phi)\, Rd\Phi = p_h\, Rd\Phi \cos^2\Phi + p_v\, Rd\Phi \sin^2\Phi$$

Using the trigonometric identities

$$\cos^2\Phi = \tfrac{1}{2}(1 + \cos 2\Phi)$$

$$\sin^2\Phi = \tfrac{1}{2}(1 - \cos 2\Phi)$$

and cancelling $Rd\varphi$ from both sides of Equation (a),

$$p_r(\varphi) = \tfrac{1}{2}(1 + \cos 2\varphi)\, p_h + \tfrac{1}{2}(1 - \cos 2\varphi)\, p_v$$

$$= \tfrac{1}{2}(p_h + p_v) + \tfrac{1}{2}(p_h - p_v) \cos 2\varphi \qquad (1)$$

The ratios of p_h/p_v to be studied are 0.25, 0.50, 0.75 and 1.0. In addition, these pressures are time-dependent, so $p_r(\varphi)$ must be a time-dependent pressure and is therefore expressed as $p_r(\varphi,t)$ when the pressures considered arise from the blast pressure acting on the surface of the ground. Let $p_h(t) = Cp_v(t)$. Then Equation (1) becomes:

$$p_r(\varphi,t) = C\, p_v(t) + p_v(t)\,(1 - C) \sin^2\varphi \qquad (2)$$

This equation is evaluated for various values of C as follows:

$$\text{For } C = 0.25,\ p_r(\varphi,t) = (0.25 + 0.75 \sin^2\varphi)\, p_v(t) \qquad (3)$$

$$\text{For } C = 0.50,\ p_r(\varphi,t) = (0.50 + 0.50 \sin^2\varphi)\, p_v(t) \qquad (4)$$

$$\text{For } C = 0.75,\ p_r(\varphi,t) = (0.75 + 0.25 \sin^2\varphi)\, p_v(t) \qquad (5)$$

$$\text{For } C = 1.00,\ p_r(\varphi,t) = p_v(t) \qquad (6)$$

Equations (3) through (6) express the time-dependent unit radial pressure acting on the arch rib at any point φ for the various assumed ratios of the horizontal pressure $p_h(t)$ to the vertical pressure $p_v(t)$. Evaluation of these equations is set forth in Table I.

3.2 Distributed Load Functions

Any radial load profile $p_r(\varphi)$, such as that shown in Figure 3.1, when acting upon a segment of a circular arch rib with a central angle θ, may be represented as a distributed load by a trigonometric series in the following manner:

$$p_r(\varphi) = p_1 \sin \frac{\pi\varphi}{\theta} + p_2 \sin \frac{2\pi\varphi}{\theta} + \text{----} + p_n \sin \frac{n\pi\varphi}{\theta} + \text{----} \tag{7}$$

The coefficient p_n is obtained by multiplying both sides of Equation (7) by $\sin \frac{n\pi\varphi}{\theta}$ and integrating over the length of the arch rib.

$$\int_o^\theta p_r(\varphi) \sin \frac{n\pi\varphi}{\theta} R d\varphi = \int_o^\theta p_1 \sin \frac{\pi\varphi}{\theta} \sin \frac{n\pi\varphi}{\theta} R d\varphi$$

$$+ \int_o^\theta p_2 \sin \frac{2\pi\varphi}{\theta} \sin \frac{n\pi\varphi}{\theta} R d\varphi$$

$$+ \text{----} + \int_o^\theta p_n \sin^2 \frac{n\pi\varphi}{\theta} R d\varphi + \text{--} \tag{8}$$

The value of the integral $\int_o^\theta \sin \frac{m\pi\varphi}{\theta} \sin \frac{n\pi\varphi}{\theta} R d\varphi$ is zero provided that m and n are integers and m does not equal n. Equation (8) then yields:

$$\int_o^\theta p_r(\varphi) \sin \frac{n\pi\varphi}{\theta} R d\varphi = R\, p_n \left[\frac{\varphi}{2} - \frac{\sin \frac{2n\pi\varphi}{\theta}}{\frac{4n\pi\varphi}{\theta}} \right]_o^\theta$$

$$= \tfrac{1}{2} p_n R\theta$$

$$\therefore p_n = \frac{2}{\theta R} \int_o^\theta p_r(\varphi) \sin \frac{n\pi\varphi}{\theta} R d\varphi \tag{9}$$

If $p_r(\varphi)$ can be expressed analytically, the value of p_n may be found by integration. If $p_r(\varphi)$ is an irregular load profile for which there is no convenient analytical expression, the integral may be evaluated by numerical methods since the integral $\int p_r(\varphi) \sin \frac{n\pi\varphi}{\theta} R d\varphi$ represents the area under the load profile multiplied by $\sin \frac{n\pi\varphi}{\theta}$.

The sign convention adopted throughout this thesis is that a positive load acts inwardly and a negative load acts outwardly. The

harmonic components of loading $p_n \sin \frac{n\pi\varphi}{\theta}$ shown in Figure 3.1 are in qualitative agreement with the original load $p_r(\varphi)$; therefore the sign of the coefficient p_2 is definitely negative. The sign of the coefficient p_3 has been taken as negative, although no positive statement can be made that this is the case for the original load $p_r(\varphi)$ in Figure 3.1.

Included in Figure 3.1 are two cases of uniform radial loading. It can be shown that the effects of $\sum p_n \sin \frac{n\pi\varphi}{\theta}$ on the crown and haunch of the arch may be represented by such uniformly distributed loads.

If the load profile $p_r(\varphi)$ is time-dependent, it is expressed as $p_r(\varphi,t)$. The procedure described above may be used to determine the coefficient $p_n(t)$, with the qualification that $p_n(t)$ must be evaluated at a specified time.

Reference (5) contains a full development of the methods of harmonic analysis as applied to structural engineering problems.

3.3. Basis for the Determination of Analogous Loads

As stated at the beginning of this chapter, the analogous loads $p_a(t)$ and p_a are derived by equating their moments to the sum of the moments of the distributed loads $\sum p_n(t) \sin \frac{n\pi\varphi}{\theta}$ and $\sum p_n \sin \frac{n\pi\varphi}{\theta}$, respectively. The time dependency of $p_a(t)$ is not considered in this section since the load $\sum p_n(t) \sin \frac{n\pi\varphi}{\theta}$ is assumed to be acting statically at the instant the analogous load $p_a(t)$ is evaluated.

Moment equations for all load profiles in Figure 3.1 are found in this section after general equations for the right reaction of any two-hinged semicircular arch are established. Since the blast load and soil load are expressed in terms of a general function $\sum p_n \sin \frac{n\pi\varphi}{\theta}$, one set of moment equations suffices for both analogous loads.

3.3.1. General Equations for the Right Reactions of Circular-Segment Arches

Since the circular-segment two-hinged arch, Figure 3.2, is one degree indeterminate, one equation based on Castigliano's theorem, Reference (4), is used for the determination of the reactions. The horizontal thrust at the right reaction is chosen as the redundant. It is assumed that the arch rib may be treated as a thin ring, making it unnecessary to consider the theory of curved beams. The effects of rib shortening also are not considered.

The following geometrical relations are derived in accordance with Figure 3.2:

Figure 3.2a

$$BC = 2R \sin\tfrac{1}{2}\varphi$$

$$AB = BC \cos\tfrac{1}{2}(\theta - \varphi) = 2R \sin\tfrac{1}{2}\varphi \cos\tfrac{1}{2}(\theta - \varphi)$$

$$AC = BC \sin\tfrac{1}{2}(\theta - \varphi) = 2R \sin\tfrac{1}{2}\varphi \sin\tfrac{1}{2}(\theta - \varphi)$$

$$BD = 2R \sin\tfrac{1}{2}\theta$$

Figure 3.2b

$$DF = 2R \sin\tfrac{1}{2}(\theta - \beta)$$

$$EF = 2R \sin\tfrac{1}{2}(\theta - \beta) \cos\tfrac{1}{2}(\theta - \beta)$$

$$= \text{moment arm of P about D}$$

Figure 3.2c

$$FG = R \sin(\varphi - \beta)$$

$$= \text{moment arm of P about G}$$

Figure 3.2d

$$AB = \text{moment arm of V about C}$$

$$AC = \text{moment arm of H about C}$$

$$DB = \text{moment arm of V about D}$$

In Figure 3.2d, the total strain energy U in the arch rib due to the moment M caused by the radial load P acting at a point on the rib located by β may be expressed as

$$U = \int \frac{M^2}{2EI}\, ds = \int \frac{M^2}{2EI}\, R d\varphi$$

Since the abutments are assumed not to move, the contribution of the right reaction H to the strain energy is zero and may be expressed as

$$\frac{\partial U}{\partial H} = \int \frac{M \partial M}{\partial H} R d\varphi = 0 \qquad (a)$$

Two equations are required to express the moment in the arch rib; one equation for angle φ less than or equal to β, and one for φ equal to or greater than β. For $0 < \varphi \leq \beta$,

$$M_1 = V(AB) - H(AC)$$
$$= 2VR \sin \tfrac{1}{2}\varphi \cos\tfrac{1}{2}(\theta - \varphi) - 2HR \sin\tfrac{1}{2}\varphi \sin\tfrac{1}{2}(\theta - \varphi) \qquad (b)$$

$$\frac{\partial M_1}{\partial H} = -2R \sin\tfrac{1}{2}\varphi \sin\tfrac{1}{2}(\theta - \varphi) \qquad (c)$$

For $\beta \leq \varphi < \theta$,

$$M_2 = V(AB) - H(AC) - P(FG) \qquad (d)$$
$$= 2VR \sin\tfrac{1}{2}\varphi \cos\tfrac{1}{2}(\theta - \varphi) - 2HR \sin\tfrac{1}{2}\varphi \sin\tfrac{1}{2}(\theta-\varphi) - PR \sin(\varphi-\beta)$$

$$\frac{\partial M_2}{\partial H} = -2R \sin\tfrac{1}{2}\varphi \sin\tfrac{1}{2}(\theta - \varphi) \qquad (e)$$

Substituting Equations (b) through (e) into Equation (a),

$$0 = \int M_1 \frac{\partial M_1}{\partial H} R d\varphi + \int M_2 \frac{\partial M_2}{\partial H} R d\varphi$$
$$= \int_0^{\beta} [\, 2VR \sin\tfrac{1}{2}\varphi \cos\tfrac{1}{2}(\theta-\varphi) - 2HR \sin\tfrac{1}{2}\varphi \sin\tfrac{1}{2}(\theta-\varphi)\,]$$
$$[\, -2R \sin\tfrac{1}{2}\varphi \sin\tfrac{1}{2}(\theta-\varphi)\,] R d\varphi +$$
$$\int_{\beta}^{\theta} [\, 2VR \sin\tfrac{1}{2}\varphi \cos\tfrac{1}{2}(\theta-\varphi) - 2HR \sin\tfrac{1}{2}\varphi \sin\tfrac{1}{2}(\theta-\varphi)$$
$$- PR \sin(\varphi-\beta)\,][-2R \sin\tfrac{1}{2}\varphi \sin\tfrac{1}{2}(\theta-\varphi)\,] R d\varphi \qquad (f)$$

Solving Equation (f) for H yields

$$H = \frac{\left[\begin{array}{l} 4\int_0^{\theta} VR^3 \sin^2\frac{\theta}{2}\sin(\frac{\theta-\varphi}{2})\cos(\frac{\theta-\varphi}{2})d\varphi \\ -2\int_{\beta}^{\theta} PR^3 \sin(\varphi-\beta)\sin\frac{\varphi}{2}\sin(\frac{\theta-\beta}{2})d\varphi \end{array}\right.}{4\int_0^{\theta} R^3 \sin^2\frac{\varphi}{2}\sin^2(\frac{\theta-\varphi}{2})\,d\varphi} \qquad (g)$$

Referring to Figure 3.2, the sum of the moments equated about the left reaction gives

$$V = \frac{P(EF)}{DB} = \frac{2PR\sin(\frac{\theta-\beta}{2})\cos(\frac{\theta-\beta}{2})}{2R\sin\frac{\theta}{2}} = \frac{P\sin(\theta-\beta)}{2\sin\frac{\theta}{2}} \qquad (10)$$

Substituting Equation (10) into Equation (g),

$$H = \frac{P\left\{\frac{\sin(\theta-\beta)}{\sin\frac{\theta}{2}}\left[\frac{1}{2} - \frac{\theta}{4}\sin\theta - \frac{1}{2}\cos\theta\right] + \left[\cos\frac{\theta}{2} - \frac{3}{4}\cos(\frac{\theta}{2}-\beta) - \frac{1}{4}\cos(\frac{3\theta}{2}-\beta) + (\frac{\beta-\theta}{2})\sin(\frac{\theta}{2}-\beta)\right]\right\}}{\frac{\theta}{2} + \theta\cos^2(\frac{\theta}{2}) - 3\sin\frac{\theta}{2}\cos\frac{\theta}{2}} \qquad (11)$$

Equations (10) and (11) define the right reaction of any circular-segment two-hinged arch acted upon by a radial load P located at any angle β.

3.3.2. Moment Equations for 180 Degree Arches

For a semicircular arch, the central angle θ is π, and Equation (11) reduces to

$$H = \frac{P}{\pi}\left[\sin\beta + (\beta - \pi)\cos\beta\right] \qquad (12)$$

Using Equation (12), the horizontal right reaction may now be found for the harmonic load component $p_n \sin\frac{n\pi\varphi}{\theta}$.

For $P = p_1 \sin\frac{\pi\varphi}{\theta}\, Rd\varphi = p_1 \sin\varphi\, Rd\varphi$, since $\theta = \pi$,

$$H = \frac{1}{\pi}\int_0^{\pi} p_1 \sin\varphi[\sin\varphi + (\varphi-\pi)\cos\varphi]\, Rd\varphi = \frac{p_1 R}{4}$$

For $P = -p_2 \sin\frac{2\pi\varphi}{\theta}\, Rd\varphi$,

$$H = \frac{1}{\pi}\int_0^{\pi} -p_2 \sin 2\varphi[\sin\varphi + (\varphi-\pi)\cos\varphi]\, Rd\varphi = \frac{2}{3} p_2 R$$

For $P = -p_3 \sin 3\varphi\, Rd\varphi$,

$$H = \frac{1}{\pi}\int_0^{\pi} -p_3 \sin 3\varphi[\sin\varphi + (\varphi-\pi)\cos\varphi]\, Rd\varphi = \frac{3}{8} p_3 R$$

The loading configurations $p_n \sin\frac{n\pi\varphi}{\theta}$ are shown in Figure 3.1.

It is also necessary to investigate the effect of the uniform antisymmetrical load p_a and the uniform symmetrical load p_s shown in Figure 3.1. For the uniform antisymmetrical load,

$$H = \frac{1}{\pi}\int_0^{\frac{\pi}{2}} -p\,[\sin\varphi + (\varphi-\pi)\cos\varphi]\, Rd\varphi + \frac{1}{\pi}\int_{\frac{\pi}{2}}^{\pi} p[\sin\varphi + (\varphi-\pi)\cos\varphi] Rd\varphi = pR$$

For the uniform symmetrical load,

$$H = \frac{1}{\pi}\int_0^{\frac{\pi}{3}} -p[\sin\varphi + (\varphi-\pi)\cos\varphi]\, Rd\varphi + \frac{1}{\pi}\int_{\frac{\pi}{3}}^{\frac{2\pi}{3}} p[\sin\varphi + (\varphi-\pi)\cos\varphi]\, Rd\varphi$$

$$+ \frac{1}{\pi}\int_{\frac{2\pi}{3}}^{\pi} p\,[\sin\varphi + (\varphi-\pi)\cos\varphi]\, Rd\varphi = \frac{1}{3}\sqrt{3}\, pR$$

Equation (10) is used to find the right vertical reaction. With $\theta = \pi$, Equation (10) reduces to $V = \frac{1}{2} P \sin\varphi$.

For $P = p_1 \sin \frac{\pi\varphi}{\theta}\, Rd\varphi$, $V = \frac{1}{2}\int_0^{\pi} p_1 \sin^2\varphi\, Rd\varphi = \frac{1}{4}p_1\pi R$

For $P = -p_2 \sin \frac{2\pi\varphi}{\theta}\, Rd\varphi$, $V = -\frac{1}{2}\int_0^{\pi} p_2 \sin 2\varphi \sin\varphi\, Rd\varphi = 0$

For $P = -p_3 \sin \frac{3\pi\varphi}{\theta}\, Rd\varphi$, $V = -\frac{1}{2}\int_0^{\pi} p_3 \sin 3\varphi \sin\varphi\, Rd\varphi = 0$

For the uniform antisymmetrical load,

$$V = \frac{1}{2}\int_0^{\frac{\pi}{2}} -p \sin\varphi\, Rd\varphi + \frac{1}{2}\int_{\frac{\pi}{2}}^{\pi} p \sin\varphi\, Rd\varphi = 0$$

For the uniform symmetrical load

$$V = \frac{1}{2}\int_0^{\frac{\pi}{3}} -p \sin\, Rd\, + \frac{1}{2}\int_{\frac{\pi}{3}}^{\frac{2\pi}{3}} p \sin\varphi\, Rd\varphi$$

$$- \frac{1}{2}\int_{\frac{2\pi}{3}}^{\pi} p \sin\varphi\, Rd\varphi = 0$$

The value of zero for the last four loads was to be expected from the symmetry of the arch and the loading configurations. It is interesting to note that the two-hinged semicircular arch is statically determinate for the last four loadings.

All the above values for the right reactions for a 180° arch are tabulated in Table II.

The moment at any point on the arch in Figure 3.1 located by φ due to a distributed load $p_1 \sin \frac{\pi\beta}{\theta}\, Rd\beta$ acting at β is

$$dM = -p_1 \sin\beta [R \sin(\varphi-\beta)]\, Rd\beta$$

The total moment at φ is

$$M = -H(AC) + V(AB) - \int_0^{\varphi} p_1 \sin\beta \, [R \sin(\varphi-\beta)] \, R d\beta$$

$$= -\frac{p_1 R}{4}\left[2R \sin\frac{\varphi}{2} \sin\left(\frac{\pi-\varphi}{2}\right)\right] + \frac{p_1 \pi R}{4}\left[2R \sin\frac{\varphi}{2} \cos\left(\frac{\pi-\varphi}{2}\right)\right]$$

$$+ p_1 R^2 \left[\tfrac{1}{2} \sin\varphi \sin^2\beta - \cos\varphi \left(\frac{\beta}{2} - \frac{\sin 2\beta}{4} \right)\right]_0^{\varphi}$$

$$= \tfrac{1}{4} p_1 R^2 \left[\pi - (\pi-2\varphi) \cos\varphi - 3 \sin\varphi \right]$$

A similar procedure is used to find the moment at φ due to the other loading configurations in Figure 3.1. The results are tabulated in Table III.

3.3.3. Moment Equations for 120 Degree Arches

When the central angle of the arch is 120 degrees, Equation (11) reduces to

$$H = \frac{P\left\{\dfrac{\sin\left(\frac{2\pi}{3} - \beta\right)}{\sin\frac{\pi}{3}}\left[\tfrac{1}{2} - \frac{\pi}{6}\sin\frac{2\pi}{3} - \tfrac{1}{2}\cos\frac{2\pi}{3}\right] + \cos\frac{\pi}{3} - \frac{3}{4}\cos\left(\frac{\pi}{3} - \beta\right) - \tfrac{1}{4}\cos(\pi-\beta) + \dfrac{\beta - \frac{2\pi}{3}}{2}\sin\left(\frac{\pi}{3} - \beta\right)\right\}}{\frac{\pi}{3} + \frac{2\pi}{3}\cos^2\frac{\pi}{3} - 3\sin\frac{\pi}{3}\cos\frac{\pi}{3}}$$

$$= \frac{P\left[(\cos\beta + \frac{1}{\sqrt{3}}\sin\beta)\left(\frac{3}{4} - \frac{\sqrt{3}}{12}\pi\right) + \tfrac{1}{2} - \left(\frac{1}{8} + \frac{\pi}{2\sqrt{3}}\right)\cos\beta + \left(\frac{\pi}{6} - \frac{3\sqrt{3}}{8}\right)\sin\beta + \frac{\sqrt{3}}{4}\beta\cos\beta - \tfrac{1}{4}\beta\sin\beta\right]}{\frac{\pi}{2} - \frac{3\sqrt{3}}{4}}$$

$$= P\left[1.83979 - 2.70578 \cos\beta + 0.16665 \sin\beta + 1.59330 \beta \cos\beta - 0.91990 \beta \sin\beta \right] \qquad (13)$$

Equation (13) may be used to find the right horizontal reaction of an arch with a 120 degree central angle acted upon by a concentrated radial load P located at any angle β. The reaction for $p_1 \sin \frac{\pi\varphi}{\theta} Rd\varphi$ is found as follows:

$$H = \int_0^{\frac{2\pi}{3}} p_1 \sin \tfrac{3}{2}\varphi \left[1.83979 - 2.70578 \cos\varphi + 0.16665 \sin\varphi + 1.59330\, \varphi\cos\varphi - 0.91990\, \varphi\sin\varphi \right] Rd\varphi = 0.53076 p_1 R$$

The horizontal reactions for the remaining harmonic loads and the uniform loads are found in the same manner, and are set forth in Table II.

Equation (10) is used to find the vertical reaction.

For $p_1 \sin \frac{\pi\varphi}{\theta} Rd\varphi$,

$$V = \int_0^{\frac{2\pi}{3}} \left[\frac{1}{2 \sin \frac{\pi}{3}} \right] p_1 \sin \tfrac{3}{2}\varphi \sin \left(\tfrac{2\pi}{3} - \varphi\right) Rd\varphi = 0.6\, p_1 R$$

The remaining vertical reactions have been found, and are stated in Table II.

For a segment $Rd\beta$ at β loaded with $p_1 \sin \frac{\pi\beta}{\theta} Rd\beta$, the moment at φ in Figure 3.1 is

$$dM = -p_1 \sin \tfrac{3}{2}\beta [R \sin(\varphi-\beta)] Rd\beta$$

and the total moment at φ is

$$M = -0.53076\, p_1 R[AC] + 0.6 p_1 R[AB] - \int_0^{\varphi} p_1 \sin \tfrac{3}{2}\beta [R\sin(\varphi-\beta)] Rd\beta$$

$$= -0.53076\, p_1 R \left[2R \sin \tfrac{\varphi}{2} \sin\left(\frac{\frac{2\pi}{3} - \varphi}{2}\right) \right] + 0.6\, p_1 R \left[2R \sin \tfrac{\varphi}{2} \cos\left(\frac{\frac{2\pi}{3} - \varphi}{2}\right) \right] - \int_0^{\varphi} p_1 \sin \tfrac{3}{2}\beta\, [R \sin(\varphi-\beta)] Rd\beta$$

$$= (0.78499 - 1.35965 \sin\varphi - 0.78499 \cos\varphi + 0.8 \sin \tfrac{3\varphi}{2})\, p_1 R^2$$

The moment equations for the remaining load configurations shown in Figure 3.1 for an arch with a 120 degree central angle have been found and are contained in Table III.

3.3.4. Procedure in Determining Analogous Loads

The moment equations tabulated in Table III have been evaluated for every ten degrees. The results are tabulated in Table IV and shown in Figures 3.3 and 3.4. These values are for static loads. They do not indicate the dynamic moment which may exist at any time in the arch.

Inspection of Figures 3.3 and 3.4 shows that the effect of the analogous antisymmetrical load is almost identical to that of the load $p_2 \sin \frac{2\pi\varphi}{\theta}$. If p_2 has a value of one, then the value of the antisymmetrical load must be slightly less than one if the effect of each is to be the same. However, the antisymmetrical load must also include the effect of the loads $p_1 \sin \frac{\pi\varphi}{\theta}$ and $p_3 \sin \frac{3\pi\varphi}{\theta}$. Therefore, the moment that $\sum p_n \sin \frac{n\pi\varphi}{\theta}$ causes at a point $\theta/4$ is first determined, and subsequently a value of the antisymmetrical load is found which will cause the same moment at $\theta/4$. The point $\theta/4$ is selected since the unsymmetrical blast load produces the maximum effect at this point. The time must remain constant for each numerical evaluation of $p_a(t)$, as described below.

The actual blast load on the arch is $p_r(\varphi, t)$. At any given time the load profile $p_r(\varphi, t)$ can be determined and analyzed to give a distributed load $\sum p_n(t) \sin \frac{n\pi\varphi}{\theta}$. By assuming that $\sum p_n(t) \sin \frac{n\pi\varphi}{\theta}$ acts statically, its effects may be found at $\theta/4$. An analogous load can be found which causes the same effect. By repeating this operation at various times, the pressure-time diagram of $p_a(t)$ can be determined. This load must then be applied dynamically to determine its actual effect on the arch.

In determining the static load of the earth, the analogous load is found by equating the moments at $\theta/4$ of the distributed static load $\sum p_n \sin \frac{n\pi\varphi}{\theta}$ with the moment of the antisymmetrical load. Since the earth pressure is not a dynamic load, only one evaluation is needed.

Further inspection of Figures 3.3 and 3.4 shows that the effect of the distributed loads $\sum p_n \sin \frac{n\pi\varphi}{\theta}$ on the central third of the arch may be represented by the symmetrical load which acts in compression on the central third of the arch and in tension on the outer thirds. This load is designated p_s . If the distributed load is a time-dependent load, the same procedure is used in finding the pressure-time diagram for $p_s(t)$ as that used for $p_a(t)$.

TABLE I

COEFFICIENTS FOR RESOLVING VERTICAL AND HORIZONTAL PRESSURE INTO RADIAL PRESSURE

Angle	Radial pressure $p_r(\varphi,t)$ in terms of vertical pressure			
	Assumed ration p_h/p_v			
	0.25	0.50	0.75	1.00
0	0.250	0.500	0.750	1.00
10	0.273	0.515	0.758	1.00
20	0.338	0.559	0.779	1.00
30	0.438	0.625	0.813	1.00
40	0.560	0.707	0.853	1.00
50	0.690	0.794	0.897	1.00
60	0.813	0.875	0.938	1.00
70	0.913	0.942	0.971	1.00
80	0.978	0.985	0.993	1.00
90	1.000	1.000	1.000	1.00
100	0.978	0.985	0.993	1.00
110	0.913	0.942	0.971	1.00
120	0.813	0.875	0.938	1.00
130	0.690	0.794	0.897	1.00
140	0.560	0.707	0.853	1.00
150	0.438	0.625	0.813	1.00
160	0.338	0.559	0.779	1.00
170	0.273	0.515	0.758	1.00
180	0.250	0.500	0.750	1.00

TABLE II

RIGHT REACTIONS OF CIRCULAR-SEGMENT ARCHES WITH H AND V IN TERMS OF pR

Arch Section	Loading				
	$p_1 \sin \frac{\pi\varphi}{\theta}$	$-p_2 \sin \frac{2\pi\varphi}{\theta}$	$-p_3 \sin \frac{3\pi\varphi}{\theta}$	Antisymmetrical	Symmetrical
Hinged, $\theta = 180^\circ$					
H	0.25000	0.66667	0.37500	1.0000	0.57735
V	0.78540	0	0	0	0
Hinged, $\theta = 120^\circ$					
H	0.53076	0.32475	0.20045	0.50000	0.31243
V	0.60000	-0.18750	-0.11688	-0.28868	-0.18199

TABLE III

MOMENT EQUATIONS FOR MOMENT AT φ IN TERMS OF $p_n R^2$

Loading	Arch Section	Condition
	Two-hinged, $\theta = 180^\circ$	
$p_1 \sin \frac{\pi\varphi}{\theta}$	$0.25 [\pi - (\pi - 2\varphi) \cos \varphi - 3 \sin\varphi]$	$0 \leq \varphi \leq \pi$
$-p_2 \sin \frac{2\pi\varphi}{\theta}$	$-0.66667 \sin \varphi \cos \varphi$	$0 \leq \varphi \leq \pi$
$-p_3 \sin \frac{3\pi\varphi}{\theta}$	$0.125 \sin \varphi - \sin^3 \varphi \cos^2 \varphi$	$0 \leq \varphi \leq \pi$
Antisymmetrical	$1 - \cos \varphi - \sin \varphi$	$0 \leq \varphi \leq \frac{\pi}{2}$
Symmetrical	$1 - \cos \varphi - 0.57735 \sin \varphi$	$0 \leq \varphi \leq \frac{\pi}{3}$
Symmetrical	$1.15470 \sin \varphi - 1$	$\frac{\pi}{3} \leq \varphi \leq \frac{2\pi}{3}$
	Two-hinged, $\theta = 120^\circ$	
$p_1 \sin \frac{\pi\varphi}{\theta}$	$0.78499 - 1.35965 \sin \varphi - 0.78499 \cos \varphi + 0.8 \sin \frac{3\varphi}{2}$	$0 \leq \varphi \leq \frac{2\pi}{3}$
$-p_2 \sin \frac{2\pi\varphi}{\theta}$	$-0.125 \sin 3 \varphi$	$0 \leq \varphi \leq \frac{2\pi}{3}$
$-p_3 \sin \frac{3\pi\varphi}{\theta}$	$-0.00100 + 0.00174 \sin\varphi + 0.00100 \cos\varphi - 0.05915 \sin \frac{9}{2} \varphi$	$0 \leq \varphi \leq \frac{2\pi}{3}$
Antisymmetrical	$1 - 0.57735 \sin \varphi - \cos \varphi$	$0 \leq \varphi \leq \frac{\pi}{3}$
Symmetrical	$0.99861 - 0.36157 \sin \varphi - 0.98861 \cos \varphi$	$0 \leq \varphi \leq \frac{2\pi}{9}$
Symmetrical	$0.92401 \sin \varphi + 0.53347 \cos \varphi - 1.00139$	$\frac{2\pi}{9} \leq \varphi \leq \frac{4\pi}{9}$

TABLE IV

MOMENT COEFFICIENTS IN TERMS OF $p_n R^2$

(Positive moment causes compression in outside fiber)

Arch Section	φ	Loading				
		$p_1 \sin \frac{\pi\varphi}{\theta}$	$-p_2 \sin \frac{2\pi\varphi}{\theta}$	$-p_3 \sin \frac{3\pi\varphi}{\theta}$	Antisymmetrical	Symmetrical
Two-hinged						
	0	0	0	0	0	0
$\theta = 180^\circ$	10	-0.03260	-0.11401	0.01664	-0.15846	-0.08507
	20	-0.04514	-0.21426	0.00742	-0.28171	-0.13716
	30	-0.04305	-0.28867	-0.03125	-0.36603	-0.15470
	40	-0.03094	-0.32827	-0.07550	-0.40883	-0.13716
	45	-0.02262	-0.33333	-0.08837	-0.41422	-0.11536
	50	-0.01351	-0.32827	-0.08998	-0.40883	-0.08507
	60	+0.00497	-0.28867	-0.05413	-0.36603	0
	70	+0.02094	-0.21426	0.02039	-0.28171	0.08506
	80	+0.03164	-0.11401	0.09430	-0.15846	0.13716
	90	+0.03540	0	0.12500	0	0.15470
Two-hinged						
	0	0	0	0	0	0
$\theta = 120^\circ$	10	-0.01762	-0.06250	-0.05055	-0.08507	-0.04762
	20	-0.01819	-0.10825	-0.06761	-0.13716	-0.06343
	30	-0.00946	-0.12500	-0.05009	-0.15470	-0.04700
	40	0.00201	-0.10825	0.00089	-0.13716	0.00123
	50	0.01110	-0.06250	0.03380	-0.08507	0.04939
	60	0.01449	0	0.05116	0	0.06556

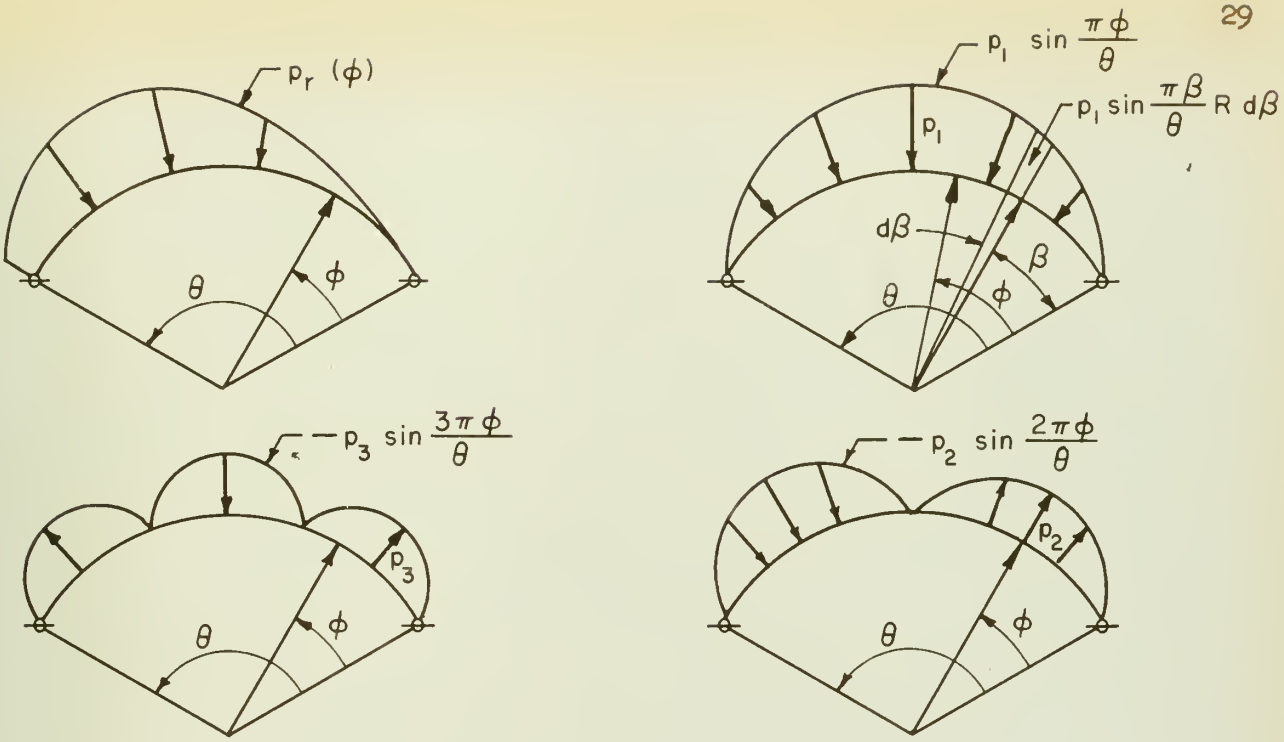

(a) Radial Load Profile $p_r(\varphi)$ and Harmonic Load Components

$$p_n \sin \frac{n\pi\varphi}{\theta}$$

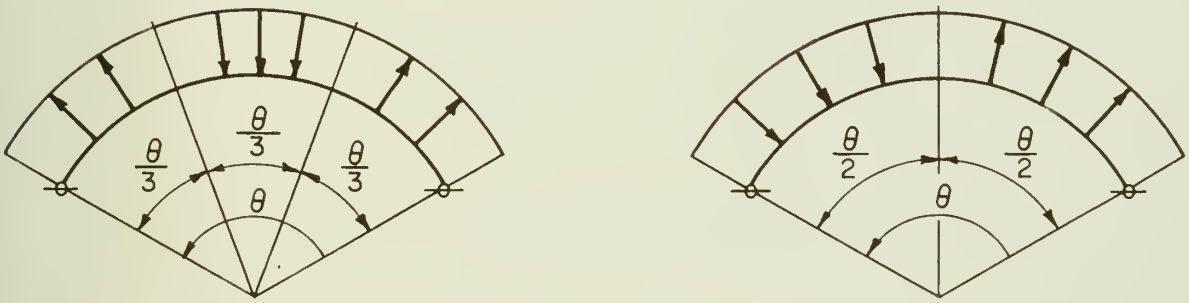

(b) Uniform Symmetrical and Antisymmetrical Loadings

Figure 3.1 Various Load Configurations

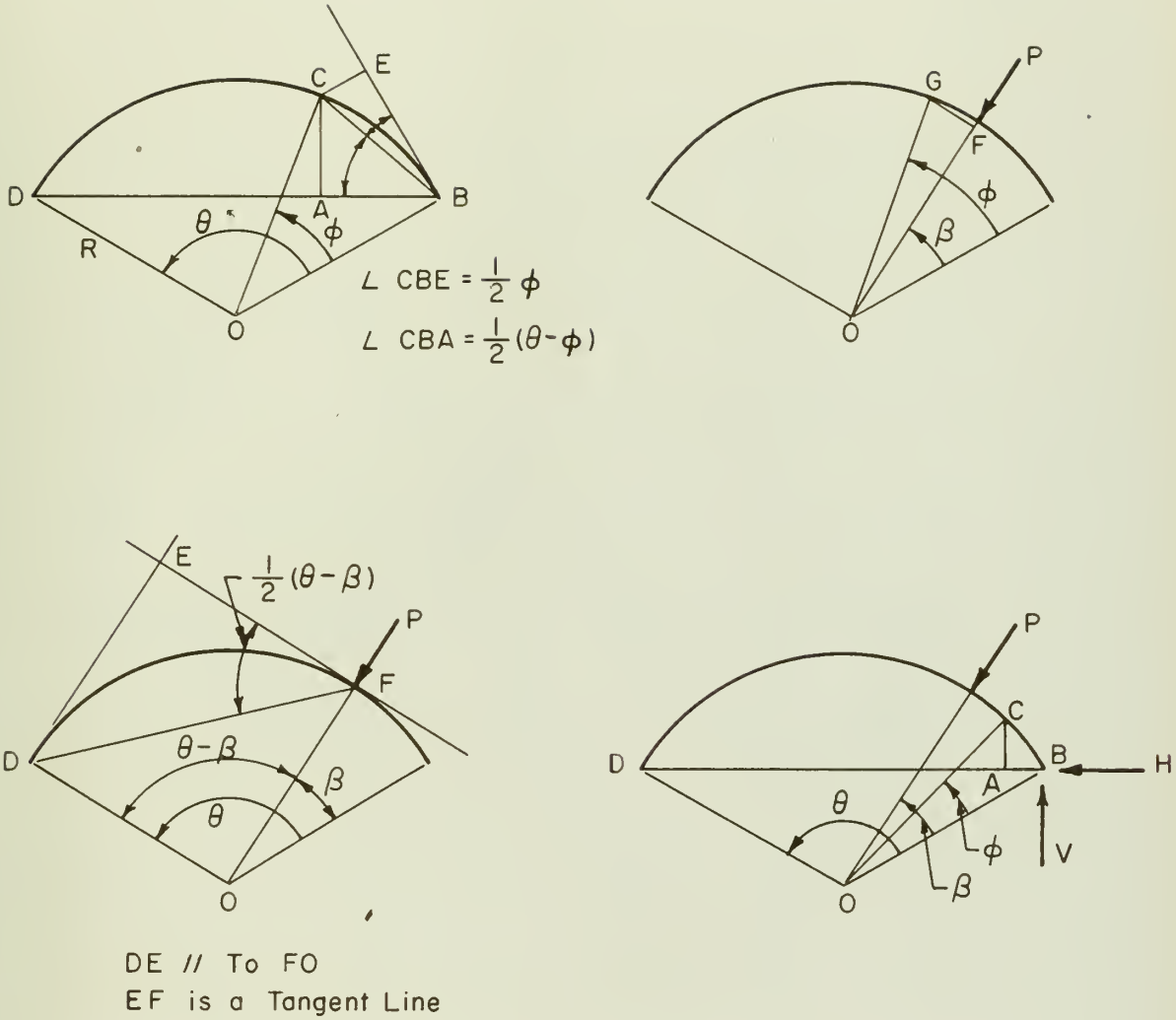

Figure 3.2 Geometry of a Circular Arch Segment

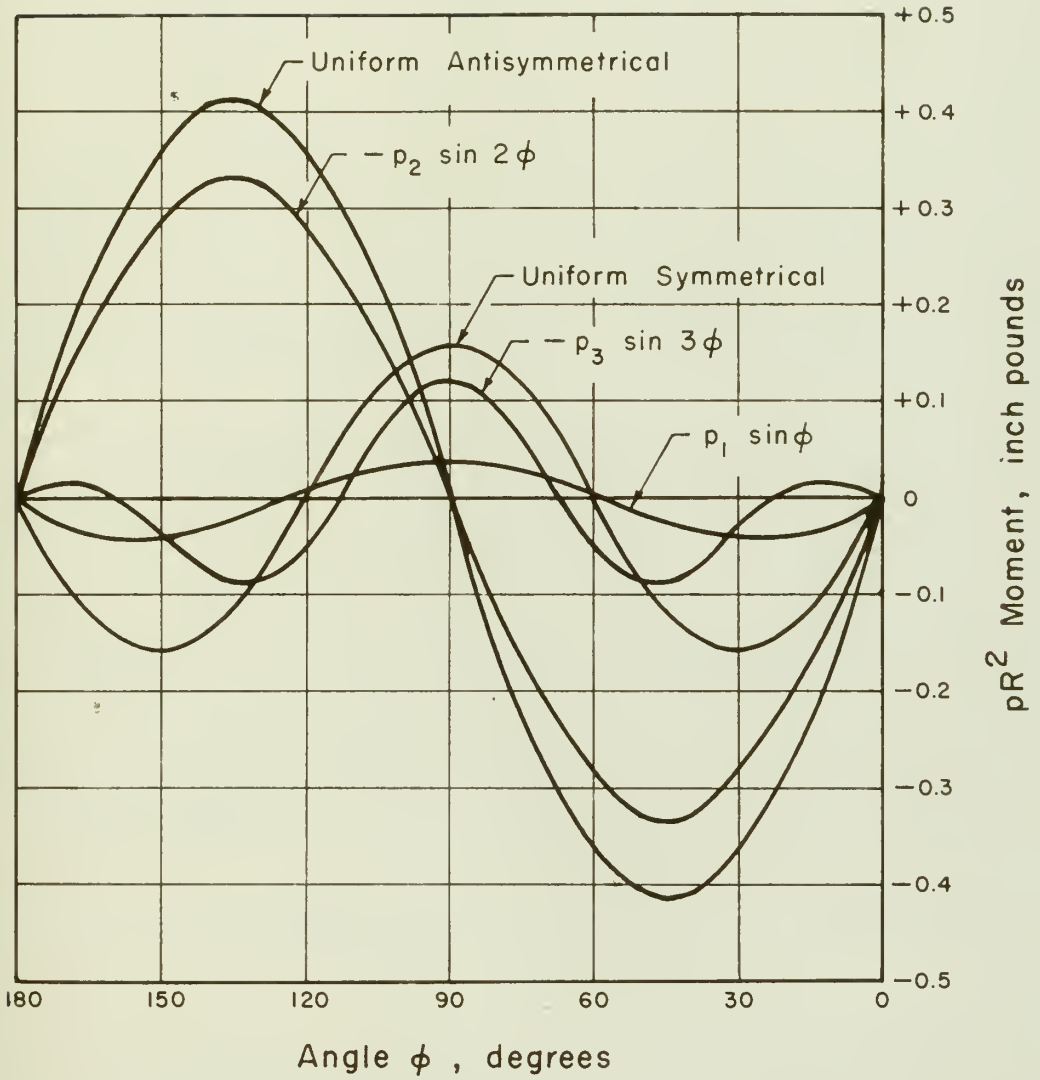

Figure 3.3 Moment vs Angle φ for 180 Degree Central Angle Two-Hinged Arch

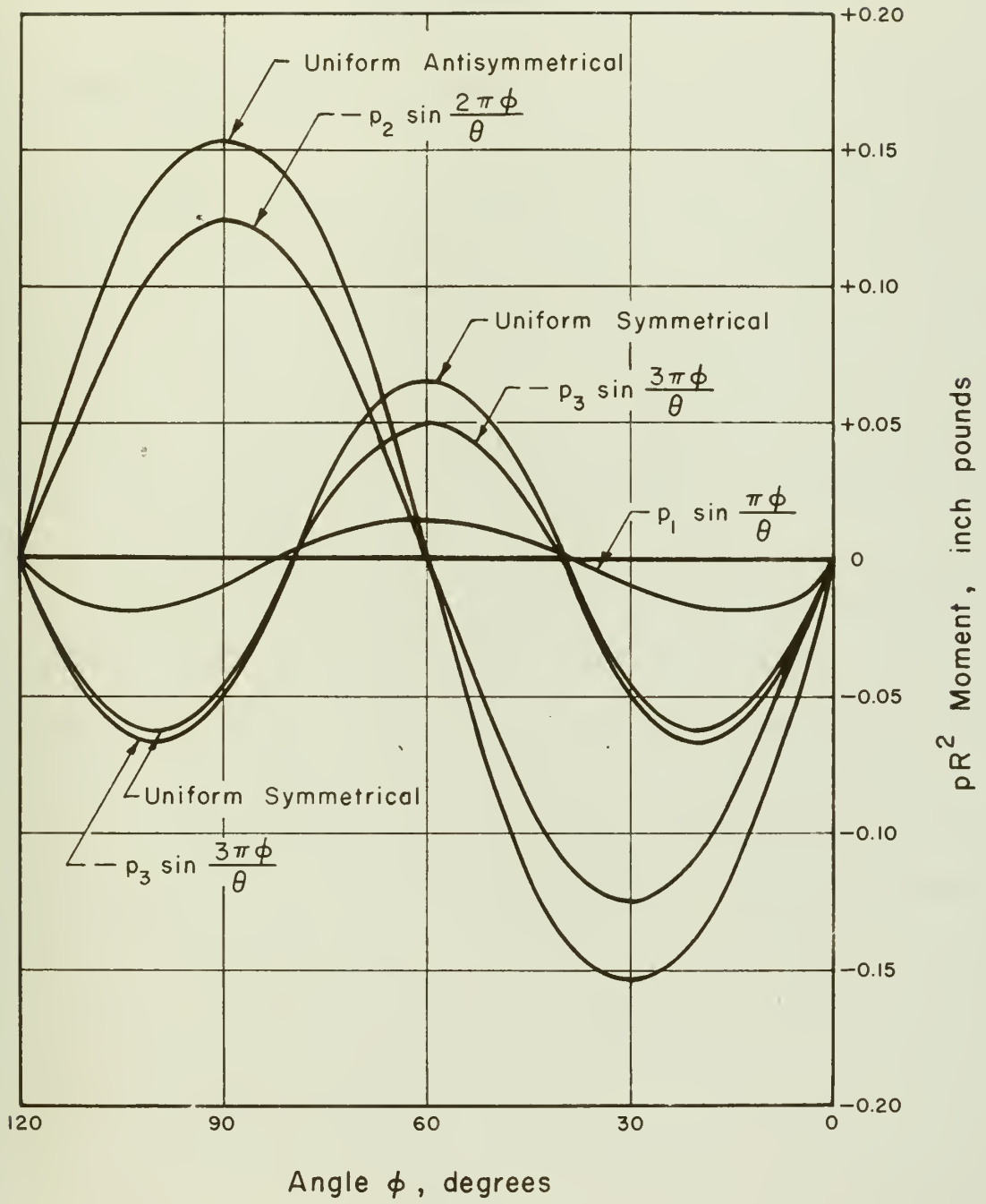

Figure 3.4 Moment vs Angle φ for 120 Degree Central Angle Two-Hinged Arch

CHAPTER IV

BLAST PRESSURE LOADING

4.1 Pressure-Time Relations at a Point

As stated in the general discussion of the variables, Section 2.1, the blast pressure acting on the surface of the ground above the point of interest causes a vertical pressure at that point. Accompanying this vertical pressure is a horizontal pressure of varying magnitude, depending on the soil. The horizontal pressure may be as low as fifteen percent in loose, dry soil, fifty percent in moist soil, and one hundred percent in saturated soil, Reference (1). One of the purposes of this thesis is to study the effects of this variation.

The vertical pressure is propagated downward with a velocity equal to the seismic velocity of the soil. At the point of interest, the time for the pressure to increase to a maximum is a function of the vertical transit line. The effect of varying the rise time will be studied.

It has been shown in Section 3.1 that the horizontal pressure may be expressed in terms of the vertical pressure. Vertical pressure-time relations at a point on the arch in terms of surface pressure are therefore required to define the total radial load profile $p_r(\varphi,t)$ acting on the arch. The equations below are derived from the geometry of Figure 4.1.

The velocity of the wave propagation is:

$$v = \frac{C_s U}{\sqrt{C_s^2 + U^2}} \qquad (14)$$

where v = velocity of propagation of the earth pressure wave

C_s = seismic velocity of the soil

U = surface blast wave velocity

The time required for the pressure wave to arrive at any point φ on the arch rib is:

$$t_a = \frac{R - R \sin(\varphi - \beta)}{v} \tag{15}$$

where φ = angle locating a point on the arch rib

R = radius of the arch

t_a = time measured after initial contact of the pressure wave with the arch rib

β = $\arctan \frac{C_s}{U}$

The time required for the pressure at φ to rise to its peak is:

$$t_r = \frac{R - R \sin\varphi + H_c}{C_s} \quad , \quad \text{for } t_r = t_t \tag{16}$$

$$t_r = \frac{R - R \sin\varphi + H_c}{2C_s} \quad , \quad \text{for } t_r = \tfrac{1}{2} t_t$$

where H_c = depth of cover on the crown

t_r = rise time of the pressure

t_t = vertical transit time of the pressure wave to φ

$$t_t = \frac{R - R \sin\varphi + H_c}{C_s}$$

The vertical pressure-time variation at a point on the arch rib is shown qualitatively in Figure 2.2. The pressure-time diagram is assumed to be a straight line in the rise part of the diagram and to have an exponential decay rate after reaching its peak value P_m. The total impulse of the force pulse at any point must be the same as the total impulse of the surface force pulse. This means that as the rise time increases, the decay rate must also increase in order to maintain the same impulse in

the force pulse. It is assumed in this study that the decay rate at the shallow points in the soil considered in this thesis is the same as the decay rate of the surface force pulse. This is a reasonable assumption since the maximum unsymmetrical loading occurs within the first few milliseconds after the blast wave begins to act on the arch.

The decay rate for a side-on overpressure P_m having a positive phase duration t_d may be obtained from Reference (6). The decay rates for the two overpressure levels studied in this thesis are shown in Figure 4.2. For the 100 psi overpressure, t_d is assumed to be 1500 milliseconds, while for 200 psi overpressure, t_d is assumed to be 1640 milliseconds. The weapon yield is 1 MT.

The complete vertical pressure-time diagram for any point can be determined only by numerical evaluation of the pressure on that point at various times. A sample calculation of a pressure-time diagram follows.

Assume that a 180 degree central angle arch with a radius of twelve and one-half feet is subjected to a 200 psi overpressure blast wave originating from a 1 MT weapon. The duration of the positive phase of the loading is 1640 milliseconds. The arch is buried in soil having a seismic velocity of 1000 fps, with zero depth of cover on the crown. The time of rise of the earth pressure at a point in the soil is assumed to equal the vertical transit time of the earth pressure wave. The ratio of the horizontal to vertical pressure is assumed to be 0.25.

Reference (7) gives the following equation for the shock velocity U of the surface blast wave:

$$U = c_o(1 + 6p/7P_o)^{\frac{1}{2}}$$

where c_o = ambient sound velocity ahead of the shock

p = peak overpressure behind the shock

P_o = ambient pressure ahead of the shock

$\therefore U = 1130\,(1 + 1200/103)^{\frac{1}{2}} = 4023$ fps

By Equation (14), $v = \dfrac{UC_s}{\sqrt{C_s^2 + U^2}} = \dfrac{1000 \times 4023}{\sqrt{1000^2 \times 4023^2}} = 972$ fps

By Equation (15), $\beta = \arctan(1000/4023) = 13^\circ 58'$

$$t_a = \frac{12.5}{972}\,[1 - \sin(\varphi - 13^\circ 58')]\text{, seconds}$$

$$= 12.86\,[1 - \sin(\varphi - 13^\circ 58']\text{, milliseconds}$$

By Equation (16) $t_r = \dfrac{12.5}{1000}\,(1 - \sin\varphi)$, seconds

$$= 12.5\,(1 - \sin\varphi)\text{, milliseconds}$$

Let $\varphi = 40^\circ$. Then

$$t_a = 12.86\,[1 - \sin(40^\circ - 13^\circ 58')] = 7.2 \text{ ms}$$

$$t_r = 12.5\,(1 - \sin 40^\circ) = 4.5 \text{ ms}$$

Therefore at $\varphi = 40$ degrees, the earth pressure wave arrives 7.2 ms after the wave initially contacts the arch rib at $\varphi = 90^\circ + 13^\circ 58'$. The vertical pressure rises at a rate of 200/4.5 = 45 psi per ms. At 8 ms, the pressure is (8 - 7.2)45 = 36 psi. At 10 ms, the pressure is (10 - 7.2)45 = 126 psi. At 11.7 ms, the pressure reaches a maximum value equal to the surface overpressure, or 200 psi. Thereafter the pressure decays at a rate assumed to be equal to the decay rate for the surface overpressure as shown in Figure 4.2. Inspection of Figure 4.2 shows that the decay may be represented accurately by a straight line down to a value of $\Delta P/\Delta P_m = 0.65$ and $\Delta t/t_d = \sim 0.02$. The pressure decrement is then

0.35(200) = 70 psi, and the time interval is 0.02(1640) = ~ 35ms. So the pressure decays at a rate of 70/35 = 2 psi per ms. Therefore at 12 ms, the pressure is 200 - 2(12 - 11.7) = 199 psi. At 14 ms, the pressure is (199 - 4) = 195 psi. This procedure is continued until a time greater than (35 + 11) ms is reached. Then the time interval is expressed as a fraction of t_d and $\Delta P/\Delta P_m$ is read from Figure 4.2. The complete pressure-time relation for φ = 40 degrees is recorded in Appendix B, Table B5.

To obtain the complete vertical pressure-time relations for the entire arch, the above procedure is accomplished for every ten degrees on the arch. Table B5, Appendix B, shows the vertical pressure-time variation for the entire arch up to 200 milliseconds. The unsymmetrical loading is readily seen. For example, at ten milliseconds the windward side of the arch has pressure acting on its entirety, whereas the leeward side is not fully loaded until after sixteen milliseconds. The unsymmetrical loading shifts from the windward side to the leeward side during the time the blast pressure acts. This effect may be seen at thirty milliseconds. The pressure on the windward side, φ greater than ninety degrees, averages some eight pounds less than the pressure on the leeward side. The effect of the decay rate may be seen by comparing the pressure at the crown with that at the abutments. For example, at twenty-four milliseconds the pressure at the crown has reached its maximum and decayed to approximately seventy-five percent of the maximum surface pressure, while the pressure at the abutment is approximately equal to the maximum surface pressure.

4.2. Harmonic Analysis of Radial Blast Load with Time a Constant

Based on the vertical pressures tabulated in Table B5, a radial load profile $p_r(\varphi,t)$ can be determined for any instant of time given in

that table. After $p_r(\varphi,t)$ has been defined, the distributed load $\sum p_n(t) \sin \frac{n\pi\varphi}{\theta}$ can be evaluated. A sample calculation, for t = 10 milliseconds, is given in Tables V and VI.

In Table V, the data in column "$p_v(t)$" is obtained from Table B5, while that in column "p_r coefficient" is derived from Table I for p_h/p_v = 0.25. The data in column "$p_r(\varphi,t)$" of Table V is derived by multiplying $p_v(t)$ by the p_r coefficient. The resulting radial pressure load profile $p_r(\varphi,t)$ is shown graphically in Figure 4.3. The coefficients $p_n(t)$ of Equation (9) are determined by numerical integration. This is done by multiplying the load ordinate at each ten degree interval by $\frac{\pi R}{18} \sin \frac{n\pi\varphi}{\theta}$, adding the results and multiplying the sum by $\frac{2}{\theta R}$. The resulting distributed radial loading $\sum p_n(t) \sin \frac{n\pi\varphi}{\theta}$, with t = 10 milliseconds, is shown as a dotted line in Figure 4.3.

Table VI contains the harmonic analysis of the same blast wave acting on a 150 inch radius arch with a central angle of 120 degrees. The radial pressure $p_r(\varphi,t)$ in Table V from 30 degrees through 150 degrees is used in Table VI from 0 degrees through 120 degrees. The resulting distributed radial loading $\sum p_n(t) \sin \frac{n\pi\varphi}{\theta}$ is shown in Figure 4.3.

Inspection of the data in column "$p_r(\varphi,t)$", Table VI, reveals that there is a radial pressure of ten or more pounds acting at all points on the arch rib. Therefore, a uniform all-around pressure of ten pounds may be subtracted from the radial pressure before the harmonic analysis is made, since it is desired to resolve harmonically only the radial pressure causing flexure in the arch rib. The column "p_r adjusted" contains the remaining radial pressure.

The coefficients $p_n(t)$ of Equation (9) are found by numerical integration. This is done by multiplying the load ordinate at each ten degree interval by $\frac{\pi R}{18} \sin \frac{n\pi\varphi}{\theta}$, adding the results, and multiplying by $\frac{2}{\theta R}$.

The resulting distributed load, $p_u(t) + \sum p_n(t) \sin \frac{n\pi\varphi}{\theta}$, with t = 10 milliseconds, is shown as a dotted line in Figure 4.3.

It is assumed that the first three terms of the series $\sum p_n \sin \frac{n\pi\varphi}{\theta}$ adequately represent the loading on the arch for the purposes of this thesis.

The radial load on the 180 degree arch at a time t = 10 milliseconds is:

$$p_r(\varphi,t) = 166 \sin\varphi - 13 \sin 2\varphi - 26 \sin 3\varphi$$

Since the time is constant, the load may be considered to be a static load. An analogous load may be determined which will have the same effect on a given point of the arch. Let the point be located at φ = 45 degrees. Inspection of Figure 3.3 shows that the components $\sum p_n \sin \frac{n\pi\varphi}{\theta}$ all cause negative moment at this point. Using the coefficients in Table IV, the moment of the load is

$$M = [166(-0.02262) + 13(-0.33333) + 26(-0.08837)]\, R^2$$
$$= [-3.75 - 4.33 - 2.30]\, R^2 = -10.38R^2$$

A uniformly distributed antisymmetrical load acting in on the windward half of the arch and out on the leeward half produces a moment of $0.41422p_aR^2$ at φ = 45 degrees. Therefore

$$p_a = \frac{10.38R^2}{0.41422R^2} = 25 \text{ psi for a time t = 10 ms}$$

However, the actual load on the arch is time-dependent and consequently p_a must be a time-dependent load, $p_a(t)$. To define the pressure-time diagram for $p_a(t)$, the load $p_r(\varphi,t)$ on the arch is harmonically analyzed at various times.

The analogous load for the crown may be found in a similar manner. The moment caused by the above load at the crown is

$$M = [166(0.03540) + 26(0.125)]\, R^2$$
$$= 9.13\, R^2 \text{ inch pounds}$$

A symmetrical load p_s acting in compression on the central third of the arch and in tension on the outer thirds of the arch produces a moment of $0.1547\, p_s R^2$ at the crown

$$\therefore p_s(t) = \frac{9.13R^2}{0.1547R^2} = 59 \text{ psi}, \quad t = 10 \text{ ms}$$

4.3 Blast Loading Approximations

Appendix B contains the results of numerous harmonic analyses of the blast load on an arch arising from a 1 MT nuclear weapon. The analyses were made and analogous loads found as described in the preceding section. These analyses were made in order to determine the effects of the variables discussed in Chapter II on the loading the arch receives, and to provide a basis for idealizing the blast load on the structure without the necessity for actually harmonically analyzing the blast load.

The blast load must be defined in relation to the effect being studied. In this thesis, the effect studied is the deflection of the arch due to flexural stresses, the area of primary interest being the haunch of the arch. The effect of the unsymmetrical blast load on the haunch of the arch is most conveniently related to an analogous uniformly-distributed load which acts inwardly on one half of the arch and outwardly on the other half. The effect of the blast load on the crown is conveniently related to a uniform load acting in compression on the central third of the arch and in tension on the outer thirds. Values of such loads for various assumed conditions are shown in Tables B11 and B12.

After the blast load has been related to the specific effect being studied, a load-time curve must be established to show the variation of the load with time. It will be noted in Tables B11 and B12 that the analogous loads are for a specified time only, and that they vary appreciably with time. Appendix B contains a few typical analogous load-time curves. Similar plots were made of all analogous loads.

Study of these load-time curves revealed that the peak values of the analogous loads are some fairly uniform function of the maximum surface overpressure P_m for all assumed values of the variables. In addition, the shapes of these load-time curves are approximately initially peaked triangular load pulses, which decay rapidly to a relatively small value and then continue to decay at a much slower rate. The duration of the rapid decay phase of the loading corresponds approximately to the time required for the pressure to engulf the arch. The duration of the slow decay phase of the loading is relatively much longer.

The peak values of the analogous loads found in Appendix B are shown in Table VII and plotted in Figures 4.4 and 4.5. The data in Appendix B and Figures 4.4 and 4.5 may be qualitatively summarized as follows:

(a) For any given overpressure, the peak value of the analogous load for the haunch increases as the value of the seismic velocity of the soil increases. This is explained by the fact that a higher seismic velocity allows the pressure to penetrate the soil to a greater extent and thus a larger segment of the arch on the windward side is loaded before the leeward side is loaded.

(b) For any given overpressure, the peak value of the analogous load for the crown decreases as the seismic velocity of the soil increases. This is explained by considering the effect of the load profile $p_r(\varphi,t)$ on the integral $\int_{\varphi_1}^{\varphi_2} p_r(\varphi,t) \sin \frac{n\pi\varphi}{\theta} Rd\varphi$. When C_s has a relatively high value in comparison with U, a greater portion of the segment from φ_1 to φ_2 is located on the windward side of the arch and the values of the sine function of the angle φ are both positive and negative. When C_s has a lower value in comparison with U, the load profile $p_r(\varphi,t)$ is located more nearly in the central third of the arch, where the value of the sine function of the angle φ is negative. This increases the numerical value of the analogous crown load.

(c) The higher ratios of p_h/p_v increase the peak value of the analogous load for the haunch. This is explained by the fact that the area of the total radial load profile $p_r(\varphi,t)$ is greater for the higher ratios, and thus the total unsymmetrical load is greater.

(d) The p_h/p_v ratio has little effect on the peak value of the analogous crown load. The peak value of the crown load is primarily a function of the location of the load, i.e., the central third of the arch. In this area, the value of the coefficient for determining the resultant of the horizontal and vertical forces is approximately one for all values of p_h/p_v. Consequently, changing the ratio has little effect on the radial load.

(e) The assumed rise time has relatively little effect on the peak value of the analogous loads. The peak values of both loads are reached very early in the loading of the arch when the pressure wave has not penetrated the soil to any extent. For shallow depths, the rise time is practically equal to the rise time of the surface pressure, which is assumed to be instantaneous.

(f) Although the higher ratios of p_h/p_v cause a higher peak value of the analogous haunch load, they actually cause a less severe dynamic load effect. If the ratio is high, the pressure, after the pressure wave has engulfed the arch, is more nearly a uniform compression, causing less flexural action in the arch. On the other hand, if the ratio is low, the uniformity of the compression is reduced, increasing the flexural action in the arch. For the higher ratios of p_h/p_v it is found that the analogous loads change direction, thereby creating a negative phase of loading. The peak value of the pressure in this negative phase is small, but could possibly cause an outward movement of the crown of the arch since it has a relatively long duration.

4.3.1 180 Degree Arches

Since the blast loading may act over all, or over part, of the arch segment, one approximation to the peak analogous loads may be obtained by considering the blast loading acting on the arch in such a way that the maximum value is given to each component of loading in the series

$\sum p_n(t) \sin \frac{n\pi\varphi}{\theta}$. The ratio of the horizontal pressure to the vertical pressure which causes the most severe dynamic loading is 0.25, therefore this value is used in the following derivations. The effect of the rise time of the pressure and the time of arrival of the pressure wave is not considered. The vertical pressure at all points on the arch is assumed to be equal to P_m. The unit radial pressure at any point is, by Equation (3),

$$p_r(\varphi,t) = (0.25 + 0.75 \sin^2\varphi)\, P_m$$

Using Equation (9),

$$p_n(t) = \frac{2}{\theta R} \int p_r(\varphi,t) \sin \frac{n\pi\varphi}{\theta} R d\varphi$$

$$\text{maximum} \quad p_1(t) = \frac{2P_m}{\pi R}\int_0^{\pi} (0.25 + 0.75 \sin^2\varphi) \sin\varphi \, R d\varphi = 0.955\, P_m$$

$$\text{maximum} \quad p_2(t) = \frac{2P_m}{\pi R}\int_{\frac{\pi}{2}}^{\pi} (0.25 + 0.75 \sin^2\varphi) \sin 2\varphi \, R d\varphi = -0.398\, P_m$$

$$\text{maximum} \quad p_3(t) = \frac{2P_m}{\pi R}\int_{\frac{\pi}{3}}^{\frac{2\pi}{3}} (0.25 + 0.75 \sin^2\varphi) \sin 3\varphi \, r d\varphi = -0.408\, P_m$$

The maximum effect of the blast loading which may occur, under an assumed ratio of $p_h/p_v = 0.25$, can never exceed the effect of the sum of maximum values of the harmonic components found in this manner. The value of the individual maximum values found, and the effect of the sum, are always reduced when the seismic velocity of the soil, the shock velocity of the surface blast wave, and the pressure-time relationships are considered.

If these components acted statically and separately, they would produce the following moments at the leeward haunch and crown:

$$M = -\left[0.023(0.955P_m)R^2 + 0.333(0.398P_m)R^2 + 0.088(0.408P_m)R^2\right]$$

$$= -0.190\ P_m R^2$$

$$M_c = 0.035(0.955P_m)R^2 + 0.125(0.408P_m)R^2 = 0.085\ P_m R^2$$

The peak value of the analogous haunch load is

$$p_a(t) = \frac{0.190\ P_m R^2}{0.414\ R^2} = 0.46\ P_m$$

The peak value of the analogous crown load is

$$p_s(t) = \frac{0.084\ P_m R^2}{0.1547} = 0.54\ P_m$$

These values of the analogous loads can never occur, and, for want of a better name, they are designated as the maximax analogous loads. They are shown in Figure 4.4 so that they may be compared with the analogous loads found by actual harmonic analysis. Such comparisons indicates that these approximations are conservative. The following reductions are arbitrarily made:

$$\text{Maximum } p_a(t) = 0.37\ P_m \tag{17}$$

$$\text{Maximum } p_s(t) = 0.45\ P_m \tag{18}$$

Equations (17) and (18) are plotted in Figure 4.4.

To obtain an idea of the magnitude of these analogous loads, they may be related to a uniformly distributed load acting on a simply supported beam. Inspection of Figure 3.3 shows that the moment caused by the analogous load p_a on the haunch of the arch is very similar to the simple beam moment. The moment at 45 degrees caused by the analogous load is

$$M = 0.37(0.41422)\ P_m R^2$$

Assume that the simple beam has a length equal to the length of half the arch, or $L = \frac{\pi R}{2}$. The moment is $wL^2/8$. Equating this to the moment in the arch, it is found that:

$$w = \frac{8 \times 9.37 \times 0.41433\ P_m R^2}{\left(\frac{\pi R}{2}\right)^2}$$

$$= 0.5\ P_m$$

A similar analogy may be drawn for the analogous load acting on the crown, with the exception that the length of the simple beam is now one-third the length of the arch, or $\frac{\pi R}{3}$. The moment in the arch at 90 degrees due to the analogous load is

$$M = 0.45(0.1547)\ P_m R^2$$

and

$$w = \frac{8M}{L^2} = \frac{8 \times 0.45 \times (0.1547)\ P_m R^2}{\left(\frac{\pi R}{3}\right)^2}$$

$$= 0.5\ P_m$$

The above maximax loads occur within approximately two to four milliseconds after the loading begins to act on the arch. This fact is evident by inspection of the data in Appendix B. These loads decrease rapidly since $p_2(t)$ becomes practically zero when the pressure wave has engulfed the arch, and $p_3(t)$ also decreases. However, $p_1(t)$ and $p_3(t)$ are still acting. It is now assumed that the pressure has completely engulfed the arch. Since the pressure has engulfed the arch, the all-around uniform pressure may be subtracted from the expression for $p_r(\varphi,t)$. Then

$$p_r(\varphi,t) = 0.75 \sin^2\varphi\ P_m$$

This radial pressure may be resolved into harmonic components. It is found that

$$p_1(t) = \frac{2P_m}{\pi R} \int_o^{\pi} (0.75 \sin^2\varphi) \sin\varphi \, R d\varphi = 0.637 \, P_m$$

$$p_3(t) = \frac{2P_m}{\pi R} \int_o^{\pi} (0.75 \sin^2\varphi) \sin 3\varphi \, R d\varphi = -0.127 \, P_m$$

The moment in the haunch at 45 degrees caused by these two components is

$$M_h = -\left[0.023(0.637P_m)R^2 + 0.088(0.127P_m)R^2\right] = -0.026 \, P_m R^2$$

The haunch analogous load is

$$p_a(t) = \frac{0.026P_m R^2}{0.414} = 0.06 \, P_m \qquad (19)$$

The components $p_1(t)$ and $p_3(t)$ act for the total duration of the surface blast pressure. Reference (2) states that the duration of the positive phase of the side-on overpressure may be considered as

$$t_i = 0.40 \left(\frac{100}{p_m}\right)^{2/3} W^{1/3} \qquad (20)$$

where W = weapon size in MT

t_i = the effective duration in seconds of a triangular pulse having the same impulse as the actual shock.

The total duration of $p_1(t)$ and $p_3(t)$ is considered to be t_i.

The time required for $p_2(t)$ to become practically zero is found by using Equations (15) and (16), with the angle $\varphi = 0$.

This time is defined as:

$$t_d' = t_a + t_r = \text{duration of initial triangular impulse}$$

$$= \frac{R + R \sin\beta}{\dfrac{C_s U}{\sqrt{C_s^2 + U^2}}} + \frac{R}{2C_s} \quad , \text{ with } t_r = \tfrac{1}{2} t_t$$

The time t_d' defines t for the load $p_a(t) = 0.06\, p_m$

4.3.2 120 Degree Arches

Approximations of the blast load acting on a 120 degree arch may be derived in the same manner as that used in finding the approximations for the 180 degree arch, as described in Section 4.3.1. It is necessary to modify Equation (3) by substituting $(\varphi + 30)$ for φ, since in Equation (3) φ is measured from a horizontal radial line joining the arch abutment with the center of the circular segment. Equation (3) becomes

$$p_r(\varphi, t) = [0.25 + 0.75 \sin^2(\varphi + 30)]\, P_m$$

$$= \left[\frac{1}{4} + \frac{9}{16}\sin^2\varphi + \frac{3\sqrt{3}}{8}\sin\varphi\cos\varphi + \frac{3}{16}\cos^2\varphi\right] P_m$$

$$\text{Let } p_n(t) = \frac{2}{\theta R}\int p_r(\varphi, t) \sin\frac{n\pi\varphi}{\theta}\, R d\varphi$$

Then the maximum possible values of $p_n(t)$ are

$$\text{Maximum } p_1(t) = \frac{2P_m}{\frac{2}{3}\pi R}\int_0^{\frac{2\pi}{3}} \left(\frac{1}{4} + \frac{9}{16}\sin^2\varphi + \frac{3\sqrt{3}}{8}\sin\varphi\cos\varphi + \frac{3}{16}\cos^2\varphi\right) \sin\frac{3}{2}\varphi\, R d\varphi$$

$$= 1.103\, P_m$$

$$\text{Maximum } p_2(t) = \frac{2P_m}{\frac{2}{3}\pi R} \int_{\frac{\pi}{3}}^{\frac{2\pi}{3}} \left(\frac{1}{4} + \frac{9}{16}\sin^2\varphi + \frac{3\sqrt{3}}{8}\sin\varphi\cos\varphi + \frac{3}{16}\cos^2\varphi \right) \sin 3\varphi \, R d\varphi$$

$$= -0.505\, P_m$$

$$\text{Maximum } p_3(t) = \frac{2P_m}{\frac{2}{3}\pi R} \int_{\frac{2\pi}{9}}^{\frac{4\pi}{9}} \left(\frac{1}{4} + \frac{9}{16}\sin^2\varphi + \frac{3\sqrt{3}}{8}\sin\varphi\cos\varphi + \frac{3}{16}\cos^2\varphi \right) \sin\frac{9}{2}\varphi \, R d\varphi$$

$$= -0.417\, P_m$$

The harmonic components $p_n(t) \sin \frac{n\pi\varphi}{\theta}$ would produce moment at the haunch and crown as shown below, if the blast load is considered to act statically. The moment coefficients are obtained from Table IV, for $\varphi = 30$ and 60 degrees.

$$M_h = -\left[0.009(1.103P_m)R^2 + 0.125(0.505P_m)R^2 + 0.050(0.417P_m)R^2\right]$$

$$= -0.094\, P_m R^2$$

$$M_c = 0.014(1.103P_m)R^2 + 0.051(0.417P_m)R^2$$

$$= 0.037\, P_m R^2$$

Using the moment coefficient for $\varphi = 30$ and 60 degrees in Table IV, the analogous loads are found to be

$$\text{Maximum } p_a(t) = \frac{0.094\, P_m R^2}{0.1547R^2}$$

$$= 0.61\, P_m$$

$$\text{Maximum } p_s(t) = \frac{0.037\ P_m R^2}{0.06556 R^2}$$

$$= 0.56\ P_m$$

These values are plotted in Figure 4.5 so that they may be compared with the actual analogous loads found by harmonic analysis, as given in Appendix B. Since they are conservative, the following arbitrary reductions are made:

$$\text{Maximum } p_a(t) = 0.45\ P_m \tag{21}$$

$$\text{Maximum } p_s(t) = 0.41\ P_m \tag{22}$$

These equations are plotted in Figure 4.5.

These loads may be related to a simple beam load of $0.5\ P_m$ by the same method as that described in section 4.3.1 for a 180 degree arch.

After the pressure wave has engulfed the arch, there is a uniform all-around pressure acting which must be subtracted from the radial pressure in order to determine the loading which causes flexural action. This uniform pressure is

$$p_u = (0.25 + 0.75 \sin^2 30)\ P_m = \frac{7}{16} P_m$$

The remaining radial pressure which is to be resolved harmonically is

$$p_r(\varphi) - p_u = \left(\frac{1}{4} + \frac{9}{16} \sin^2\varphi + \frac{3\sqrt{3}}{8} \sin\varphi \cos\varphi + \frac{3}{16} \cos^2\varphi \right) P_m - \frac{7}{16} P_m$$

$$= \left(-\frac{3}{16} + \frac{9}{16} \sin^2\varphi + \frac{3\sqrt{3}}{8} \sin\varphi \cos\varphi + \frac{3}{16} \cos^2\varphi \right) P_m$$

Then

$$p_1(t) = \frac{2P_m}{\frac{2}{3}\pi R} \int_o^{\frac{2\pi}{3}} \left(-\frac{3}{16} + \frac{9}{16}\sin^2\varphi + \frac{3\sqrt{3}}{8}\sin\varphi\cos\varphi + \frac{3}{16}\cos^2\varphi\right) \sin\frac{3}{2}\varphi \, R d\varphi$$

$$= 0.546 \, P_m$$

$$p_3(t) = \frac{2P_m}{\frac{2}{3}\pi R} \int_o^{\frac{2\pi}{3}} \left(-\frac{3}{16} + \frac{9}{16}\sin^2\varphi + \frac{3\sqrt{3}}{8}\sin\varphi\cos\varphi + \frac{3}{16}\cos^2\varphi\right) \sin\frac{9}{2}\varphi \, R d\varphi$$

$$= -0.020 \, P_m$$

These loads would produce the following moment at the haunch and crown of the arch if they acted statically:

$$M_h = -\left[0.009(0.546P_m)R^2 + 0.050(0.020P_m)R^2\right]$$

$$= -0.006 \, P_m R^2$$

$$M_c = 0.014(0.546P_m)R^2 + 0.051(0.020P_m)R^2$$

$$= 0.009 \, P_m R^2$$

The analogous antisymmetrical load for the haunch is

$$p_a(t) = \frac{0.006 \, P_m R^2}{0.155R^2}$$

$$= 0.04 \, P_m \qquad (23)$$

The analogous load for the crown is

$$p_s(t) = \frac{0.009P_m R^2}{0.06556R^2}$$

$$= 0.14 \, P_m \qquad (24)$$

The time t that defines the analogous loads in Equations (23) and (24) is the time required for the pressure wave to engulf the arch and rise to its maximum value at the abutments. This time is expressed by Equations (15) and (16). The angle φ in both of these equations is thirty degrees.

4.3.3 Summary

The blast load acting on the arch may be defined by numerically evaluating at specific times the coefficient $p_n(t)$ for the distributed load $\sum p_n(t) \sin \frac{n\pi\varphi}{\theta}$. The load-time curve for the analogous loads is obtained by equating the static effects of the distributed load $\sum p_n(t) \sin \frac{n\pi\varphi}{\theta}$ to those of the analogous loads. This is the procedure employed in Appendix B. The procedure is extremely tedious, and, in fact, unnecessary, since the blast load is not accurately known. Therefore, a more convenient method such as that established in Subsections 4.3.1 and 4.3.2 is desirable.

In these subsections, the blast load acting on the arch has been idealized to two initially peaked triangular force pulses. For investigating the effect of the blast load on the haunch of a 180 degree arch, the peak value of the first pulse is $0.37P_m$, and the peak value of the second pulse is $0.06P_m$. For similar investigation of a 120 degree arch the peak value of the first pulse is $0.45\ P_m$, whereas the peak value of the second pulse is $0.04\ P_m$. In each instance the duration of the first pulse is the time required for the pressure wave to engulf the arch, and the duration of the second pulse is equal to the effective duration of the blast loading.

TABLE V

HARMONIC ANALYSIS OF BLAST LOADING ON 180° ARCH
($p_v(t)$ obtained from Table B5, Appendix B, for t = 10 ms)

φ	$p_v(t)$	p_r coef.	$p_r(\varphi,t)$	sin φ	$p_r(\varphi,t)$ sin φ	sin 2φ	$p_r(\varphi,t)$ sin 2φ	sin 3φ	$p_r(\varphi,t)$ sin 3φ	$p_1(t)$ sin φ	$p_2(t)$ sin2φ	$p_3(t)$ sin3φ	$\sum p_n(t)$ sin $n\varphi$
0	0	0.250	0	0	0	0	0	0	0	0	0	0	0
10	0	0.273	0	0.174	0	0.342	0	0.500	0	29	-4	-13	12
20	0	0.338	0	0.342	0	0.643	0	0.866	0	57	-8	-22	27
30	22	0.438	10	0.500	5	0.866	9	1.000	10	83	-11	-26	46
40	126	0.560	71	0.643	46	0.985	70	0.866	61	107	-13	-22	72
50	196	0.690	135	0.766	103	0.985	133	0.500	67	127	-13	-13	101
60	191	0.813	155	0.866	134	0.866	134	0	0	144	-11	0	133
70	186	0.913	170	0.940	160	0.643	109	-0.500	-85	156	-8	13	161
80	183	0.978	179	0.985	176	0.342	61	-0.866	-155	164	-4	22	182
90	181	1.000	181	1.000	181	0	0	-1.000	-181	166	0	26	192
100	180	0.978	176	0.985	173	-0.342	-60	-0.866	-152	164	4	22	190
110	182	0.913	166	0.940	156	-0.643	-107	-0.500	-83	156	8	13	177
120	184	0.813	150	0.866	130	-0.866	-130	0	0	144	11	0	155
130	188	0.690	130	0.766	100	-0.985	-128	0.500	65	127	13	-13	127
140	194	0.560	109	0.643	70	-0.985	-107	0.866	94	107	13	-22	98
150	195	0.438	85	0.500	42	-0.866	-74	1.000	85	83	11	-26	68
160	105	0.338	35	0.342	12	-0.643	-23	0.866	30	57	8	-22	43
170	46	0.273	13	0.174	2	-0.342	-4	0.500	7	29	4	-13	20
180	3	0.250	1	0	0	0	0	0	0	0	0	0	0
			SUM		1490		-117		-237				
			SUM x $\frac{1}{9}$		166		-13		-26				

$$p_r(\varphi,t) = p_1(t)\sin\varphi + p_2(t)\sin 2\varphi + p_3(t)\sin 3\varphi$$

$$\therefore p_r(\varphi,t) = 166\sin\varphi - 13\sin 2\varphi - 26\sin 3\varphi \text{ , with } t = 10 \text{ ms}$$

TABLE VI

HARMONIC ANALYSIS OF BLAST LOADING ON 120° ARCH

($p_r(\varphi,t)$ obtained from Table III)

φ	$p_r(\varphi,t)$	Adj. $p_r(\varphi,t)$	$\sin\frac{3}{2}\varphi$	$p_r(\varphi,t)$ $\sin\frac{3}{2}\varphi$	$\sin 3\varphi$	$p_r(\varphi,t)$ $\sin 3\varphi$	$\sin\frac{9}{2}\varphi$	$p_r(\varphi,t)$ $\sin\frac{9}{2}\varphi$	$p_1(t)$ $\sin\frac{3}{2}\varphi$	$p_3(t)$ $\sin\frac{9}{2}\varphi$	Σ $p_u(t) + p_n(t)\sin\frac{n\pi\varphi}{\theta}$
0	10	0	0	0	0	0	0	0	0	0	10
10	71	61	0.259	16	0.500	31	0.707	43	49	18	77
20	135	125	0.500	63	0.866	108	1.000	125	95	25	130
30	155	145	0.707	103	1.000	145	0.707	103	134	18	162
40	170	160	0.866	139	0.866	139	0	0	164	0	174
50	179	169	0.966	163	0.500	85	-0.707	-119	183	-18	175
60	181	171	1.000	171	0	0	-1.000	-171	189	-25	174
70	176	166	0.966	160	-0.500	-83	-0.707	-117	183	-18	175
80	166	156	0.866	135	-0.866	-135	0	0	164	0	174
90	150	140	0.707	99	-1.000	-140	0.707	99	134	18	162
100	130	120	0.500	60	-0.866	-104	1.000	120	95	25	130
110	109	99	0.259	26	-0.500	-48	0.707	70	49	18	77
120	85	74	0	0	0	0	0	0	0	0	10
		SUM		1135		-2		+153			
		SUM x $\frac{1}{6}$		189		0		+25			

$$p_r(\varphi,t) = p_u(t) + p_1(t)\sin\tfrac{3}{2}\varphi + p_2(t)\sin 3\varphi + p_3(t)\sin\tfrac{9}{2}\varphi$$

$$= 10 + 189\sin\tfrac{3}{2}\varphi + 25\sin\tfrac{9}{2}\varphi\ , \qquad \text{with } t = 10 \text{ ms}$$

TABLE VII

PEAK VALUE OF ANALOGOUS LOADS $p_a(t)$ AND $p_s(t)$ FOUND BY HARMONIC ANALYSIS

P_m (psi)	C_s (fps)	180 Degree Arch				120 Degree Arch				Radius (ft)	Ratio t_r/t_t
		$p_h/p_v = 0.25$		$p_h/p_v = 1.00$		$p_h/p_v = 0.25$		$p_h/p_v = 1.00$			
		$p_a(t)$	$p_s(t)$	$p_a(t)$	$p_s(t)$	$p_a(t)$	$p_s(t)$	$p_a(t)$	$p_s(t)$		
100	1000	25	41	32	41	37	37	41	35	12.5	1
200	1000	45	84	55	84	70	76	78	74	12.5	1
100	2000	32	35	43	25	43	28	50	23	12.5	1
200	2000	60	72	76	66	81	58	93	45	12.5	1
200	1000	48	83	58	84	71	70	89	82	25	0.5
200	2000	64	68			85	51			25	0.5

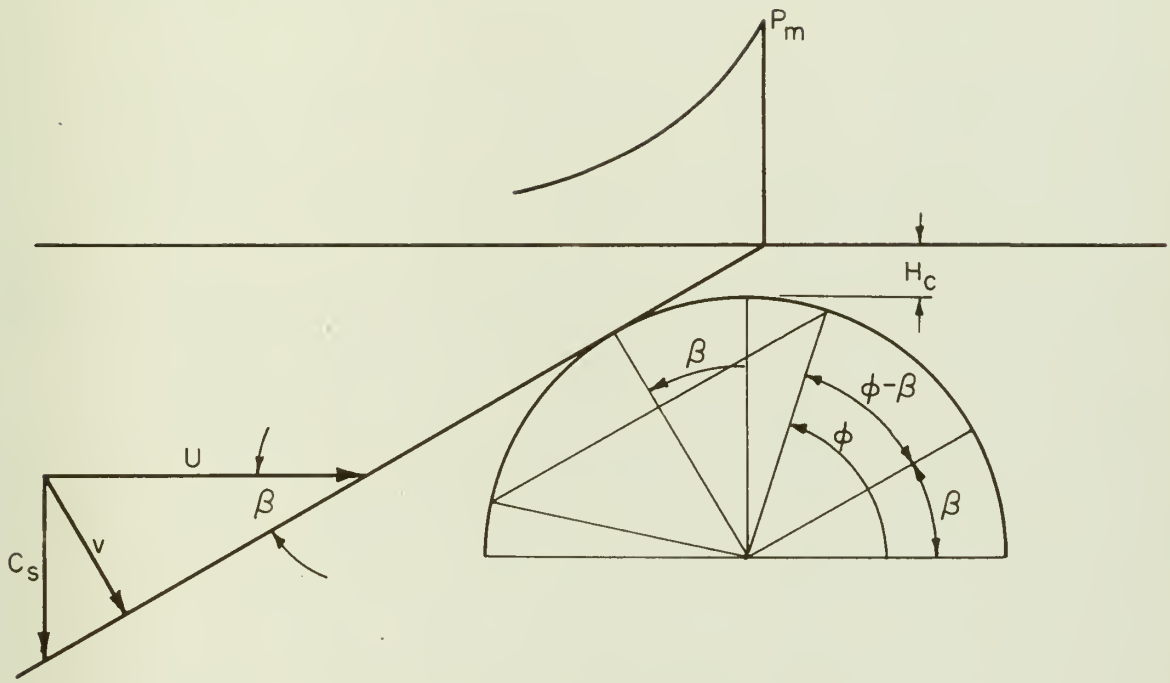

Figure 4.1 Geometry of Blast Loading on a 180 Degree Central Angle Circular Segment Arch

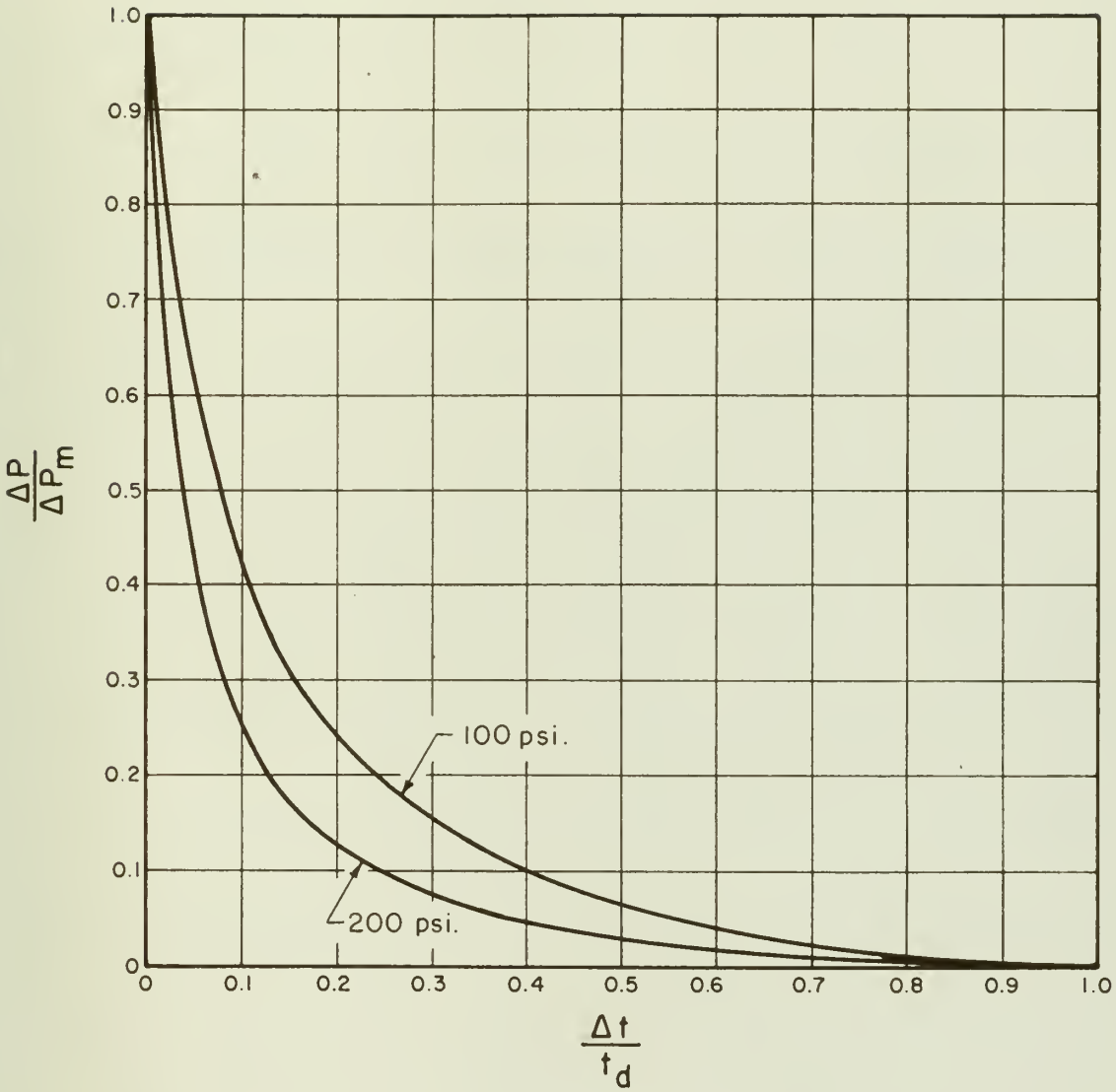

Figure 4.2 Overpressure as a Function of Time

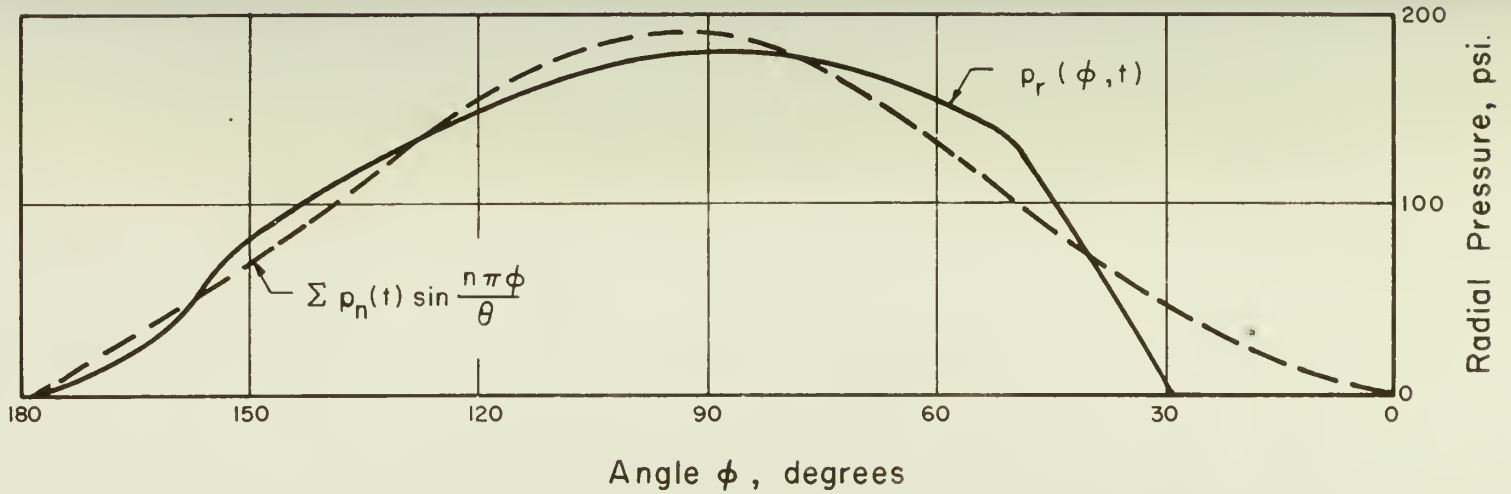

(a) 180 Degree Arch

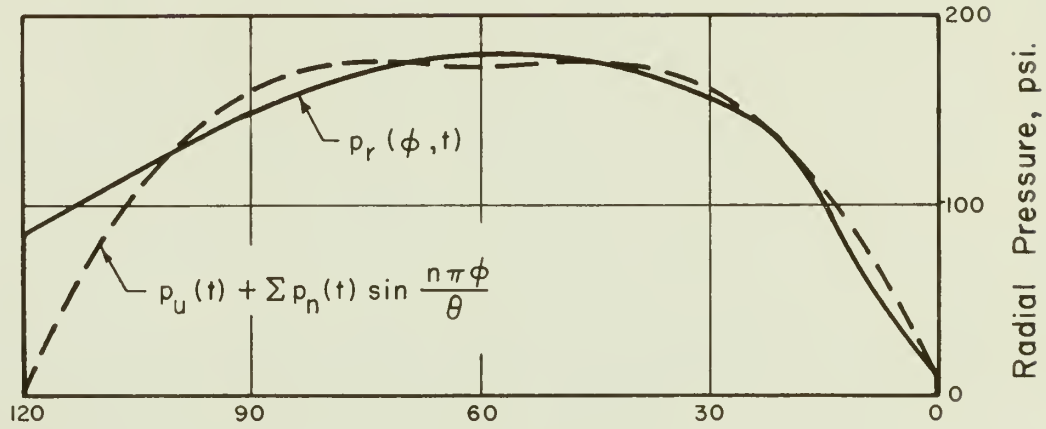

(b) 120 Degree Arch

Figure 4.3 Blast Loading on 180 and 120 Degree Central Angle 150 Inch Radius Arches at Time t = 10 ms

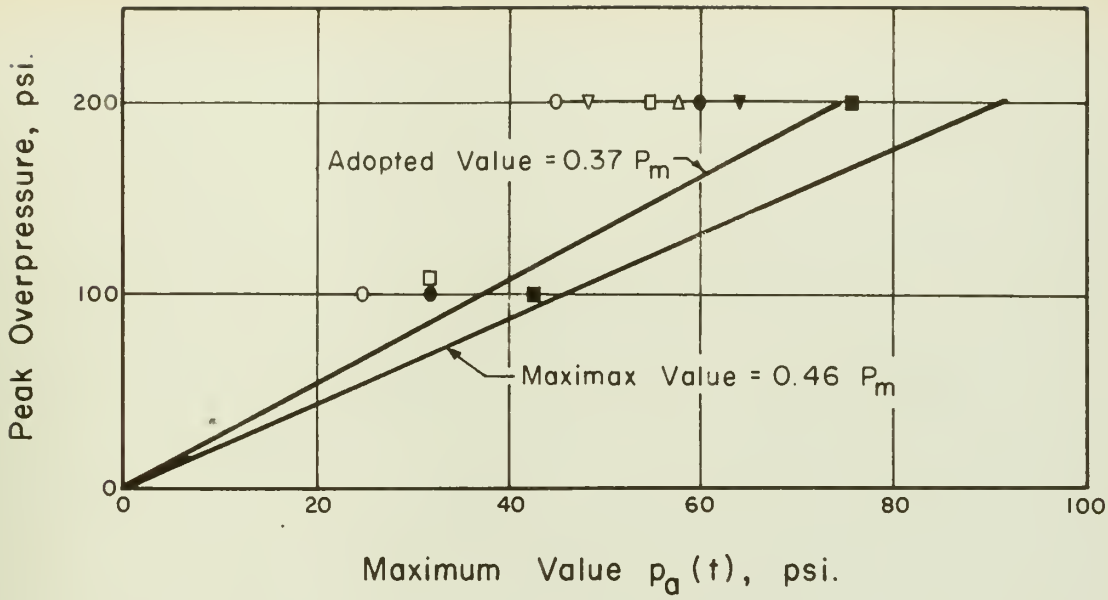

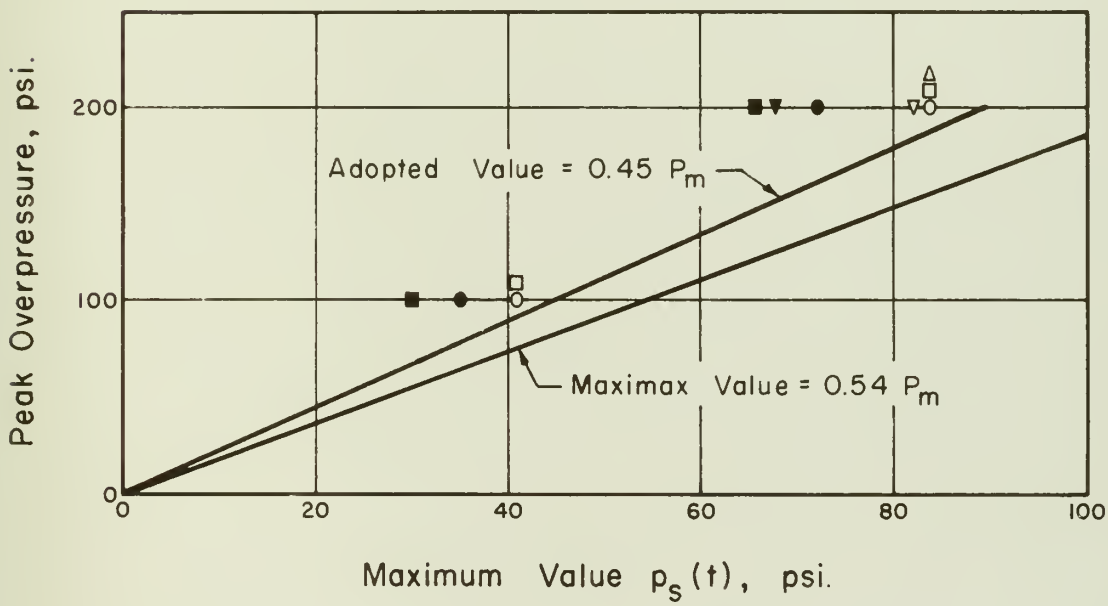

CODE

$C_s = 1000$	$C_s = 2000$	$\frac{p_h}{p_v}$	$\frac{t_r}{t_t}$
○	●	0.25	1.0
□	■	1.00	1.0
▽	▼	0.25	0.5
△		1.00	0.5

Figure 4.4 Peak Values of Analogous Loads: Antisymmetrical $p_a(t)$ and Symmetrical $p_s(t)$ for a 180 Central Angle Arch

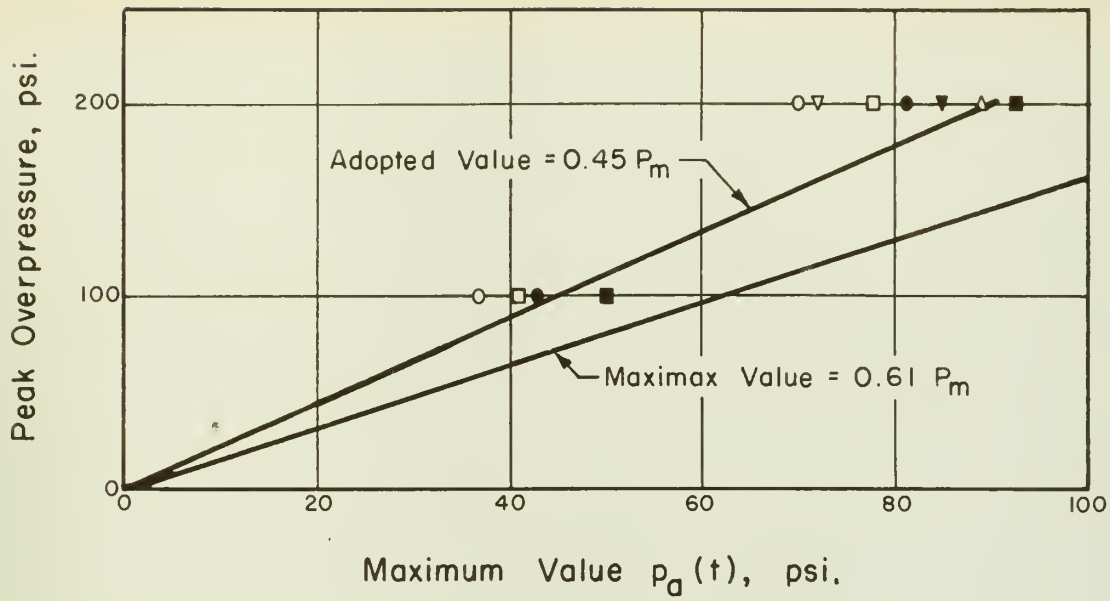

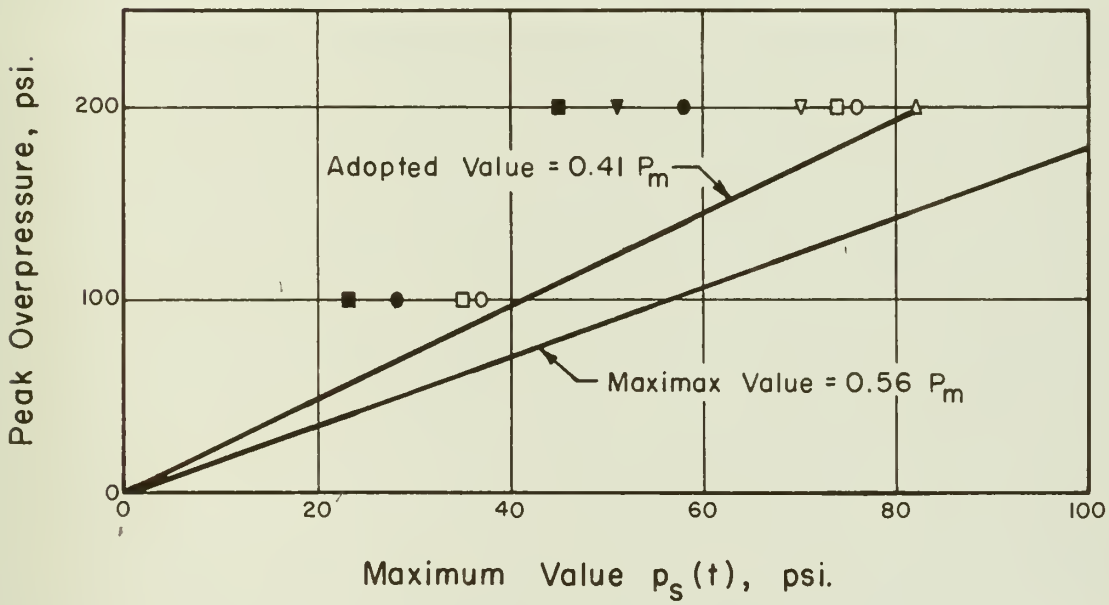

CODE

$C_s = 1000$	$C_s = 2000$	$\frac{p_h}{p_v}$	$\frac{t_r}{t_t}$
○	●	0.25	1.0
□	■	1.00	1.0
▽	▼	0.25	0.5
△		1.00	0.5

Figure 4.5 Peak Values of Analogous Loads: Antisymmetrical $p_a(t)$ and Symmetrical $p_s(t)$ for a 120 Degree Central Angle Arch

CHAPTER V

PASSIVE EARTH PRESSURE LOADING

If there were no soil surrounding the arch, it would deflect into the dotted configuration shown in Figure 5.1 under the unsymmetrical blast loading. However, the soil restricts this deflection by passive earth pressure and the inertia of the soil mass. To evaluate the passive earth pressure, the segment of the arch on the leeward side from the springing line to the crown is assumed to act as a retaining wall. The soil volume and the relative plane of slip are shown in Figure 5.1.

Under actual conditions, the body of soil located on the windward side of the arch would most certainly be affected by the blast pressure and would have to move downward and laterally into the arch to load it. The energy required to accelerate this mass would lower the energy level in the blast pressure. In addition, after the surface pressure wave passes the arch, there would be a vertical pressure of varying intensity acting downward on the soil body on the leeward side of the arch. This would increase the shear strength of the soil, the passive earth pressure, and the inertia force. Evaluation of these later effects would be extremely difficult and is omitted in this study. This results in a conservative approach.

5.1 Unit Passive Earth Pressure

Rankine's formula for the total horizontal passive earth pressure force P_p acting on the vertical plane AV with a height h in Figure 5.1 is

$$P_p = \tfrac{1}{2} w h^2 K$$

where $K = \dfrac{1 + \sin \varphi'}{1 - \sin \varphi'}$, φ' being the angle of internal friction of the soil

and w = unit weight of the soil.

The unit horizontal pressure along the plane AV in Figure 5.1 varies directly as y varies, y being the distance below the ground surface. This pressure then may be expressed as

$$p_p = wyK \tag{25}$$

5.1.1 180 Degree Arches

For a semicircular arch with no cover on the crown and $\varphi' = 30$ degrees, since $y = R(1 - \sin\varphi)$, Equation (25) becomes

$$p_p = wR(1 - \sin\varphi)\frac{1 + 0.5}{1 - 0.5} = 3wR(1 - \sin\varphi) \tag{26}$$

The angle φ is measured from the horizontal radial line which joins the abutment with the center of the circular segment.

In addition to the horizontal passive pressure, it is necessary to consider the weight of the soil above the arch rib. This soil exerts a unit pressure

$$p_v = wR(1 - \sin\varphi) \tag{27}$$

Using Equations (1), (26), and (27), the resultant radial earth pressure is

$$\begin{aligned} p_r(\varphi) &= \tfrac{1}{2}(p_v + p_p) + \tfrac{1}{2}(p_p - p_v)\cos 2\varphi \\ &= \tfrac{1}{2}[wR(1 - \sin\varphi) + 3wR(1 - \sin\varphi)] \\ &\quad + \tfrac{1}{2}[3wR(1 - \sin\varphi) - wR(1 - \sin\varphi)]\cos 2\varphi \\ &= 2wR(1 - \sin\varphi) + wR(1 - \sin\varphi)\cos 2\varphi \end{aligned} \tag{28}$$

In Figure 5.1, the angle β, which defines the inclination of the plane of shear AS with the vertical plane AV, is

$\beta = \frac{1}{2}(90^\circ + \varphi')$, φ' being the angle of internal friction of the soil

$= \frac{1}{2}(90^\circ + 30^\circ) = 60^\circ$ for $\varphi' = 30^\circ$

From the geometry of Figure 5.1, the total weight of the soil associated with the passive earth pressure is

$$W_s = \left[\tfrac{1}{2} R(R \tan 60) + R^2 - \frac{\pi R^2}{4} \right] w = 1.08\ wR^2 \qquad (29)$$

Equation (28) is for an arch with no cover on the crown. If there is a depth of cover H_c on the crown, a uniformly distributed horizontal pressure $3wH_c$, as derived from Equation (25), and a uniformly distributed vertical pressure wH_c, must be added to the radial pressure acting on the arch. For an arch with a central angle of 180 degrees, the resulting radial pressure due to H_c, as obtained by Equation (1), is

$$\begin{aligned} p_r(\varphi) &= \tfrac{1}{2}(p_v + p_p) + \tfrac{1}{2}(p_p - p_v)\cos 2\varphi \\ &= \tfrac{1}{2}(wH_c + 3wH_c) + \tfrac{1}{2}(3wH_c - wH_c)\cos 2\varphi \\ &= 2\ wH_c + wH_c \cos 2\varphi \end{aligned} \qquad (30)$$

The total radial pressure on a 180 degree arch with a depth of cover H_c is found by adding the pressures derived from Equations (28) and (30).

$$\begin{aligned} p_r(\varphi) &= 2wR\ (1 - \sin\varphi) + wR\ (1 - \sin\varphi)\cos 2\varphi \\ &\quad + 2wH_c + wH_c \cos 2\varphi \end{aligned}$$

5.1.2 120 Degree Arches

Equation (28) is valid only for a semi-circular arch with the angle φ measured from the horizontal radial line. For an arch with no cover on the crown and a central angle of 120 degrees, Equation (28) is modified by substituting $(\varphi + 30^\circ)$ for φ. This yields

$$\begin{aligned} p_r(\varphi) &= 2wR\ [1 - \sin(\varphi + 30)] + wR\ [1 - \sin(\varphi + 30)]\cos 2(\varphi + 30) \\ &= wR\ \Big(2 - \frac{3\sqrt{3}}{4}\sin\varphi - \frac{3}{4}\cos\varphi - \frac{1}{2}\cos 3\varphi \\ &\quad - \frac{\sqrt{3}}{2}\sin 2\varphi + \frac{1}{2}\cos 2\varphi \Big) \end{aligned} \qquad (31)$$

If there is a depth of cover H_c on the crown of the 120 degree arch, the resulting radial pressure due solely to H_c is

$$p_r(\varphi) = \tfrac{1}{2}(p_h + p_v) + \tfrac{1}{2}(p_h - p_v)\cos 2\varphi$$

$$= \tfrac{1}{2}(3wH_c + wH_c) + \tfrac{1}{2}(3wH_c - wH_c)\cos 2(\varphi + 30)$$

$$= 2\,wH_c + \tfrac{1}{2}\,wH_c \cos 2\varphi - \frac{\sqrt{3}}{2}\,wH_c \sin 2\varphi \qquad (32)$$

The angle φ is measured from the radial line joining the abutment with the center.

The total unit radial pressure of a 120 degree arch having a depth of cover H_c on the crown is found by adding Equations (31) and (32). The result is

$$p_r(\varphi) = wR\left(2 - \frac{3\sqrt{3}}{4}\sin\varphi - \frac{3}{4}\cos\varphi - \tfrac{1}{2}\cos 3\varphi\right.$$

$$\left. - \frac{\sqrt{3}}{2}\sin 2\varphi + \tfrac{1}{2}\cos 2\varphi\right) + 2\,wH_c$$

$$+ \tfrac{1}{2}\,wH_c \cos 2\varphi - \frac{\sqrt{3}}{2}\,wH_c \sin 2\varphi \qquad (33)$$

The total weight of the soil associated with this force is

$$W_s = \left[\tfrac{1}{2}(R + H_c)^2 \tan 60 - \frac{\pi R^2}{6}\right] w$$

$$= 0.342\,wR^2 + 1.732\,wRH_c + 0.866\,wH_c^2$$

5.2 Distributed Earth Pressure Load

In considering the unsymmetrical blast loading on the arch rib, it is advantageous to resolve this loading into harmonic components since the resulting distributed loads $\sum p_n(t) \sin \frac{n\pi\varphi}{\theta}$ are easier to treat analytically than the actual irregular blast load. This advantage does not exist for the passive earth pressure loading, since original analytical

expressions are available which may be studied in determining the effect of the passive earth pressure on the arch. However, resolution of the passive earth pressure into harmonic loadings does facilitate visualization of the fact that the earth pressure may be thought of as a distributed resistance $\sum p_n \sin \frac{n\pi\varphi}{\theta}$ in the arch rib. In addition, a desirable uniformity of approach is provided for the entire problem.

Equation (28) expresses the unit radial pressure acting on a 180 degree arch with zero depth of cover on the crown. The total force acting on the arch rib may be resolved into harmonic components by Equation (9).

$$p_r(\varphi) = 2wR(1 - \sin\varphi) + wR(1 - \sin\varphi)\cos 2\varphi$$

$$p_n = \frac{2}{\theta R}\int p_r(\varphi) \sin \frac{n\pi\varphi}{\theta} R d\varphi$$

$$p_1 = \frac{2}{\pi R}\int_0^{\frac{\pi}{2}} [2wR(1 - \sin\varphi) + wR(1 - \sin\varphi)\cos 2\varphi]\sin \frac{\pi\varphi}{\theta} R d\varphi$$

$$= 0.948\ wR$$

$$p_2 = \frac{2}{\pi R}\int_0^{\frac{\pi}{2}} p_r(\varphi) \sin \frac{2\pi\varphi}{\theta} R d\varphi = 0.509\ wR$$

$$p_3 = \frac{2}{\pi R}\int_0^{\frac{\pi}{2}} p_r(\varphi) \sin \frac{3\pi\varphi}{\theta} R d\varphi = 1.180\ wR$$

Equation (33) expresses the radial pressure acting on a 120 degree arch having a depth of cover H_c on the crown. The total radial force resulting from this pressure may be resolved into harmonic loading components as follows:

$$p_r(\varphi) = wR\left(2 - \frac{3\sqrt{3}}{4}\sin\varphi - \frac{3}{4}\cos\varphi - \frac{1}{2}\cos 3\varphi - \frac{\sqrt{3}}{2}\sin 2\varphi + \frac{1}{2}\cos 2\varphi\right) + wH_c\left(2 + \frac{1}{2}\cos 2\varphi - \frac{\sqrt{3}}{2}\sin 2\varphi\right)$$

$$p_n = \frac{2}{\theta R}\int p_r(\varphi)\sin\frac{n\pi\varphi}{\theta}\,Rd\varphi$$

$$p_1 = \frac{2}{\frac{2}{3}\pi R}\left[\int_0^{\frac{\pi}{3}}\left[2 - \frac{3\sqrt{3}}{4}\sin\varphi - \frac{3}{4}\cos\varphi - \frac{1}{2}\cos 3\varphi - \frac{\sqrt{3}}{2}\sin 2\varphi + \frac{1}{2}\cos 2\varphi\right]\sin\frac{3}{2}\varphi\,Rd\varphi + wH_c\int_0^{\frac{\pi}{3}}\left(2 + \frac{1}{2}\cos 2\varphi - \frac{\sqrt{3}}{2}\sin 2\varphi\right)\sin\frac{3}{2}\varphi\,Rd\varphi\right]$$

$$= 0.111\,wR + 0.864\,wH_c$$

$$p_2 = \frac{2}{\frac{2}{3}\pi R}\int_0^{\frac{\pi}{3}} p_r(\varphi)\sin 3\varphi\,Rd\varphi = 0.181\,wR + 0.987\,wH_c$$

$$p_3 = \frac{2}{\frac{2}{3}\pi R}\int_0^{\frac{\pi}{3}} p_r(\varphi)\sin\frac{9}{2}\varphi\,Rd\varphi = 0.198\,wR + 0.557\,wH_c$$

5.3 Analogous Earth Pressure Load

In order that the effect of the unsymmetrical blast load on the arch rib may be determined conveniently, the blast load is represented as an analogous uniformly distributed radial load acting in compression on the windward side of the arch and in tension on the leeward side. This greatly facilitates the study of the dynamic effects of this load since the problem

of dealing with a time-dependent unsymmetrical load is reduced to that of dealing with a time-dependent uniform load. The problem may be simplified further by letting this uniform load define the parameters of the dynamic load acting on the single-degree-of-freedom system.

It is logical to extend the concept of analogous loads to the unsymmetrical passive earth pressure acting on the arch. In the first place, a desirable uniformity of approach to the entire problem is obtained. In addition, by defining the earth pressure load as an antisymmetrical radial load acting in compression on the leeward side of the arch and in tension on the windward side, the value of this pressure can be considered as integral part of the resistance of the arch rib, since the direction of the earth pressure is directly opposite to that of the blast pressure. Furthermore, this resistance provided to the arch by the soil may be used to define the resistance of the single-degree-of-freedom system.

The loading components $\sum p_n \sin \frac{n\pi\varphi}{\theta}$ defined in Section 5.2 , coupled with the moment coefficients from Table IV, are used to define the analogous loads for 180 and 120 degree arches. The resulting analogous loads define the maximum, or yield, resistance given the arch rib by the soil, since the passive earth pressure is evaluated at its peak value. The resistance is evaluated as a function of the moment in the arch rib at a point located by $\theta/4$, the same point used to define the analogous load for the blast pressure.

For a 180 degree arch with no cover on the crown, the resisting moment due to the soil is

$$M = -0.023(0.948\ wR)R^2 + 0.333(0.509\ wR)R^2 + 0.088(1.180\ wR)R^2$$

$$= 0.252\ wR^3$$

The analogous load is

$$p_a = \frac{0.252\ wR^3}{0.414\ R^2}$$

$$= 0.611\ wR \qquad (34)$$

For a 120 degree arch with a depth of cover H_c on the crown, the resisting moment due to the soil pressure is

$$M = -0.009(0.111wR + 0.864wH_c)R^2 + 0.125(0.181wR + 0.987wH_c)R^2$$

$$+ 0.050(0.198wR + 0.557WH_c)R^2$$

$$= 0.034wR^3 + 0.144wH_cR^2$$

The analogous load is

$$p_a = \frac{0.034wR^3 + 0.144wH_cR^2}{0.155R^2}$$

$$= 0.219wR + 0.929WH_c \qquad (35)$$

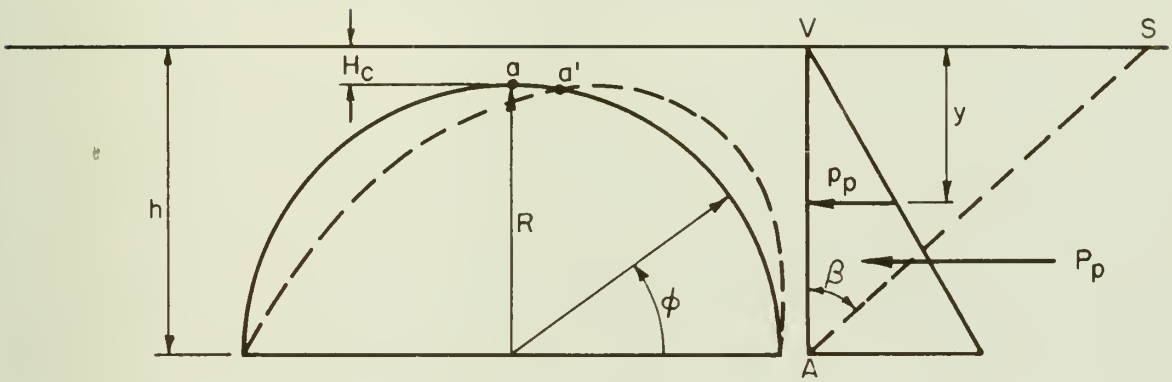

Figure 5.1 Passive Earth Pressure on a 180 Degree Central Angle Arch

CHAPTER VI

ANALYSIS OF THE RESPONSE OF THE ARCH TO THE DYNAMIC LOAD

The arch rib is idealized as a single-degree-of-freedom system, and the flexural resistance and mass of the arch rib per se are ignored. A method of dynamic analysis developed by Dr. N. M. Newmark, References (8) and (9), is used to predict the response of the arch rib to the given pressure pulse.

For the arches investigated in this thesis, it is found that the response of each is in the plastic, or yielded, part of the assumed elasto-plastic resistance diagram for the soil. Had the response been less than the deflection required to establish the passive earth pressure, the differential equation of motion stated in the introductory chapter of this study would have been used to find the maximum response.

6.1 Method of Analysis

For an initially peaked triangular force pulse acting on a single-degree-of-freedom system having an elasto-plastic resistance function, Figure 6.1, Dr. Newmark presented in Reference (8) the following approximate equation to predict the maximum response of the structure:

$$\frac{p_{max}}{q_e} = \frac{T}{\pi t_1}\sqrt{2\mu - 1} + \frac{1 - \frac{1}{2\mu}}{1 + 0.7\frac{T}{t_1}} \qquad (36)$$

where p_{max} = maximum value of the pulse loading

q_e = yield resistance of the structural element

μ = ductility ratio = maximum deflection/yield deflection

$= x_m/x_e$

T = natural period of vibration of the structure = $2\pi\sqrt{\frac{mx_e}{q_e}}$

t_1 = duration of the loading

Another technique developed by Dr. Newmark, Reference (9), can be used to define the dynamic behavior of the structure for other pulse shapes which may be represented by several initially peaked triangular force pulses, Figure 6.1. The relationship between the peak pressure and the maximum response of the structure is defined approximately as

$$\frac{f_1}{F_1} + \frac{f_2}{F_2} = \frac{p_{max}}{q_e}\left[\frac{c_1}{F_1} + \frac{c_2}{F_2}\right] = 1 \qquad (37)$$

where F_1, F_2 = damage pressure levels for initially peaked triangular force pulses of duration t_1/T and t_2/T, respectively, acting separately

c_1, c_2 = ratio of the peak pressure of the first and and second replacement triangles to the total peak pressure

f_1, f_2 = $c_1(p_m/q_e)$ and $c_2(p_m/q_e)$, respectively, the maximum value of the individual force pulses

To apply the above described methods of dynamic analysis to the situation at hand it is assumed that:

(1) The configuration of the arch rib is defined by the radial deflection of the haunch at a point located at $\theta/4$. The structure is idealized as a single-degree-of-freedom system.

(2) The blast loading on the arch is considered to be a uniformly distributed antisymmetrical loading. The unit value of this loading defines the forcing function acting on the single-degree-of-freedom system.

(3) The shape of the blast loading force pulse consists of two initially peaked triangular force pulses. The duration of the first pulse, t_1, is defined as the time required for the blast wave to engulf the arch

rib and rise to its maximum pressure at the leeward abutment, a time equal to t_a plus t_r. The total duration of both pulses is defined as the effective duration of the blast loading, t_i.

(4) The resistance provided to the arch rib by the passive earth pressure is considered to be a uniformly distributed antisymmetrical load. The unit value of this resistance defines the resistance function of the single-degree-of-freedom system.

(5) The weight of the soil associated with the passive earth pressure is uniformly distributed along the arch rib. This unit weight defines the unit mass of the single-degree-of-freedom system.

(6) The passive earth pressure reaches its maximum value when the radial deflection of the arch at a point $\theta/4$ is 0.1%R. The resistance diagram of this pressure is elasto-plastic and defines the resistance function of the idealized single-degree-of-freedom system.

(7) The period of vibration of the arch is defined as $T = 2\pi\sqrt{mx_e/q_e}$, where m results from the unit weight found in (5), x_e is 0.1%R, and q_e is the unit passive earth pressure resistance found in (4).

The general nature of assumptions (1) through (7) above is shown in Figure 6.2.

Numerical values of the parameters in Equation (36) are presented in Table VIII. Using these parameters, the maximum responses of arches with various radii subjected to 100 and 200 psi overpressures have been determined and are plotted in Figure 6.3. It is assumed that the arch is buried in soil with a seismic velocity of 2000 fps. The resistance and mass of the arch rib have not been included, and soil arching effects are not considered.

6.2 Sample Calculation

A sample calculation of the response of an arch under an assumed set of conditions follows.

Let: C_s = 2000 fps = 2 ft/ms; W = 1 MT; P_m = 100 psi; U = 3000 fps = 3 ft/ms

w = 120 pcf; R = 200 in. = 16.67 ft.; θ = 180 degrees

$t_r = \frac{1}{2} t_t$; $H_c = 0$

The parameters are:

$$p_{max} = 0.37\, P_m = 0.37(100) = 37 \text{ psi}$$

$$p'_{max} = 0.06\, P_m = 0.06(100) = 6 \text{ psi}$$

$$t_1 = \frac{R - R\sin(\varphi - \beta)}{\frac{C_s U}{\sqrt{C_s^2 + U^2}}} + \frac{R - R\sin\varphi}{2C_s}$$

$$= \frac{16.67\left[1 - \sin\left(0 - \arctan\frac{2}{3}\right)\right]}{\frac{6}{\sqrt{13}}} + \frac{16.67}{4}$$

$$= 20 \text{ ms}$$

$$t_2 = 0.4\left(\frac{100}{P_m}\right)^{2/3} W^{1/3}$$

$$= 400 \text{ ms}$$

$$T = 0.0076\sqrt{R} = 0.0076\sqrt{200} = 0.107 \text{ sec.} = 107 \text{ ms}$$

$$x_e = 0.001\, R = 0.001(200) = 0.2 \text{ in.}$$

$$q_e = 0.611\, wR = \frac{0.611(120)}{1728}\, 200 = 8.5 \text{ psi}$$

The force pulse is shown in Figure 6.2. Equations (36) and (37) must be evaluated by trial and error. Reference (9), Chart I, may also be used to evaluate Equation (36).

Assume that $\mu = 12$. For the first initially peaked triangular force pulse having a duration of 20 ms, the damage pressure level necessary for a maximum deflection of $x_m = 12x_e$ is

$$\frac{p_{max}}{q_e} = \frac{T}{\pi t_1}\sqrt{2\mu - 1} + \frac{1 - \frac{1}{2\mu}}{1 + 0.7(T/t_1)}$$

$$= \frac{107}{20\pi}\sqrt{24 - 1} + \frac{1 - \frac{1}{24}}{1 + 0.7(107/20)} = 8.4 = F_1$$

For the second initially peaked triangular force pulse having a duration of 400 ms, the damage pressure level necessary for a maximum deflection of $x_m = 12x_e$ is

$$\frac{p_{max}}{q_e} = \frac{107}{400\pi}\sqrt{24 - 1} + \frac{1 - \frac{1}{24}}{1 + 0.7(107/400)} = 1.2 = F_2$$

The small increase in the peak value of the second pulse due to the extension of the pressure line from t = 20 ms to t = 0 ms, an increase of $\frac{20}{380}(6) = 0.3$ psi, is ignored.

The actual peak pressure in the first force pulse is 31 psi; the actual peak pressure in the second force pulse is 6 psi; and the actual ratio of the total peak force to the resistance is

$$\frac{p_{max}}{q_e} = \frac{37}{8.5} = 4.37$$

Equation (37) may now be evaluated to determine if the assumed value of $\mu = 12$ is satisfactory.

$$\frac{p_{max}}{q_e}\left[\frac{c_1}{F_1}+\frac{c_2}{F_2}\right]=1.0$$

where $c_1=\frac{31}{37}=0.84$ $\qquad c_2=\frac{6}{37}=0.16$

$$\therefore\ 4.37\left(\frac{0.84}{84}+\frac{0.16}{1.2}\right)=1.02=\sim 1.0$$

Therefore the assumed value of 12 for μ is satisfactory, and the maximum deflection is

$$x_m=\mu x_e$$
$$=12(0.2)$$
$$=2.4 \text{ inches}$$

6.3 Discussion of Results

Figure 6.3 contains the quantitative results of the analyses of the response of various sized arches. The results may be qualitatively summarized as follows:

(1) For any given overpressure level, the response of the arch increases as the radius of the arch decreases. This is partially explained by considering how the load on the arch and the resistance given to the arch by the earth pressure are defined. The blast pressure is defined as a function of the peak overpressure only. The value of the analogous, uniformly-distributed, anti-symmetrical load is not a function of the radius of the arch. The earth pressure is defined as a function of the radius of the arch and varies directly as the radius varies. Consequently, the response of the arch to any

given overpressure varies indirectly as the radius of the arch varies.

Other factors which probably influence the response of the arch have not been studied in this thesis. One of these is the value of the resistance of the arch per se. For arches of smaller radii, this resistance may be relatively large compared to the resistance given the arch by the earth pressure.

(2) For equal radius arches, the response of the arch to any given overpressure level increases as the central angle of the arch decreases.

(3) The effect of the second triangular force pulse is very important since it has a relatively long duration. Several analyses of the response of a 120 degree arch to a 100 psi overpressure were made, in which the effect of this second force pulse was not considered. The response of a 200 inch radius arch was found to be approximately three inches, compared to a value of sixteen inches when the effect of the second pulse is included.

(4) Increasing the depth of cover on the crown reduces the effect of the blast load on the arch. The effect of the depth of burial of the arch may be related conveniently to the ratio of the depth of burial of the arch abutment to one-half of the arch span. When this ratio is one, for arches having radii of 200 inches or more and central angles greater than 120 degrees, the flexural action caused by an overpressure of 100 psi resulting from a 1 MT weapon may

be ignored. For a 180 degree arch, this ratio is one when there is no cover on the crown, and the deflection is approximately two inches. For a 120 degree arch, this ratio is approximately 0.9 when there is a depth of cover of 0.3R on the crown, and the deflection is approximately one inch.

TABLE VIII

PARAMETERS FOR DYNAMIC ANALYSIS OF SOIL RESISTANCE

Parameter	180 Degree Arch $H_c = 0$	120 Degree Arch $H_c = 0$	120 Degree Arch $H_c = 0.3R$
p_{max}	$0.37P_m$	$0.45P_m$	$0.45P_m$
p'_{max}	$0.06P_m$	$0.04P_m$	$0.04P_m$
t_1	$t_a + t_r$	$t_a + t_r$	$t_a + t_r$
t_2	t_i	t_i	t_i
q_e	$0.611wR$	$0.219wR$	$0.497wR$
x_e	$0.001R$	$0.001R$	$0.001R$
m	$\frac{1.08wR^2}{\pi Rg}$	$\frac{0.342wR^2}{\frac{2}{3}\pi Rg}$	$\frac{0.940wR^2}{\frac{2}{3}\pi Rg}$
T	$0.0076\sqrt{R}$	$0.0087\sqrt{R}$	$0.0096\sqrt{R}$

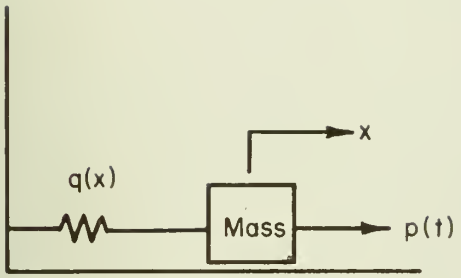

(a) Single-Degree-of-Freedom System

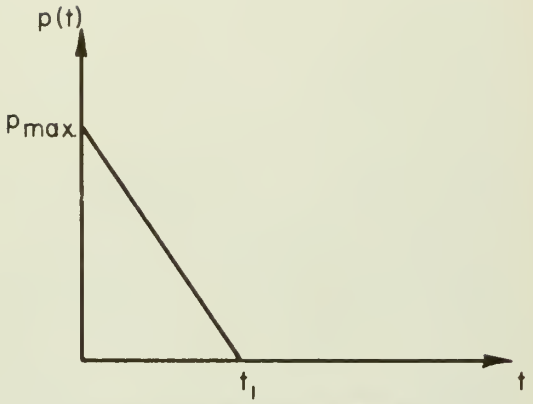

(b) Initially Peaked Triangular Force Pulse

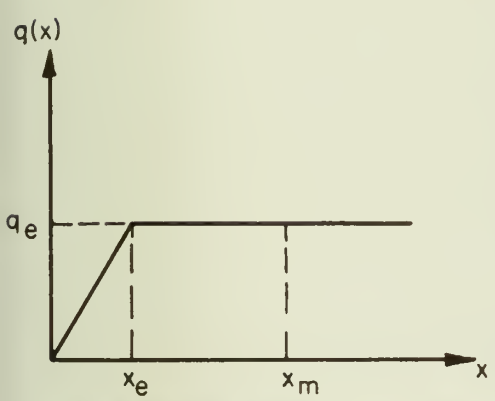

(c) Elasto-Plastic Bilinear Resistance

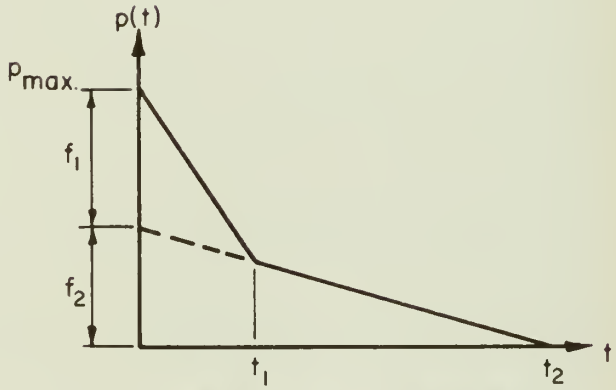

(d) Two Initially Peaked Triangular Force Pulses

Figure 6.1 Idealized Single-Degree-of-Freedom System, Force Pulses and Elasto-Plastic Bilinear Resistance

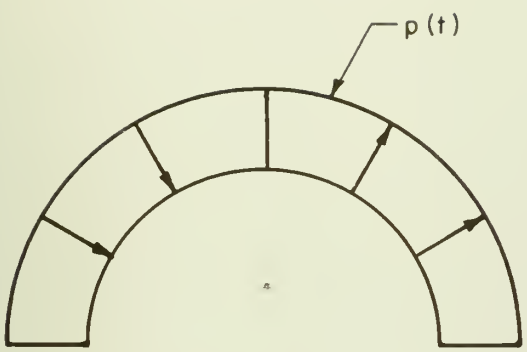

Blast Loading

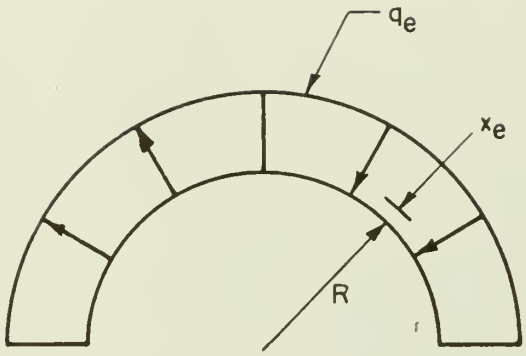

Soil Resistance

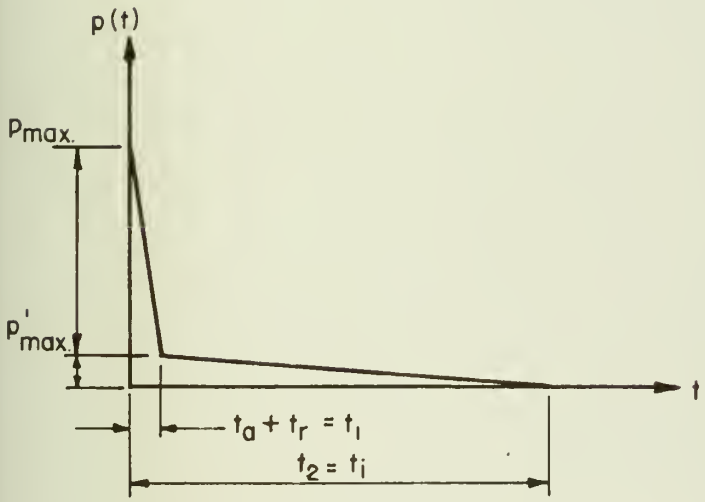

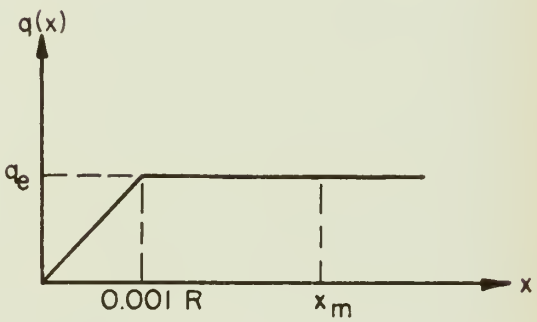

Soil Resistance Diagram

Figure 6.2 Idealized Loading and Resistance Functions of an Underground Arch Rib Subjected to Blast Pressure

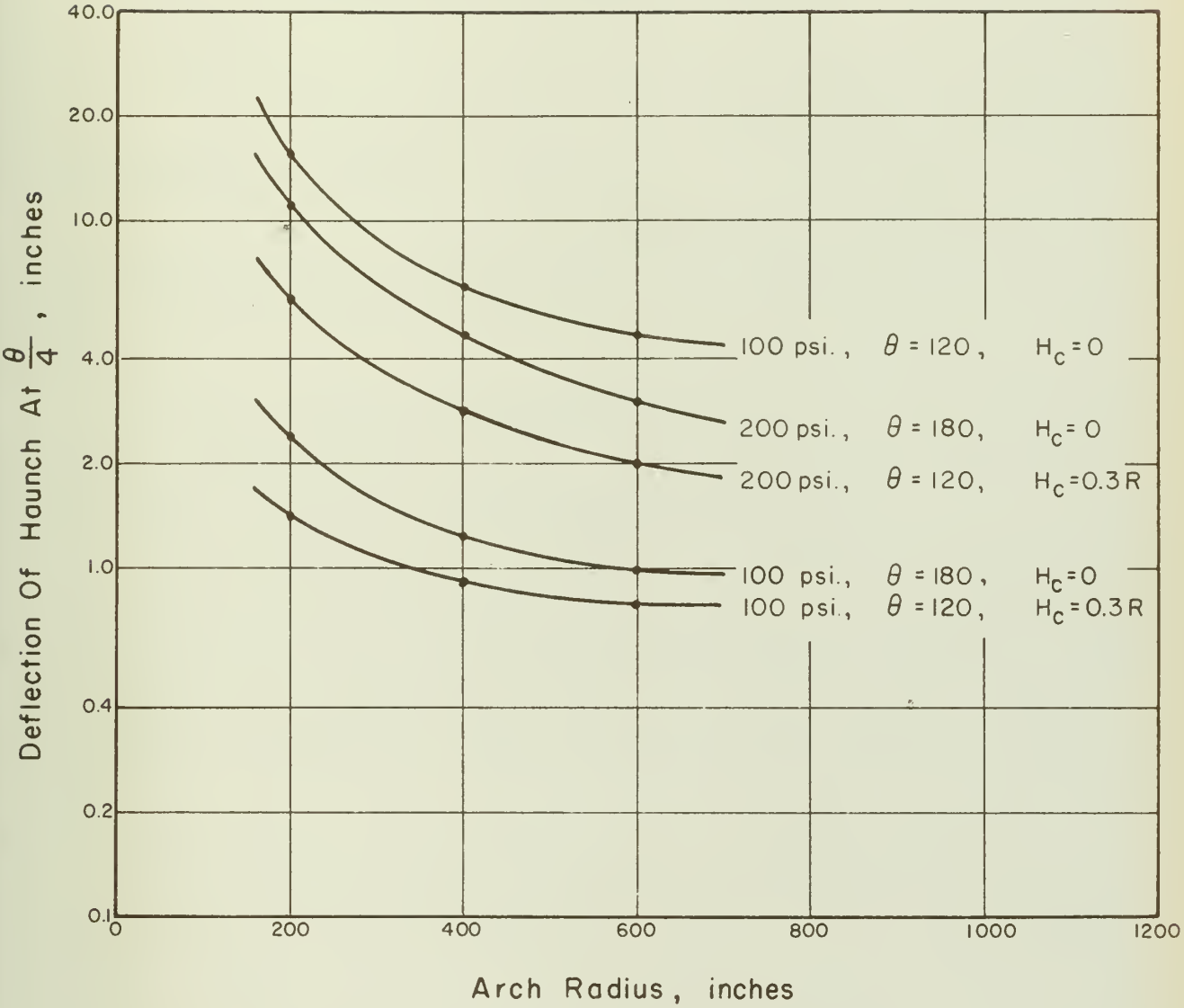

Figure 6.3 Haunch Deflection vs Arch Radius

W = 1 MT C_s = 2000 fps $t_r = \frac{1}{2}t_t$

P_m as noted H_c as noted θ as noted

CHAPTER VII

QUALITATIVE DESIGN METHOD FOR ARCH RIBS

The problem of the structural design of the arch rib has not been studied. However, the following qualitative design procedure, based on the methods used in this thesis, is suggested:

(1) Idealize the arch as a single-degree-of-freedom system, the configuration of which is defined by the radial deflection of the arch at $\theta/4$.

(2) Define the fundamental period of vibration of the structure by the mass and resistance of the soil, and the deflection of the arch at $\theta/4$ necessary to establish the full passive earth pressure.

(3) Define the forcing function as consisting of two initially-peaked triangular force pulses, the first pulse having a duration of $t_a + t_r$, the second having a duration of t_i. These forcing functions are uniformly-distributed, antisymmetrical, radial loads analogous to the actual blast loading.

(4) Assume a ductility factor μ. The end objective is to design the arch rib, not to determine the response of the soil surrounding the arch. However, since the arch cannot deflect without the soil accompanying it, this ductility factor also defines the response of the soil. The assumed value of μ should be larger than that desired for the actual arch rib.

(5) Evaluate the damage pressure level equation to determine the total resistance required of the combined arch rib-soil system.

(6) Subtract the soil resistance from the total required resistance and design the arch rib with a resistance equal to the remainder. The usually recommended allowable stresses for dynamic design are to be used.

(7) Determine the yield deflection at $\theta/4$ of the arch section designed in (6). The yield deflection must be stated in the same numerical terms as those used in (2) for finding the period of vibration of the structure.

(8) Combine the resistance of the soil and arch rib into an elasto-plastic resistance diagram. This is accomplished by making the area of the idealized bilinear resistance diagram equal to the area of the actual trilinear resistance diagram when both diagrams extend to a numerically specified deflection. The ratio x_m/x_e is assumed; the initial slope of the elastic part of the actual diagram is maintained; the value of q_e is adjusted to make the areas equal. Determine a new period of vibration for the combined arch-rib soil system, including the resistance and mass of the arch section designed in (6).

(9) Using the elasto-plastic resistance function found in (8), evaluate the damage pressure level equation to determine the maximum response of the system. The resulting ratio of the maximum deflection to the yield deflection of the system is found and compared with the ratio x_m/x_e used in combining the soil and arch resistances. If these ratios are equal, the arch section designed in (6) is satisfactory. If they are not equal, the arch section must be redesigned and (7) through (9) repeated.

The anticipated results of the design procedure outlined above are discussed below without proof.

There are two principle modes of response of an arch to blast loading, Reference (10). One of these is symmetrical, corresponding to the compression in the arch, and the other is antisymmetrical, corresponding to the flexural deformation of the arch. Consider an underground arch and assume that the arch rib has been designed for the static load of the soil

cover and the compression load of the blast force. For the arch sizes, overpressures, and weapon yield studied in this thesis, it is reasonable to expect that such arches would have a yield deflection on the haunch of at least one-half inch. For 100 psi overpressure, the maximum deflection expected of the haunch, considering the resistance of the soil only, is two inches for 180 degree arches with zero depth of cover on the crown, and approximately one inch for 120 degree arches with 0.3R cover on the crown. Therefore the ratio of the maximum deflection on the haunch to the allowable elastic deflection of the arch rib does not exceed 4:1, even though the reduction of the maximum deflection due to energy absorbed by elastic or plastic deformation of the arch rib is disregarded.

For moderately ductile structures, the above ratio, ductility factor μ, ranges from 10 to 30, Reference (8). For designing flexural members, including reinforced concrete members, the ductility factor usually is assumed to be 20.

It is therefore concluded that if the arch rib is designed so that it has a ductility factor of 20 for flexural action, and is covered as described above, no increase in the required resistance for static and blast compression load is necessary to accommodate the antisymmetrical mode of response for an overpressure of 100 psi.

CHAPTER VIII

CONCLUSIONS AND RECOMMENDATIONS

8.1 Conclusions

The following conclusions are drawn from the results obtained and the discussions thereof in the preceding chapters.

(1) Harmonic analysis provides a convenient means of analyzing unsymmetrical loads acting on arches.

(2) The peak values of dynamic loads and their load-time curves may be determined by harmonically analyzing the load at suitable time intervals.

(3) The effects of the unsymmetrical blast load acting on the arch may be studied conveniently through the use of analogous loads. When studying the effect of the blast load on the haunch, the analogous load employed is a uniformly distributed radial load which acts in compression on the windward side of the arch and in tension on the leeward side. The peak value of this load is approximately forty percent of the peak value of the overpressure. When studying the effect of the blast load on the crown, the analogous load employed is a uniformly distributed radial load which acts in compression on the central third of the arch and in tension on the outer thirds. The peak value of this load is approximately forty percent of the maximum overpressure.

(4) The effect of the unsymmetrical passive earth pressure load on the arch also may be studied through the use of an analogous load. This analogous load is a uniformly distributed radial load acting in compression on the leeward side of the arch and in tension on the windward side. It directly opposes the blast pressure load. Its value varies directly with the radius of the arch.

(5) The peak value of the analogous load employed in studying the blast effects on the haunch of the arch increases as the seismic velocity of the soil increases. The peak value of the analogous load used in studying the crown of the arch decreases as the seismic velocity of the soil increases.

(6) The relative severity of the dynamic load varies inversely with the ratio of the horizontal to vertical pressure in the soil. It is to be noted, however, that as this ratio increases, there may be a tendency for the crown of the arch to move outward.

(7) The relative rise time of the blast pressure to its peak value has little effect on the peak value of the analogous loads.

(8) The passive earth pressure contributes materially to the resistance of the arch. An overpressure of 100 pounds per square inch from a one megaton weapon causes a maximum response of approximately two inches in the 180 degree arches studied. Subjected to the same overpressure, the response of a 120 degree arch with a depth of cover on the crown equal to three-tenths of the radius is approximately one inch. This response is considered negligible.

(9) The passive earth pressure developed by the arch decreases as the central angle of the arch decreases. It is doubtful if arches with central angles of much less than 120 degrees would develop significant passive earth pressure under blast loading.

(10) The rigidity of an arch interferes with the deflection of the arch required to develop the passive earth pressure. This suggests that flexible arches have certain advantages in blast resistant construction.

(11) The method of approach presented in this thesis may be extended to consider soils with different angles of internal friction,

different unit weights, and varying water table levels, as well as to cohesive soils, provided the cohesion of the soil can be stated in terms of an equivalent angle of internal friction.

8.2 Recommendations

It is recommended that the studies made in this thesis be extended to:

(1) Consider how the blast loading on the arch is affected by the soil on the windward side of the arch.

(2) Consider how the passive earth pressure loading on the arch is affected by the increased shear strength of the soil due to the vertical blast pressure acting on the leeward side of the arch.

(3) Compare the arch behavior predicted in this thesis with available test data.

(4) Develop a quantitative procedure for design of the arch rib under impulsive loading which includes the effect of the passive earth pressure.

APPENDIX A

BIBLIOGRAPHY

1. Anderson, F. A., "Blast Phenomena from a Nuclear Burst," Journal of the Structural Division, Proceedings of the American Society of Civil Engineers, Paper 1836, St 7, November 1958.

2. "Protective Construction Review Guide," issued by Office of Secretary of Defense, January 1959. Prepared under contract SD-52 by N. M. Newmark, R. J. Hansen and others. Classified Secret Security Information.

3. Huntington, W. C., Earth Pressures and Retaining Walls, John Wiley and Sons, Inc., New York, 1957.

4. Seely, F. B., and Smith, J. O., Advanced Mechanics of Materials, Second Edition, John Wiley and Sons, Inc., New York, October 1957.

5. Hendry, A. W., and Jaeger, L. G., The Analysis of Grid Frameworks and Related Structures, Chatto and Windus, London, 1958; Prentice-Hall, Inc., New York, 1959.

6. Brode, H. L., "Numerical Solutions of Spherical Blast Waves," Journal of Applied Physics, v. 26, No. 6, pp. 766-775, June, 1955.

7. The Effects of Nuclear Weapons, Samuel Glasstone, Editor, United States Department of Defense, June, 1957.

8. Newmark, N. M., "An Engineering Approach to Blast Resistant Design," Transactions of the American Society of Civil Engineers, v. 121, Paper No. 2786, pp. 45-64, 1956.

9. Melin, J. W., and S. Sutcliffe, "Development of Procedures for Rapid Computation of Dynamic Structural Response," Civil Engineering Studies, Structural Research Series No. 171, University of Illinois, Urbana, Illinois, January, 1959.

10. Merritt, J. L. and N. M. Newmark, "Design of Underground Structures to Resist Nuclear Blast," Civil Engineering Studies, Structural Research Series No. 149, University of Illinois, Urbana, Illinois, April, 1958.

APPENDIX B

NUMERICAL CALCULATION RESULTS

This Appendix contains the results of the numerical harmonic analyses made.

In Tables B1 through B10 are tabulated the vertical pressure-time values of blast pressure on a 180 degree arch with zero depth of cover on the crown for various combinations of the variables stated in Chapter II. Since the 120 degree arch has the same radius, this table also provides the vertical pressure-time values for the blast loading on a 120 degree arch by using the values between 30 and 150 degrees.

Tables B11 and B12 contain the values of the coefficients $p_n(t)$ for the harmonic components of loading, as found by numerical analysis. These values were found by using the vertical pressures in Tables B1 through B10, applying the coefficients from Table I to convert the vertical pressure to radial pressure, and then harmonically analyzing these radial pressures. These tables also contain the values of the analogous loads $p_a(t)$ and $p_s(t)$.

The following sign convention is applicable to these loads:

(a) $p_n(t)$ is positive when the load acts inwardly

(b) $p_a(t)$ is positive when the uniformly distributed load acts in compression on the windward half of the arch and in tension on the leeward side

(c) $p_s(t)$ is positive when the uniformly distributed load acts in compression on the central third of the arch and in tension on the outer thirds.

Originally it was intended to study only twenty-five foot radius arches, some with a rise time equal to one-half the transit time and the remainder with a rise time equal to the transit time. However, after numerous calculations had been made, an error amounting to a multiple of two was found.

In order to use the previous work it became necessary to decrease the arch radius to 12.5 feet, and to increase the rise times of some of the arches to equal the transit time, and of the remainder to twice the transit time. This accounts for the data showing $t_r = 2t_t$. After the error was discovered, only arches with a twenty-five foot radius and $t_r = \frac{1}{2}t_t$ were studied. The results are of such a nature that general conclusions may be drawn without regard to the disparity in the arch sizes.

Figures B1 through B6 are typical graphs of the values of the coefficient $p_n(t)$ and the analogous loads $p_a(t)$ and $p_s(t)$.

Table B1. Vertical pressure-time plot for 180 degree 150 inch radius arch subjected to 100 psi overpressure from 1 MT weapon with C_s = 1000 fps and $t_r = t_t$

Time in ms	Vertical pressure $p_v(t)$ in pounds per square inch at φ																		
	180	170	160	150	140	130	120	110	100	90	80	70	60	50	40	30	20	10	0
1	0	0	0	0	0	0	50	100	100	100	0	0	0	0	0	0	0	0	0
2	0	0	0	0	0	38	100	100	99	99	100	0	0	0	0	0	0	0	0
4	0	0	0	11	46	100	99	98	98	98	99	100	0	0	0	0	0	0	0
8	0	11	37	74	99	98	97	96	96	96	97	98	99	59	0	0	0	0	0
12	24	50	86	99	97	96	95	94	94	94	95	96	97	99	82	24	0	0	0
16	56	89	99	97	95	94	93	92	92	92	93	94	95	97	98	88	39	10	0
20	88	99	97	95	93	92	91	90	90	90	91	92	93	95	96	98	89	49	22
24	99	97	95	93	91	90	89	88	88	88	89	90	91	93	94	96	98	85	54
28	97	95	93	91	89	88	87	86	86	86	87	88	89	91	92	94	96	99	86
32	95	93	91	89	87	86	85	84	84	84	85	86	87	89	90	92	94	97	99
36	93	91	89	87	85	84	83	82	82	82	83	84	85	87	88	90	92	95	97
40	91	89	87	85	83	82	81	80	80	80	81	82	83	85	86	88	90	93	95
60	81	79	77	75	73	72	71	70	70	70	71	72	73	75	76	78	80	83	85
120	61	59	57	55	53	52	51	50	50	50	51	52	53	55	56	58	60	63	65
200	41	39	37	35	33	32	31	30	30	30	31	32	33	35	36	38	40	43	45

Table B2. Vertical pressure-time plot for 180 degree 150 inch radius arch subjected to 100 psi overpressure from 1 MT weapon with C_s = 1000 fps and $t_r = 2t_t$

Time in ms	Vertical pressure $p_v(t)$ in pounds per square inch at φ																		
	180	170	160	150	140	130	120	110	100	90	80	70	60	50	40	30	20	10	0
2	0	0	0	0	0	20	48	100	100	100	100	0	0	0	0	0	0	0	0
4	0	0	0	6	24	54	100	99	98	98	99	80	0	0	0	0	0	0	0
8	0	5	18	38	69	99	98	97	96	96	97	98	100	29	0	0	0	0	0
12	12	24	42	70	99	97	96	95	94	94	95	96	98	98	41	12	0	0	0
16	28	43	67	100	97	95	94	93	92	92	93	94	96	98	85	44	20	5	0
20	44	63	91	98	95	93	92	91	90	90	91	92	94	96	99	76	44	24	11
24	60	82	99	96	93	91	90	89	88	88	89	90	92	94	97	99	69	43	27
28	76	100	97	94	91	89	88	87	86	86	87	88	90	92	95	97	93	63	43
32	92	98	95	92	89	87	86	85	84	84	85	86	88	90	93	95	99	82	59
36	99	96	93	90	87	85	84	83	82	82	83	84	86	88	91	93	97	100	75
40	97	94	91	88	85	83	82	81	80	80	81	82	84	86	89	91	95	98	91
44	95	92	89	86	83	81	80	79	78	78	79	80	82	84	87	89	93	96	99
60	87	84	81	78	75	73	72	71	70	70	71	72	74	76	79	81	85	88	91
120	59	57	55	54	52	51	50	49	49	49	49	50	51	52	54	55	57	59	60
200	40	39	37	36	36	35	35	34	34	34	34	34	35	36	37	38	39	40	41

Table B3. Vertical pressure-time plot for 180 degree 150 inch radius arch subjected to 100 psi overpressure from 1 MT weapon with C_s = 2000 fps and $t_r = t_t$

Time in ms	Vertical pressure $p_v(t)$ in pounds per square inch at φ																		
	180	170	160	150	140	130	120	110	100	90	80	70	60	50	40	30	20	10	0
1	0	0	0	10	30	67	100	100	100	0	0	0	0	0	0	0	0	0	0
2	0	0	14	40	75	100	99	99	99	100	0	0	0	0	0	0	0	0	0
4	8	32	62	100	99	99	98	98	98	99	99	100	0	0	0	0	0	0	0
6	40	70	100	99	98	98	97	97	97	98	98	99	100	33	0	0	0	0	0
8	72	100	99	98	97	97	96	96	96	97	97	98	99	100	53	0	0	0	0
10	100	99	98	97	96	96	95	95	95	96	96	97	98	99	100	59	14	0	0
12	99	98	97	96	95	95	94	94	94	95	95	96	97	98	99	100	62	25	3
14	98	97	96	95	94	94	93	93	93	94	94	95	96	97	98	99	100	63	35
16	97	96	95	94	93	93	92	92	92	93	93	94	95	96	97	98	99	100	67
18	96	95	94	93	92	92	91	91	91	92	92	93	94	95	96	97	98	99	99
20	95	94	93	92	91	91	90	90	90	91	91	92	93	94	95	96	97	98	99
60	75	74	73	72	71	71	70	70	70	71	71	72	73	74	75	76	77	78	79
120	52	51	51	50	50	49	49	49	49	49	49	49	50	50	51	51	52	54	55
200	35	35	35	34	34	34	34	34	34	34	34	34	35	35	35	36	36	36	37

Table B4. Vertical pressure-time plot for 180 degree 150 inch radius arch subjected to 100 psi overpressure from 1 MT weapon with C_s = 2000 fps and $t_r = 2t_t$

Time in ms	Vertical pressure $p_v(t)$ in pounds per square inch at φ																		
	180	170	160	150	140	130	120	110	100	90	80	70	60	50	40	30	20	10	0
2	0	0	7	21	37	70	100	99	99	100	0	0	0	0	0	0	0	0	0
4	4	17	31	53	81	99	99	98	98	99	99	100	0	0	0	0	0	0	0
6	20	37	55	85	99	98	98	97	97	98	98	99	100	17	0	0	0	0	0
8	36	57	79	99	98	97	97	96	96	97	97	98	99	87	26	0	0	0	0
10	52	77	100	98	97	96	96	95	95	96	96	97	98	99	70	31	7	0	0
12	68	87	99	97	96	95	95	94	94	95	95	96	97	98	100	62	31	13	2
14	84	99	98	96	95	94	94	93	93	94	94	95	96	97	99	94	55	33	18
16	100	98	97	95	94	93	93	92	92	93	93	94	95	96	98	99	79	53	34
18	99	97	96	94	93	92	92	91	91	92	92	93	94	95	97	98	100	73	50
20	98	96	95	93	92	91	91	90	80	91	91	92	93	94	96	97	99	93	66
22	97	95	94	92	91	90	90	89	89	90	90	91	92	93	95	96	98	100	82
24	96	94	93	91	90	89	89	88	88	89	89	90	91	92	94	95	97	99	98
26	95	93	92	90	89	88	88	87	87	88	88	89	90	91	93	94	96	98	99
60	78	76	75	73	72	71	71	70	70	71	72	72	73	74	76	77	79	81	82
120	54	53	52	51	50	49	49	49	49	49	49	50	51	51	52	53	54	55	55
200	36	36	36	35	35	34	34	34	34	34	34	34	35	35	36	36	37	38	38

Table B5. Vertical pressure-time plot for 180 degree 150 inch radius arch subjected to 200 psi overpressure from 1 MT weapon with C_s = 1000 fps and $t_r = t_t$

Time in ms	Vertical pressure $p_v(t)$ in pounds per square inch at φ																		
	180	170	160	150	140	130	120	110	100	90	80	70	60	50	40	30	20	10	0
1	0	0	0	0	0	0	59	200	198	200	0	0	0	0	0	0	0	0	0
2	0	0	0	0	0	48	177	198	196	197	199	0	0	0	0	0	0	0	0
4	0	0	0	3	67	186	196	194	192	193	195	198	47	0	0	0	0	0	0
6	0	0	7	67	156	196	192	190	188	189	191	194	199	48	0	0	0	0	0
8	0	8	56	131	198	192	188	186	184	185	187	190	195	186	36	0	0	0	0
10	3	46	105	195	194	188	184	182	180	181	183	186	191	196	126	22	0	0	0
12	35	84	154	196	190	184	180	178	176	177	179	182	187	192	199	86	12	0	0
14	67	122	200	192	186	180	176	174	172	173	175	178	183	188	195	150	61	6	0
16	99	160	196	188	182	176	172	170	168	169	171	174	179	184	191	199	110	44	0
18	131	198	192	184	178	172	168	166	164	165	167	170	175	180	187	195	159	82	32
20	163	196	188	180	174	168	164	162	160	161	163	166	171	176	183	191	199	120	64
22	195	192	184	176	170	164	160	158	156	157	159	162	167	172	179	187	195	158	96
24	197	188	180	172	166	160	156	154	152	153	155	158	163	168	175	183	191	190	128
26	193	184	176	168	162	156	152	150	148	149	151	154	159	164	171	179	187	196	160
28	189	180	172	164	158	152	148	146	144	145	147	150	155	160	167	175	183	192	192
30	185	176	168	160	154	148	144	142	140	141	143	146	151	156	163	171	179	188	197
60	124	122	118	112	110	106	104	104	104	104	104	106	108	110	116	118	122	126	136
120	76	74	72	70	70	68	66	66	66	66	66	68	68	70	72	74	76	80	80
200	48	46	44	44	44	44	42	42	42	42	42	42	44	44	44	46	46	48	48

Table B6. Vertical pressure-time plot for 180 degree 150 inch radius arch subjected to 200 psi overpressure from 1 MT weapon with C_s = 1000 fps and $t_r = 2t_t$

Time in ms	Vertical pressure $p_v(t)$ in pounds per square inch at φ																		
	180	170	160	150	140	130	120	110	100	90	80	70	60	50	40	30	20	10	0
2	0	0	0	0	0	24	88	199	197	197	199	0	0	0	0	0	0	0	0
4	0	0	0	2	34	93	200	195	193	193	195	24	0	0	0	0	0	0	0
6	0	0	4	34	80	162	196	191	189	189	191	195	142	24	0	0	0	0	0
8	0	4	28	66	125	198	192	187	185	185	187	191	198	93	18	0	0	0	0
10	2	23	53	98	171	194	188	183	181	181	183	187	194	162	63	11	0	0	0
12	18	42	77	130	199	190	184	179	177	177	179	183	190	198	109	43	6	0	0
14	34	61	102	162	195	186	180	175	173	173	175	179	186	194	154	75	30	3	0
16	50	80	126	196	191	182	176	171	169	169	171	175	182	190	200	107	55	22	0
18	66	99	151	197	187	178	172	167	165	165	167	171	178	186	196	139	79	41	16
20	82	118	175	193	183	174	168	163	161	161	163	167	174	182	192	171	104	60	32
22	98	137	200	189	179	170	164	159	157	157	159	163	170	178	188	200	128	79	48
24	114	156	196	185	175	166	160	155	153	153	155	159	166	174	184	196	153	98	64
26	130	175	192	181	171	162	156	151	149	149	151	155	162	170	180	192	177	117	80
28	146	194	188	177	167	158	152	147	145	145	147	151	158	166	176	188	200	136	96
30	162	197	184	173	163	154	148	143	141	141	143	147	154	162	172	184	196	155	112
32	178	193	180	169	159	150	144	139	137	137	139	143	150	158	168	180	192	174	128
34	194	189	176	165	155	146	140	135	133	133	135	139	146	154	164	176	188	193	144
36	198	185	172	161	151	142	136	131	129	129	131	135	142	150	160	172	182	197	160
38	194	181	168	157	147	138	132	127	125	125	127	131	138	146	156	168	178	193	176
40	190	177	164	153	143	134	128	123	121	121	123	127	134	142	152	164	174	189	192
42	186	173	160	149	139	130	124	119	117	117	119	123	130	138	148	160	170	185	198
120	82	80	76	74	72	70	68	68	66	66	68	68	70	72	74	76	80	82	90
180	50	48	46	46	44	42	42	42	40	40	42	42	42	44	46	46	48	50	52

Table B7. Vertical pressure-time plot for 180 degree 150 inch radius arch subjected to 200 psi overpressure from 1 MT weapon with C_s = 2000 fps and $t_r = t_t$

Time in ms	Vertical pressure $p_v(t)$ in pounds per square inch at φ																		
	180	170	160	150	140	130	120	110	100	90	80	70	60	50	40	30	20	10	0
1	0	0	0	0	37	115	200	199	199	200	0	0	0	0	0	0	0	0	0
2	0	0	5	52	128	199	197	196	196	197	199	0	0	0	0	0	0	0	0
4	3	46	103	181	197	194	192	191	191	192	194	196	200	0	0	0	0	0	0
6	67	123	200	196	192	189	187	186	186	187	189	191	195	199	64	0	0	0	0
8	130	200	195	191	187	184	182	181	181	182	184	186	190	194	199	97	10	0	0
10	194	195	190	186	182	179	177	176	176	177	179	181	185	189	194	199	108	39	0
12	195	190	185	181	177	174	172	171	171	172	174	176	180	184	189	194	200	116	60
14	190	185	180	176	172	169	167	166	166	167	169	171	175	179	184	189	195	193	124
16	185	180	175	171	167	164	162	161	161	162	164	166	170	174	179	184	190	195	187
18	180	175	170	166	162	159	157	156	156	157	159	161	165	169	174	179	185	190	196
60	112	110	108	108	106	104	104	104	104	104	104	106	108	108	110	110	116	120	122
120	72	70	68	68	66	66	66	66	66	66	66	66	68	68	70	70	72	72	74
200	44	42	42	42	42	42	42	42	42	42	42	42	42	42	42	42	44	44	44

Table B8. Vertical pressure-time plot for 180 degree 150 inch radius arch subjected to 200 psi overpressure from 1 MT weapon with C_s = 2000 fps and $t_r = 2t_t$

Time in ms	Vertical pressure $p_v(t)$ in pounds per square inch at φ																		
	180	170	160	150	140	130	120	110	100	90	80	70	60	50	40	30	20	10	0
2	0	0	2	25	62	124	199	197	197	197	199	0	0	0	0	0	0	0	0
4	2	23	51	85	151	198	195	193	193	195	198	106	0	0	0	0	0	0	0
6	34	62	100	149	198	194	190	188	188	188	190	193	197	124	31	0	0	0	0
8	66	101	149	199	194	189	186	184	184	184	186	189	193	198	120	48	5	0	0
10	98	140	198	195	187	185	181	179	179	179	181	184	188	193	200	111	54	19	0
12	130	179	196	190	185	180	177	175	175	175	177	180	184	189	196	175	103	58	30
14	162	198	192	186	180	176	172	170	170	170	172	175	179	184	191	197	152	97	62
16	194	194	187	181	176	171	168	166	166	166	168	171	175	180	187	193	200	136	94
18	196	189	183	177	171	167	163	161	161	161	163	166	170	175	182	188	195	175	126
20	192	185	179	173	167	163	159	157	157	157	159	162	166	171	178	184	191	198	158
22	187	180	174	169	162	158	154	152	152	152	154	157	161	166	173	179	186	193	190
24	183	176	170	165	158	154	150	148	148	148	150	153	157	162	169	175	182	189	197
60	122	116	112	110	108	106	104	104	104	104	104	106	108	110	110	116	122	124	126
120	72	72	70	70	68	66	66	66	66	66	66	66	68	70	70	72	72	74	76
200	44	42	42	42	42	42	42	42	42	42	42	42	42	42	42	44	44	46	48

Table B9. Vertical pressure-time plot for 180 degree 300 inch radius arch subjected to 200 psi overpressure from 1 MT weapon with C_s = 1000 fps and $t_r = \frac{1}{2} t_t$

Time	Vertical pressure $p_v(t)$ in pounds per square inch at φ																		
	180	170	160	150	140	130	120	110	100	90	80	70	60	50	40	30	20	10	0
1	0	0	0	0	0	0	0	200	199	197	0	0	0	0	0	0	0	0	0
2	0	0	0	0	0	0	118	199	198	197	0	0	0	0	0	0	0	0	0
4	0	0	0	0	0	98	199	195	194	193	196	0	0	0	0	0	0	0	0
6	0	0	0	0	45	200	195	191	190	189	192	199	0	0	0	0	0	0	0
20	5	95	200	188	180	172	167	163	162	161	164	171	178	188	199	44	0	0	0
32	200	188	176	164	156	148	143	139	138	137	140	147	154	164	175	186	199	45	0
42	180	168	156	144	136	128	123	119	118	117	120	127	134	144	155	166	179	192	166

Table B10. Vertical pressure-time plot for 180 degree 300 inch radius arch subjected to 200 psi overpressure from 1 MT weapon with C_s = 2000 fps and $t_r = \frac{1}{2} t_t$

Time	Vertical pressure $p_v(t)$ in pounds per square inch at φ																		
	180	170	160	150	140	130	120	110	100	90	80	70	60	50	40	30	20	10	0
1	0	0	0	0	0	85	200	200	200	0	0	0	0	0	0	0	0	0	0
2	0	0	0	0	72	200	198	198	198	199	0	0	0	0	0	0	0	0	0
4	0	0	0	110	199	196	194	194	194	195	198	0	0	0	0	0	0	0	0
8	0	89	200	195	191	188	186	186	186	187	190	195	199	0	0	0	0	0	0
16	196	190	184	179	175	172	170	170	170	171	174	179	183	188	194	187	20	0	0
28	172	166	160	155	151	148	146	146	146	147	150	155	159	164	170	176	184	190	197
34	160	154	148	143	139	136	134	134	134	135	138	143	147	152	158	164	172	178	185

Table B11. Values of the coefficients $p_n(t)$ for the harmonic components of loading $p_n(t) \sin \frac{n\pi\varphi}{\theta}$, antisymmetrical $p_a(t)$ and symmetrical $p_s(t)$ analogous uniform loadings, and the uniform all-around compression $p_u(t)$. (All loadings are in pounds per square inch. Time is in milliseconds. R = 150 inches. W = 1 MT. Other variables are as noted.)

(a) Condition: P_m = 100 psi C_s = 1000 fps p_h/p_v = 0.25 $t_r = t_t$

	180 Degree Arch						120 Degree Arch					
Time	$p_1(t)$	$p_2(t)$	$p_3(t)$	$p_u(t)$	$p_a(t)$	$p_s(t)$	$p_1(t)$	$p_2(t)$	$p_3(t)$	$p_u(t)$	$p_a(t)$	$p_s(t)$
1	35	-14	-25	0	19	28	56	-28	-24	0	34	31
2	52	-17	-33	0	24	38	73	-30	-26	0	37	37
4	67	-18	-32	0	25	41	90	-25	-15	0	30	32
8	81	-12	-22	0	19	36	102	- 8	5	0	11	20
12	87	-9	-11	0	14	29	91	0	10	11	2	13
16	88	-2	-5	0	8	24	52	1	-1	39	3	13
20	80	0	-4	6	5	21	47	2	-1	42	1	12
24	68	1	-6	14	4	20	46	1	-1	41	2	11
28	57	1	-9	22	4	20	45	1	-1	40	2	11
32	52	1	-10	25	4	20	42	1	-1	39	2	10
40	49	1	-9	23	4	18	42	1	-1	37	2	10
120	30	1	-5	15	2	11	26	1	0	24	1	7
200	18	1	-3	10	1	6	15	1	0	15	0	4

TABLE B11 (Continued)

(b) Condition: P_m = 100 psi C_s = 1000 fps $t_r = t_t$ p_h/p_v = 0.50

Time	180 Degree Arch						120 Degree Arch					
	$p_1(t)$	$p_2(t)$	$p_3(t)$	$p_u(t)$	$p_a(t)$	$p_s(t)$	$p_1(t)$	$p_2(t)$	$p_3(t)$	$p_u(t)$	$p_a(t)$	$p_s(t)$
1	36	-15	-26	0	20	29	51	-28	-24	0	33	30
2	53	-18	-34	0	25	40	74	-32	-25	0	38	36
4	69	-21	-32	0	28	41	93	-28	-12	0	32	30
8	85	-17	-18	0	22	34	107	-9	11	0	10	16
12	95	-10	-3	0	14	24	91	0	17	15	0	8
16	98	-4	7	0	7	16	39	1	2	55	1	7
20	83	-1	7	11	4	13	31	1	0	59	1	7
24	62	1	2	27	2	12	30	1	0	58	1	7
28	39	1	-4	43	2	12	29	1	0	57	1	7
32	31	1	-6	50	2	12	28	1	0	56	1	6
40	29	1	-6	46	2	11	27	1	0	53	1	6
120	17	1	-3	30	1	6	16	1	0	34	0	4
200	9	1	-2	20	0	4	9	1	0	22	0	2

TABLE B11 (Continued)

(c) Conditions: P_m = 100 psi C_s = 1000 fps $t_r = t_t$ p_h/p_v = 0.75

	180 Degree Arch						120 Degree Arch					
Time	$p_1(t)$	$p_2(t)$	$p_3(t)$	$p_u(t)$	$p_a(t)$	$p_s(t)$	$p_1(t)$	$p_2(t)$	$p_3(t)$	$p_u(t)$	$p_a(t)$	$p_s(t)$
1	37	-15	-26	0	20	29	52	-30	-23	0	35	29
2	55	-20	-34	0	26	40	76	-35	-23	0	40	35
4	72	-24	-31	0	30	41	96	-31	-7	0	33	27
8	92	-21	-14	0	25	32	111	-11	16	0	10	13
12	102	-13	6	0	15	18	89	0	22	20	-2	3
16	106	-5	19	0	6	10	21	1	3	72	0	2
20	85	-1	18	17	2	5	13	1	0	77	0	3
24	53	1	10	41	0	4	12	1	0	76	0	3
28	21	1	1	65	0	4	12	1	0	74	0	3
32	12	1	-2	70	0	4	13	1	0	72	0	3
40	11	1	-2	67	0	4	12	1	0	69	0	3
120	6	1	-1	44	0	2	5	1	0	45	0	1
200	3	1	1	28	1	0						

TABLE B11 (Continued)

(d) Condition: P_m = 100 psi C_s = 1000 fps $t_r = t_t$ p_h/p_v = 1.00

Time	180 Degree Arch						120 Degree Arch					
	$p_1(t)$	$p_2(t)$	$p_3(t)$	$p_u(t)$	$p_a(t)$	$p_s(t)$	$p_1(t)$	$p_2(t)$	$p_3(t)$	$p_u(t)$	$p_a(t)$	$p_s(t)$
1	37	-16	-26	0	20	29	53	-31	-23	0	36	30
2	55	-21	-34	0	27	40	78	-37	-22	0	41	35
4	75	-27	-30	0	32	41	99	-34	-6	0	35	27
8	97	-25	-9	0	27	29	111	-13	17	0	12	12
12	110	-17	14	0	17	14	90	0	29	24	-4	-2
16	114	-7	30	0	6	5	7	1	6	88	-2	-3
20	89	-1	30	22	-1	-4	2	1	2	90	-1	-1
24	47	1	19	54	-2	-5	2	1	2	88	-1	-1
28	4	2	5	86	-2	-2	2	1	2	86	-1	-1
32	4	2	5	84	-2	-2	2	1	2	84	-1	-1
40	4	2	5	80	-2	-2	2	1	2	80	-1	-1
120	4	2	5	50	-2	-2	2	1	2	50	-1	-1
200	4	2	5	30	-2	-2	2	1	2	30	-1	-1

TABLE B11 (Continued)

(e) Condition: P_m = 100 psi C_s = 1000 fps $t_r = 2t_t$ p_h/p_v = 0.25

	180 Degree Arch						120 Degree Arch					
Time	$p_1(t)$	$p_2(t)$	$p_3(t)$	$p_u(t)$	$p_a(t)$	$p_s(t)$	$p_1(t)$	$p_2(t)$	$p_3(t)$	$p_u(t)$	$p_a(t)$	$p_s(t)$
1	30	-10	-24	0	15	26	27	-20	-26	0	26	27
2	47	-12	-34	0	20	38	67	-22	-33	0	32	41
4	61	-15	-35	0	23	42	84	-23	-22	0	30	36
8	77	-11	-26	0	19	38	100	-10	-1	0	14	24
12	84	-7	-18	0	14	34	99	-2	10	5	4	15
16	86	-4	-9	0	10	27	79	0	8	19	2	12
20	83	-2	-6	3	8	24	59	1	3	33	2	11
24	77	0	-4	7	5	21	46	1	-1	42	2	11
28	71	0	-4	11	5	19	45	1	-1	41	2	11
32	64	1	-6	15	4	19	44	1	0	40	2	10
36	57	1	-7	19	4	18	42	1	-1	40	2	10
40	50	1	-8	23	4	18	41	1	-1	39	2	10
60	44	1	-10	23	4	18	36	1	0	34	2	8
120	29	0	-6	15	3	11						
200	21	0	-3	10	2	7						

TABLE B11 (Continued)

(f) Condition: P_m = 100 psi C_s = 1000 fps $t_r = 2t_t$ p_h/p_v = 0.50

Time	180 Degree Arch						120 Degree Arch					
	$p_1(t)$	$p_2(t)$	$p_3(t)$	$p_u(t)$	$p_a(t)$	$p_s(t)$	$p_1(t)$	$p_2(t)$	$p_3(t)$	$p_u(t)$	$p_a(t)$	$p_s(t)$
1	30	-10	-24	0	15	26	44	-20	-26	0	27	30
2	47	-12	-35	0	20	39	69	-23	-32	0	33	41
4	63	-16	-34	0	24	42	87	-25	-20	0	32	35
8	82	-14	-25	0	21	39	104	-12	5	0	14	20
12	90	-10	-11	0	15	29	99	-3	17	8	3	9
16	94	-7	-1	0	11	22	73	0	12	28	0	7
20	90	-3	4	5	7	17	46	1	5	48	0	7
24	79	-1	6	13	4	13	28	1	0	62	1	6
28	66	0	4	22	3	12	27	1	0	61	1	6
32	54	1	2	30	2	11	27	1	0	59	1	6
36	42	1	-1	38	2	9	26	1	0	58	1	6
40	31	0	-4	46	2	10	25	1	0	57	1	6
60	23	0	-4	44	2	8	21	1	0	51	0	5

TABLE B11 (Continued)

(g) Condition: P_m = 100 psi C_s = 1000 fps $t_r = 2t_t$ p_h/p_v = 0.75

Time	180 Degree Arch						120 Degree Arch					
	$p_1(t)$	$p_2(t)$	$p_3(t)$	$p_u(t)$	$p_a(t)$	$p_s(t)$	$p_1(t)$	$p_2(t)$	$p_3(t)$	$p_u(t)$	$p_a(t)$	$p_s(t)$
1	30	-10	-24	0	15	26	44	-21	-26	0	28	30
2	49	-13	-35	0	21	39	70	-25	-32	0	35	41
4	65	-18	-34	0	25	42	90	-27	-18	0	33	35
8	85	-17	-23	0	23	38	108	-13	10	0	14	17
12	96	-12	-6	0	16	27	101	-3	23	10	1	5
16	102	-9	8	0	11	17	66	0	16	36	-1	3
20	94	-5	14	8	6	10	33	1	7	62	-1	2
24	80	-2	16	20	3	5	10	1	0	80	0	2
28	64	1	14	32	0	3	10	1	1	76	-1	2
32	46	1	10	44	0	2	9	1	0	75	0	1
36	29	2	5	56	-1	3	9	1	1	73	-1	1
40	12	2	0	68	-1	3	8	1	0	72	0	2
60	6	2	-1	63	-1	2	7	1	0	63	0	2
120	5	1	-1	43	0	2						
200	4	0	-1	29	0	2						

TABLE B11 (Continued)

(h) Condition: P_m = 100 psi C_s = 1000 fps $t_r = 2t_t$ p_h/p_v = 1.00

	180 Degree Arch						120 Degree Arch					
Time	$p_1(t)$	$p_2(t)$	$p_3(t)$	$p_u(t)$	$p_a(t)$	$p_s(t)$	$p_1(t)$	$p_2(t)$	$p_3(t)$	$p_u(t)$	$p_a(t)$	$p_s(t)$
1	31	-10	-24	0	15	26	45	-21	-26	0	28	31
2	50	-14	-35	0	21	39	71	-25	-31	0	34	40
4	67	-20	-34	0	27	43	91	-29	-16	0	34	33
8	90	-20	-20	0	25	37	112	-15	14	0	13	15
12	103	-16	-1	0	19	24	104	-4	29	12	0	2
16	110	-11	17	0	11	11	63	0	21	44	-3	-2
20	100	-6	24	11	5	3	20	2	9	76	-3	-2
24	80	-2	25	27	1	-2	3	1	4	88	-2	-2
28	59	-2	23	43	0	-5	3	1	4	86	-2	-2
32	37	1	18	59	-3	-6	2	1	4	84	-2	-3
36	15	2	11	75	-3	-5	2	2	3	82	-2	-2
40	5	2	8	80	-3	-5	3	1	4	80	-2	-2
60	5	2	8	70	-3	-5	3	1	4	70	-2	-2
120	3	1	4	49	-1	-3						
200	2	0	3	34	-1	-2						

TABLE B11 (Continued)

(i) Condition: P_m = 100 psi C_s = 2000 fps $t_r = t_t$ p_h/p_v = 0.25

	180 Degree Arch						120 Degree Arch					
Time	$p_1(t)$	$p_2(t)$	$p_3(t)$	$p_u(t)$	$p_a(t)$	$p_s(t)$	$p_1(t)$	$p_2(t)$	$p_3(t)$	$p_u(t)$	$p_a(t)$	$p_s(t)$
1	34	-25	-10	0	24	16	43	-43	8	0	35	4
2	49	-32	-15	0	32	23	62	-48	-2	0	43	13
4	72	-27	-23	0	30	35	91	-27	-9	0	30	28
6	83	-18	-20	0	23	35	102	-11	3	0	14	21
8	87	-10	-14	0	16	31	106	-1	13	0	3	14
10	90	-4	-8	0	10	27	73	1	5	26	2	13
12	89	-1	-4	1	7	23	52	2	-1	42	1	13
14	77	1	-5	9	5	22						
16	68	1	-8	17	5	22						
18	57	1	-11	24	5	22						
20	57	1	-11	24	4	22						
60	44	1	-8	19	3	16	38	1	-1	32	1	10
120	31	2	-6	13	2	19						
200	21	0	-4	9	2	11	18	0	-1	15	1	5

TABLE B11 (Continued)

(j) Condition: P_m = 100 psi C_s = 2000 fps $t_r = t_t$ p_h/p_v = 1.00

	180 Degree Arch						120 Degree Arch					
Time	$p_1(t)$	$p_2(t)$	$p_3(t)$	$p_u(t)$	$p_a(t)$	$p_s(t)$	$p_1(t)$	$p_2(t)$	$p_3(t)$	$p_u(t)$	$p_a(t)$	$p_s(t)$
1	40	-32	-8	0	29	16	50	-52	15	0	50	0
2	59	-46	-8	0	42	20	70	-60	9	0	50	9
4	87	-46	-7	0	43	25	101	-39	0	0	37	23
6	101	-37	1	0	35	22	115	-17	17	0	16	13
8	110	-27	12	0	25	15	121	-2	35	0	-3	1
10	116	-12	24	0	11	7	47	2	16	59	-4	-2
12	115	-4	33	3	3	-2	2	2	1	94	-2	-0
14	79	1	25	35	-2	-2						
16	35	2	13	67	-2	-3						
18	3	2	3	91	-2	-2						
20	3	2	3	91	-2	-2						
60	3	2	3	70	-2	-2	2	2	1	70	-2	0
120	1	1	2	49	-1	-1						
200	1	1	1	34	-1	-1	0	0	0	34	0	0

TABLE B11 (Continued)

(k) Condition: P_m = 200 psi C_s = 1000 fps $t_r = t_t$ p_h/p_v = 0.25

	180 Degree Arch						120 Degree Arch					
Time	$p_1(t)$	$p_2(t)$	$p_3(t)$	$p_u(t)$	$p_a(t)$	$p_s(t)$	$p_1(t)$	$p_2(t)$	$p_3(t)$	$p_u(t)$	$p_a(t)$	$p_s(t)$
1							97	-51	-50	0	63	60
2	100	-30	-67	0	44	77	141	-55	-55	0	70	76
4	133	-29	-67	0	45	84	181	-41	-28	0	53	63
6	151	-22	-55	0	38	79	197	-20	1	0	27	45
10	166	-13	-26	0	26	59	189	0	25	10	3	24
14	167	-4	-9	0	17	45	111	3	6	66	2	22
18	154	-1	-1	8	10	36	84	3	-1	81	3	20
22	135	4	-6	16	6	35	80	3	-1	77	3	19
26	98	3	-12	40	6	32	75	3	0	74	2	17
30	84	3	-14	46	5	30	71	3	0	70	2	16
60	63	1	-12	31	5	24	56	2	-2	49	2	14
120	41	1	-8	19	3	16	35	1	-1	31	2	9
200							22	1	0	19	1	5

TABLE B11 (Continued)

(1) Condition: P_m = 200 psi C_s = 1000 fps $t_r = t_t$ p_h/p_v = 0.50

	180 Degree Arch						120 Degree Arch					
Time	$p_1(t)$	$p_2(t)$	$p_3(t)$	$p_u(t)$	$p_a(t)$	$p_s(t)$	$p_1(t)$	$p_2(t)$	$p_3(t)$	$p_u(t)$	$p_a(t)$	$p_s(t)$
1							98	-52	-50	0		
2	102	-32	-68	0	46	78	144	-58	-54	0		
4	138	-34	-66	0	49	84	186	-46	-23	0		
6	159	-28	-51	0	42	77	205	-24	10	0		
10	179	-19	-13	0	28	51	194	-1	38	14		
14	184	-8	13	0	14	31	85	3	10	94		
18	161	0	20	16	5	20	50	3	0	115		
22	114	3	10	48	2	18	47	3	0	110		
26	65	4	-3	80	1	17	44	3	0	105		
30	43	4	-8	91	1	16	41	3	0	100		
60	35	2	-7	62	2	14	33	2	0	70		
120	24	1	-4	38	1		22	1	-2	44		
200							14	1	0	28		

TABLE B11 (Continued)

(m) Condition: P_m = 200 psi C_s = 1000 fps $t_r = t_t$ p_h/p_v = 0.75

	180 Degree Arch						120 Degree Arch					
Time	$p_1(t)$	$p_2(t)$	$p_3(t)$	$p_u(t)$	$p_a(t)$	$p_s(t)$	$p_1(t)$	$p_2(t)$	$p_3(t)$	$p_u(t)$	$p_a(t)$	$p_s(t)$
1							100	-54	-50	0		
2	105	-34	-68	0	48	79	145	-61	-52	0		
4	144	-38	-65	0	52	85	192	-51	-16	0		
6	167	-34	-47	0	47	76	213	-28	20	0		
10	193	-25	0	0	31	44	198	-2	51	18		
14	201	-11	34	0	13	18	60	4	14	122		
18	170	-1	42	24	1	5	15	4	1	150		
22	102	3	27	72	-2	1	15	4	1	143		
26	32	4	7	120	-3	2	12	3	1	137		
30	10	4	0	148	-3	2	12	4	1	130		
60	10	2	-2	91	-1	4	13	2	0	91		
120	9	2	-1	56	-1	3	10	1	0	57		
200							6	1	0	36		

TABLE B11 (Continued)

(n) Condition: P_m = 200 psi C_s = 1000 fps $t_r = t_t$ p_h/p_v = 1.00

	180 Degree Arch						120 Degree Arch					
Time	$p_1(t)$	$p_2(t)$	$p_3(t)$	$p_u(t)$	$p_a(t)$	$p_s(t)$	$p_1(t)$	$p_2(t)$	$p_3(t)$	$p_u(t)$	$p_a(t)$	$p_s(t)$
1							101	-55	-50	0	67	62
2	107	-36	-68	0	49	79	150	-65	-51	0	78	74
4	149	-42	-63	0	55	84	198	-56	-10	0	60	53
6	176	-39	-42	0	50	74	221	-32	29	0	29	28
10	207	-32	13	0	34	36	204	-3	65	22	-7	-4
14	219	-16	55	0	13	5	35	4	18	150	-7	-6
18	179	-3	64	32	-1	-11	7	4	10	164	-6	-6
22	90	4	43	96	-7	-14	7	4	10	156	-6	-6
26	14	5	21	148	-8	-12	7	4	10	148	-6	-6
30	14	5	21	140	-8	-12	7	4	10	140	-6	-6
60	6	3	9	104	-4	-6	2	2	4	104	-3	-3
120	3	2	5	66	-2	-3	2	1	2	66	-1	-1
200							3	1	2	40	-1	-1

TABLE B11 (Continued)

(0) Condition: P_m = 200 psi C_s = 2000 fps $t_r = t_t$ p_h/p_v = 0.25

	180 Degree Arch						120 Degree Arch					
Time	$p_1(t)$	$p_2(t)$	$p_3(t)$	$p_u(t)$	$p_a(t)$	$p_s(t)$	$p_1(t)$	$p_2(t)$	$p_3(t)$	$p_u(t)$	$p_a(t)$	$p_s(t)$
1	86	-47	-45	0	52	56	118	-83	-21	0	81	43
2	117	-53	-52	0	60	68	155	-77	-29	0	81	58
4	155	-36	-46	0	47	72	197	-27	-4	0	35	48
6	168	-20	-29	0	32	62	205	-3	22	0	7	30
8	172	-8	-14	0	19	50	149	4	15	43	-1	22
10	171	-1	-5	0	11	43	94	4	-2	82	-3	20
12	148	1	-8	15	9	40	92	4	-1	79	-2	22
14	125	4	-12	31	6	38	89	3	-1	77	-3	21
16	100	3	-18	47	7	37	86	4	-1	75	-2	20
18	97	3	-18	45	7	37	83	3	-1	73	-3	20
60	65	3	-13	28	4	25	56	1	-1	47	-3	14
120	41	1	-8	18	3	16	35	1	-1	30	-1	9

TABLE B11 (Continued)

(p) Condition: P_m = 200 psi C_s = 2000 fps $t_r = t_t$ p_h/p_v = 1.00

	180 Degree Arch						120 Degree Arch					
Time	$p_1(t)$	$p_2(t)$	$p_3(t)$	$p_u(t)$	$p_a(t)$	$p_s(t)$	$p_1(t)$	$p_2(t)$	$p_3(t)$	$p_u(t)$	$p_a(t)$	$p_s(t)$
1	96	-58	-43	0	61	56	129	-99	-10	0	91	37
2	134	-74	-41	0	76	63	170	-100	-8	0	93	45
4	187	-68	-29	0	71	66	221	-42	24	0	39	32
6	210	-50	16	0	42	35	235	-7	65	0	-1	5
8	221	-26	45	0	24	14	111	5	40	97	-11	-6
10	226	-7	66	0	4	-2	5	5	6	176	-9	-4
12	148	3	54	60	-6	-10	5	5	6	171	-9	-4
14	63	6	30	124	-8	-10	5	5	6	166	-9	-4
16	10	7	13	161	-8	-8	5	5	6	161	-9	-4
18	9	6	13	156	-7	-8	5	5	6	156	-9	-4
60	3	2	5	104	-1	-3	1	2	2	104	-2	-1
120	2	1	2	66	-0	-1	0	1	1	66	-1	-1

Table B12. Values of the coefficients $p_n(t)$ for the harmonic components of loading $p_n(t) \sin \frac{n\pi\varphi}{\theta}$, antisymmetrical $p_a(t)$ and symmetrical $p_s(t)$ analogous uniform loadings, and the uniform all-around compression $p_u(t)$. (All loadings are in pounds per square inch. Time is in milliseconds. R = 300 inches. W = 1 MT. Other variables are as noted.)

(a) Condition: P_m = 200 psi C_s = 1000 fps $t_r = \frac{1}{2}t_t$ p_h/p_v = 0.25

	180 Degree Arch						120 Degree Arch					
Time	$p_1(t)$	$p_2(t)$	$p_3(t)$	$p_u(t)$	$p_a(t)$	$p_s(t)$	$p_1(t)$	$p_2(t)$	$p_3(t)$	$p_u(t)$	$p_a(t)$	$p_s(t)$
2	71	-30	-51	0	39	57	102	-59	-44	0	68	58
4	103	-36	-64	0	48	75	144	-62	-47	0	71	70
6	128	-33	-67	0	48	83	175	-47	-31	0	58	64
20	157	-9	-12	0	18	45	161	5	28	19	-4	15
32	142	3	4	0	5	29	67	5	2	72	-1	14
42	72	5	-7	41	1	10	57	5	3	63	-2	11

TABLE B12 (Continued)

(b) Condition: P_m = 200 psi C_s = 1000 fps $t_r = \frac{1}{2}t_t$ p_h/p_v = 1.00

	180 Degree Arch						120 Degree Arch					
Time	$p_1(t)$	$p_2(t)$	$p_3(t)$	$p_u(t)$	$p_a(t)$	$p_s(t)$	$p_1(t)$	$p_2(t)$	$p_3(t)$	$p_u(t)$	$p_a(t)$	$p_s(t)$
2	76	-33	-52	0	42	59	107	-65	-62	0	79	73
4	112	-44	-65	0	55	78	155	-75	-60	0	89	82
6	142	-45	-64	0	58	84	191	-64	-15	0	68	56
20	200	-26	38	0	24	15	159	7	63	44	-17	-13
32	192	3	79	0	-9	-20	11	7	15	137	-10	-9
42	22	11	32	117	-14	-21	11	7	15	118	-10	-9

TABLE B12 (Continued)

(c) Condition: P_m = 200 psi C_s = 2000 fps $t_r = \frac{1}{2}t_t$ p_h/p_v = 0.25

	180 Degree Arch						120 Degree Arch					
Time	$p_1(t)$	$p_2(t)$	$p_3(t)$	$p_u(t)$	$p_a(t)$	$p_s(t)$	$p_1(t)$	$p_2(t)$	$p_3(t)$	$p_u(t)$	$p_a(t)$	$p_s(t)$
1	61	-43	-26	0	44	35	82	-79	6	0	67	14
2	92	-55	-39	0	58	52	123	-93	-9	0	85	35
4	117	-59	-45	0	64	63	155	-80	-20	0	74	51
8	154	-38	-41	0	48	68	193	-24	-3	0	32	47
16	165	-2	-8	0	12	44	80	6	0	78	0	18
28	92	6	-16	43	4	34	79	6	0	68	0	18
34	90	6	-14	40	3	32	73	6	1	63	-1	16

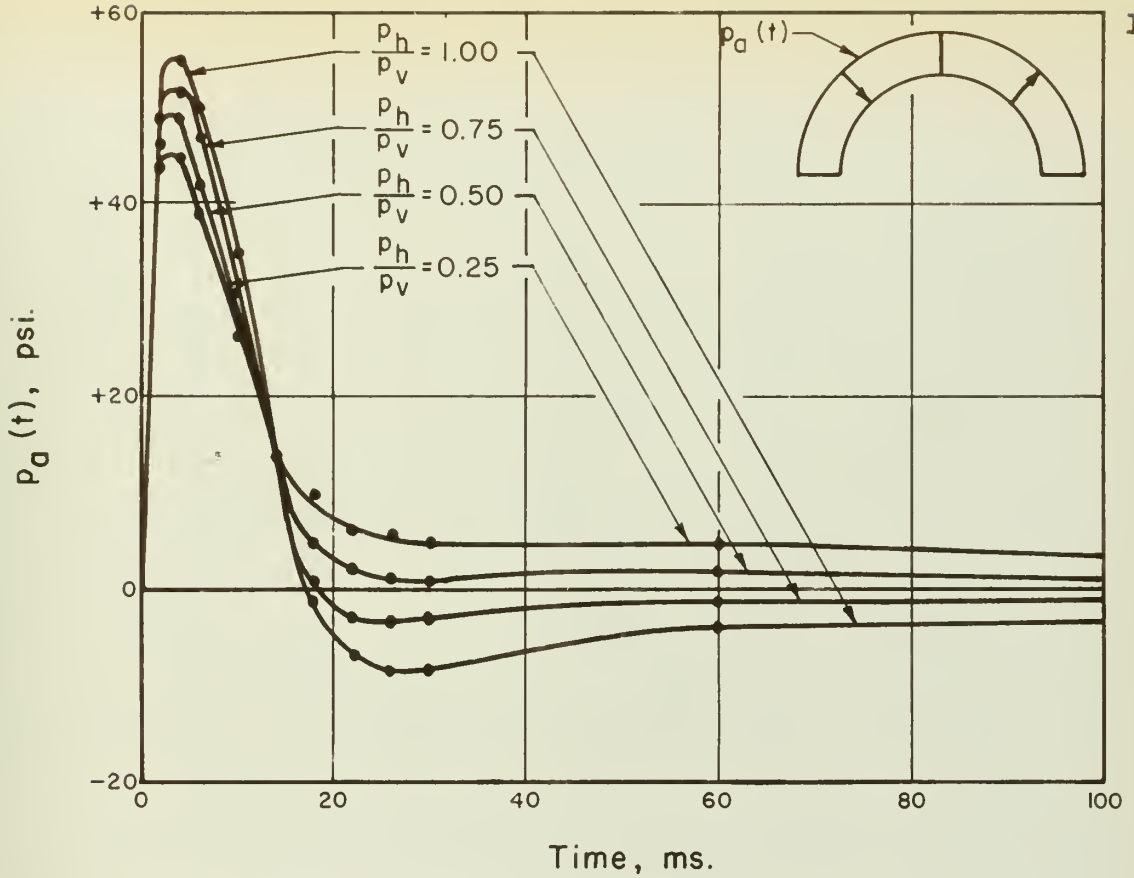

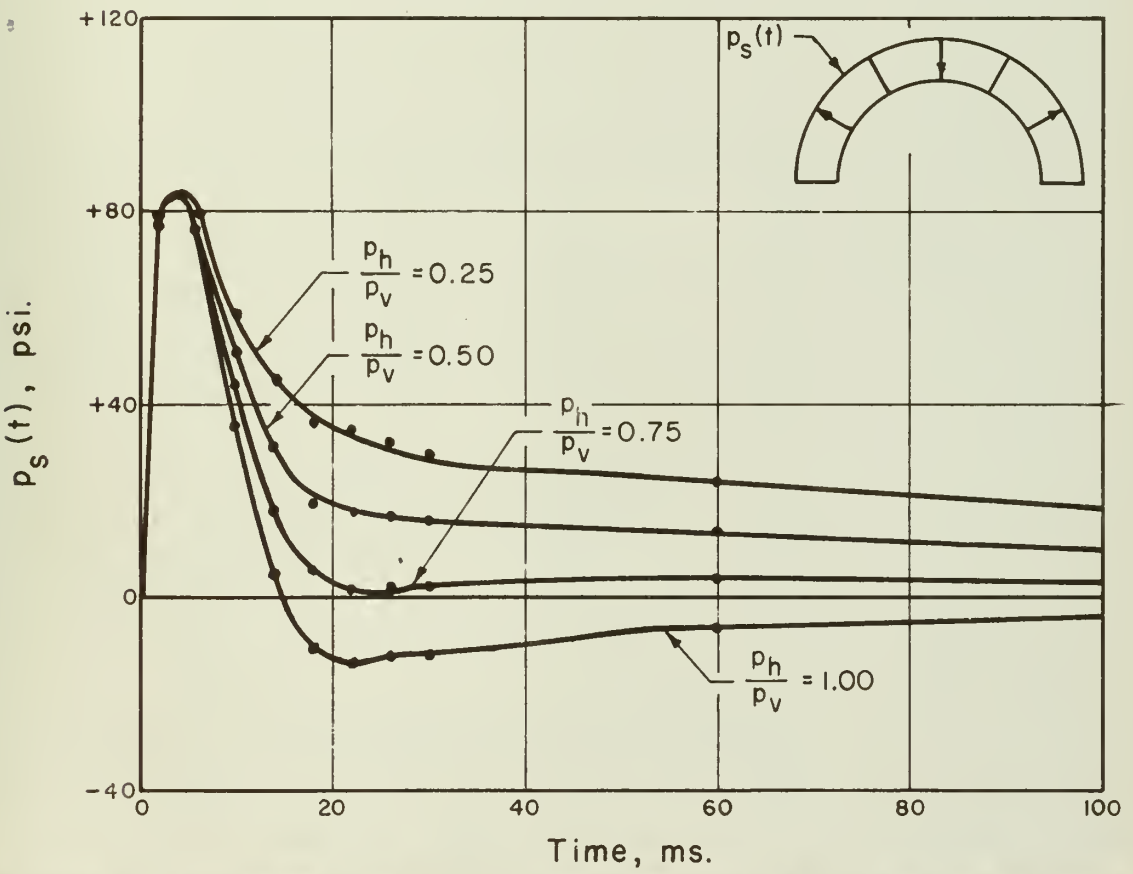

Figure B1 Antisymmetrical $p_a(t)$ and Symmetrical $p_s(t)$ Analogous Loads with R = 150 inches, C_s = 1000 fps, P_m = 200 psi, $t_r = t_t$, θ = 180 degrees, W = 1 MT, and p_h/p_v as noted

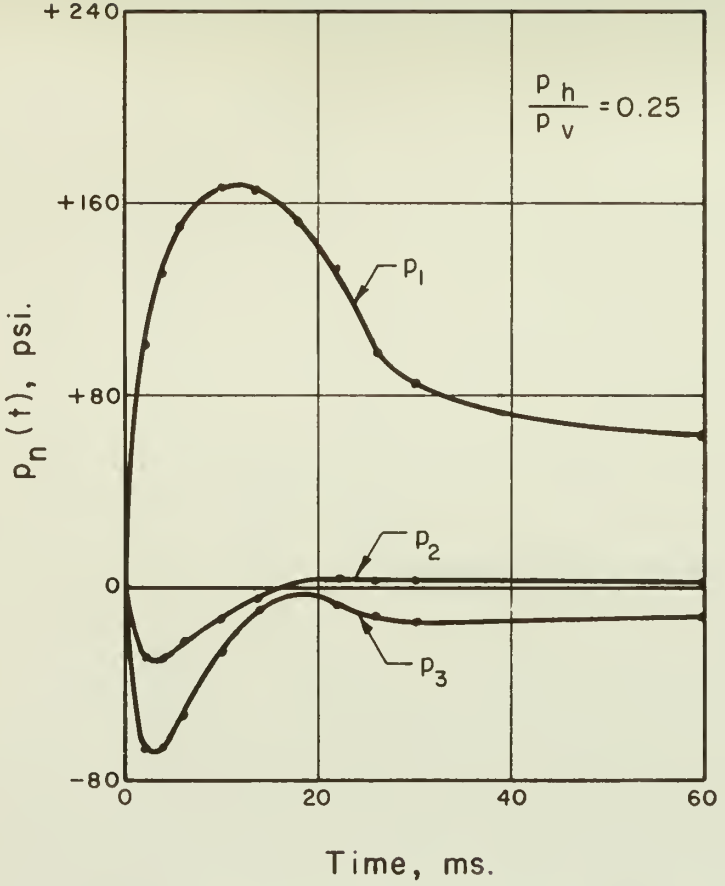

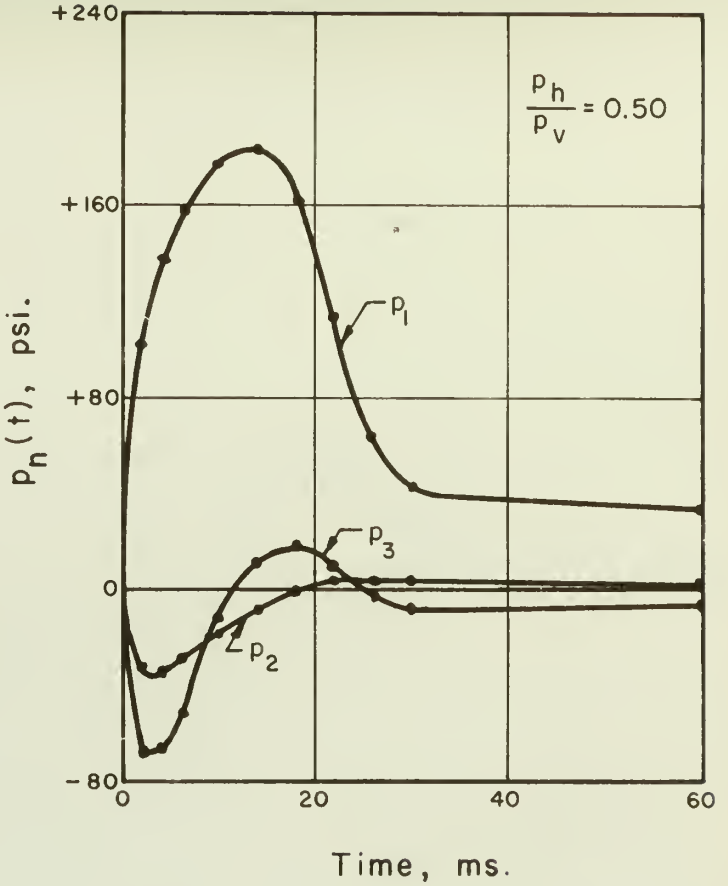

Figure B2 Values of the Coefficient $p_n(t)$ for the Distributed Load $\sum p_n(t) \sin \frac{n\pi\varphi}{\theta}$ with R = 150 inches, C_s = 1000 fps, P_m = 200 psi, $t_r = t_t$, θ = 180 degrees, W = 1 MT, p_h/p_v as noted

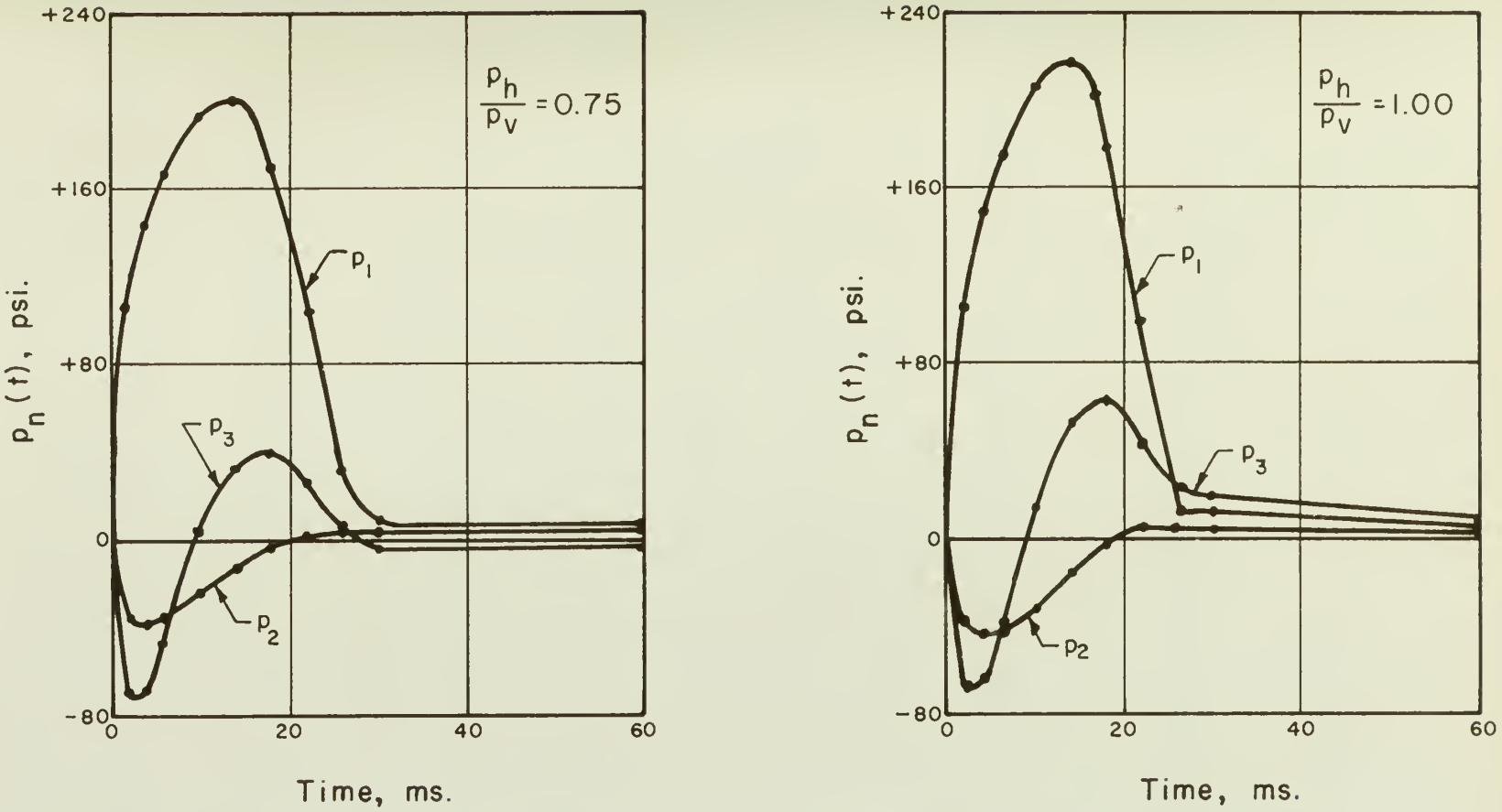

Figure B3 Values of the Coefficient $p_n(t)$ for the Distributed Load $\sum p_n(t) \sin \frac{n\pi\varphi}{\theta}$ with R = 150 inches, C_s = 1000 fps, P_m = 200 psi, $t_r = t_t$, θ = 180 degrees, W = 1 MT, p_h/p_v as noted

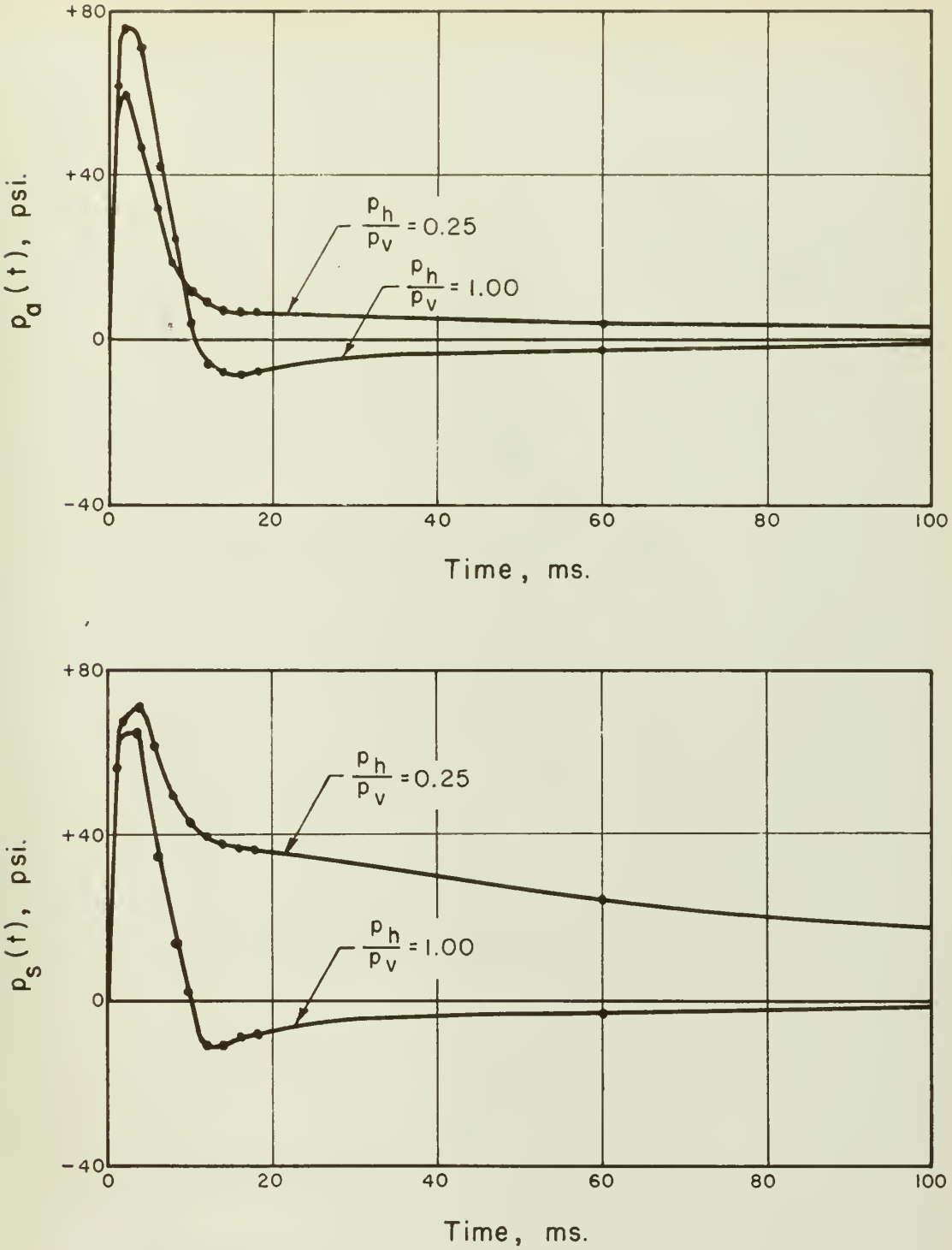

Figure B4 Antisymmetrical $p_a(t)$ and Symmetrical $p_s(t)$ Analogous Loads with R = 150 inches, C_s = 2000 fps, P_m = 200 psi, $t_r = t_t$, θ = 180 degrees, W = 1 MT, and p_h/p_v = as noted

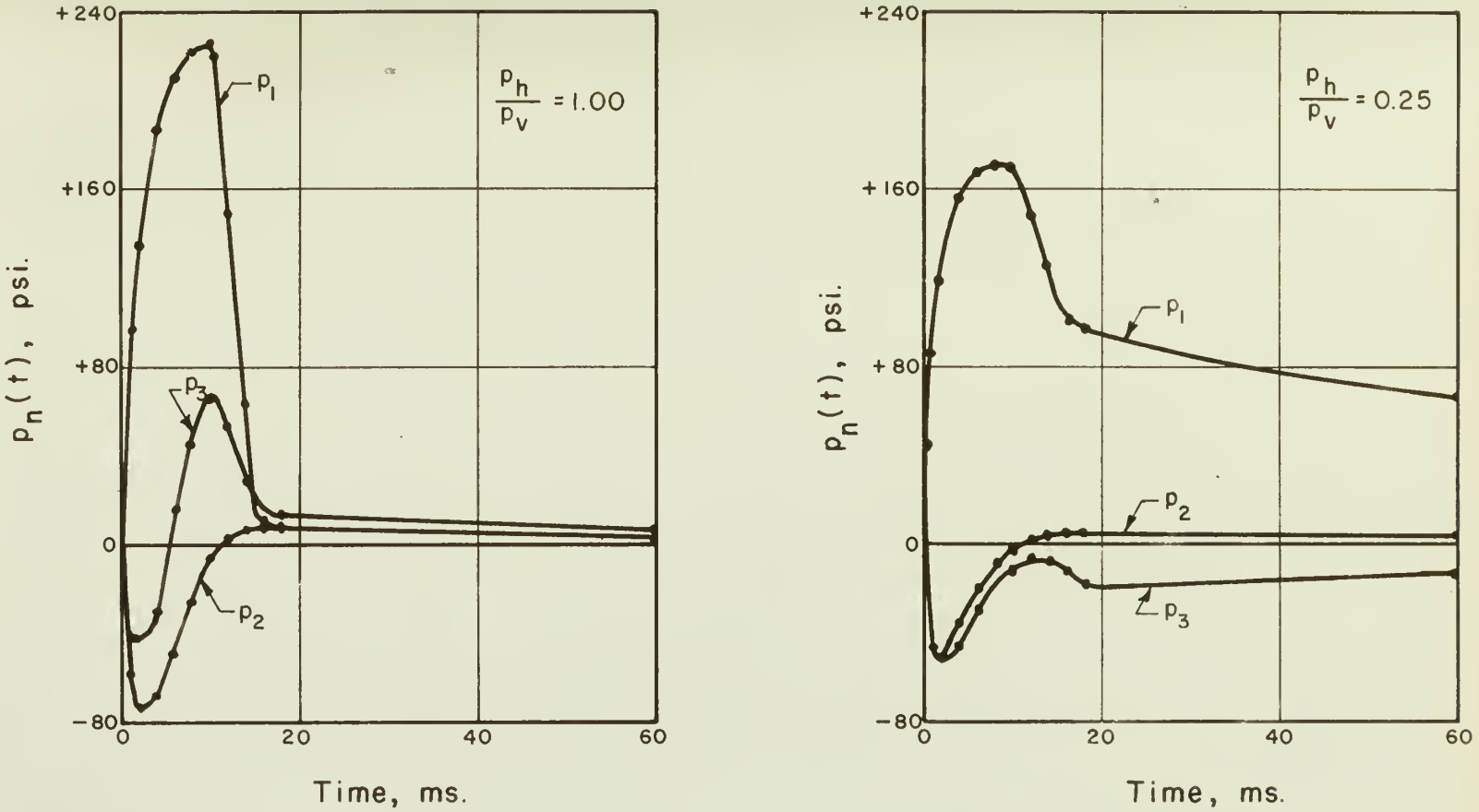

Figure B5 Values of the Coefficient $p_n(t)$ for the Distributed Load $\sum p_n(t) \sin \frac{n\pi\varphi}{\theta}$ with R = 150 inches, C_s = 2000 fps, P_m = 200 psi, $t_r = t_t$, θ = 180 degrees, W = 1 MT, p_h/p_v as noted

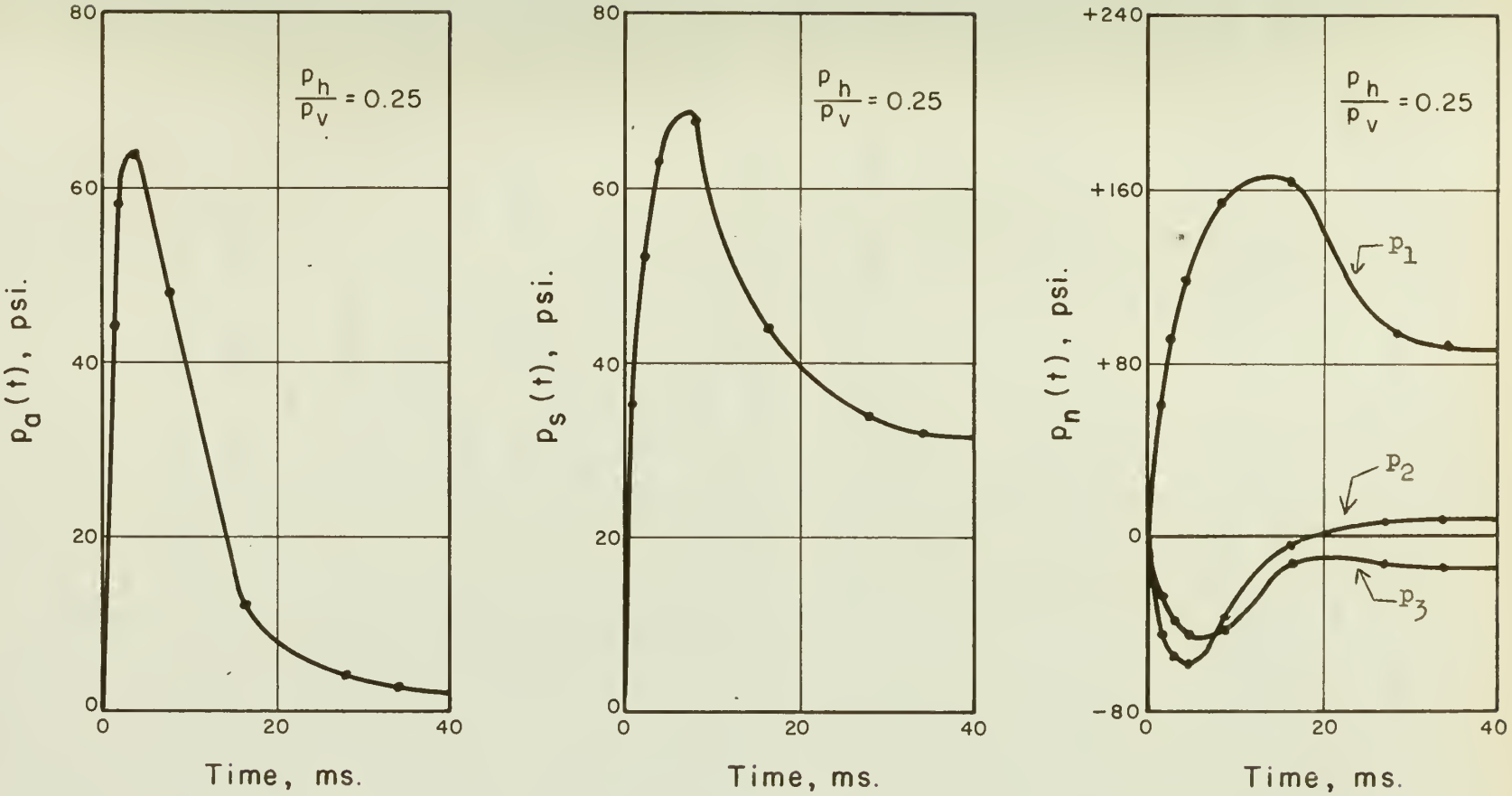

Figure B6 Antisymmetrical $p_a(t)$ and Symmetrical $p_s(t)$ Analogous Loads and Values of the Coefficient $p_n(t)$ for the Distributed Load $\sum p_n(t) \sin \frac{n\pi\varphi}{\theta}$ with R = 300 inches, C_s = 2000 fps, P_m = 200 psi, $t_r = \frac{1}{2} t_t$, θ = 180 degrees, W = 1 MT, p_h/p_v = 0.25

VITA

Lieutenant Commander Worthen Allen Walls, Civil Engineer Corps, U. S. Navy, was born near Little Rock, Arkansas, February 17, 1922. Following his graduation from Stephens High School, Stephens, Arkansas, in 1940, he attended Magnolia A and M College, Magnolia, Arkansas, for two years.

He entered the Naval Air Corps, U. S. Navy, in June of 1942 and after flight training was designated a Naval Aviator and commissioned as an Ensign, U. S. Naval Reserve, in 1943. Wartime assignments were primarily with the Pacific Fleet and included duty on the West Coast, the Aleutians, Hawaii, Saipan, Peleliu, Okinawa, Iwo Jima, and then Japan in the early days of the occupation.

After being released to inactive duty in 1946, he entered the University of Arkansas, Fayetteville, Arkansas, from which he graduated, with honors, in 1948 with the degree of Bachelor of Science in Civil Engineering. He was then employed as an engineer by Phillips Petroleum Company, Okmulgee, Oklahoma, until April, 1949.

In April, 1949, he returned to active duty and was commissioned as a Lieutenant (junior grade), Civil Engineer Corps, U. S. Navy. His first tour of duty was as Assistant Public Works Officer and Assistant Officer in Charge of Construction, Bureau of Yards and Docks Contracts, U. S. Fleet Activities, Yokosula, Japan. This duty was followed in 1951 by duty in the Public Works Department, U. S. Naval Air Station, Corpus Christi, Texas, until 1953.

In May, 1953, he entered the University of Illinois, for graduate work in Civil Engineering under a program of postgraduate education

sponsored by the U. S. Navy and received the degree of Master of Science in Civil Engineering in 1954.

Thereafter he was assigned as Assistant Resident Officer in Charge of Construction, Bureau of Yards and Docks Contracts, Seville, Spain, for three years in connection with the Spanish Bases Program. From 1957 to 1958 he served as Public Works Officer and Officer in Charge of Construction, U. S. Naval Ammunition Depot, Concord, California. He returned to the University of Illinois in 1958 to continue his advanced study in Civil Engineering under Navy sponsorship.

He is a member of the American Society of Civil Engineers, Society of American Military Engineers, and Tau Beta Pi.